Cosmic magnetic fields
and
their influence on UHE cosmic ray transport

Gustavo Medina Tanco
Inst. Ciencias Nucleares
UNAM - México

Three very basic questions

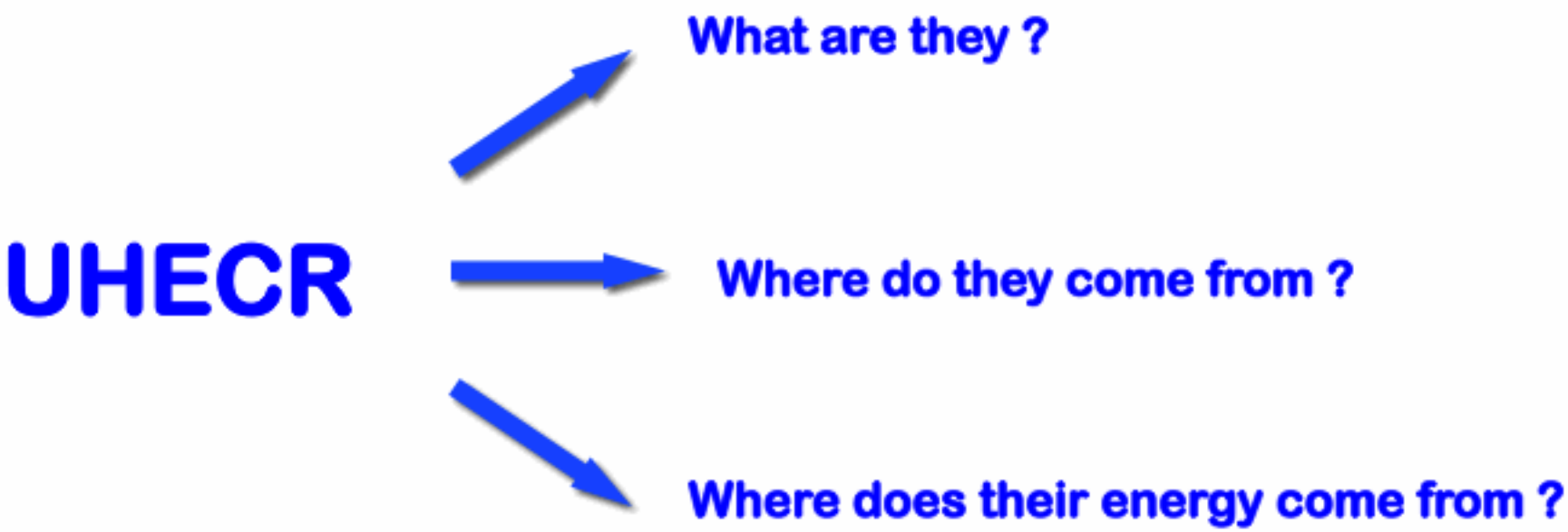

Three very limited clues

Mapping observables onto the sources: understanding propagation

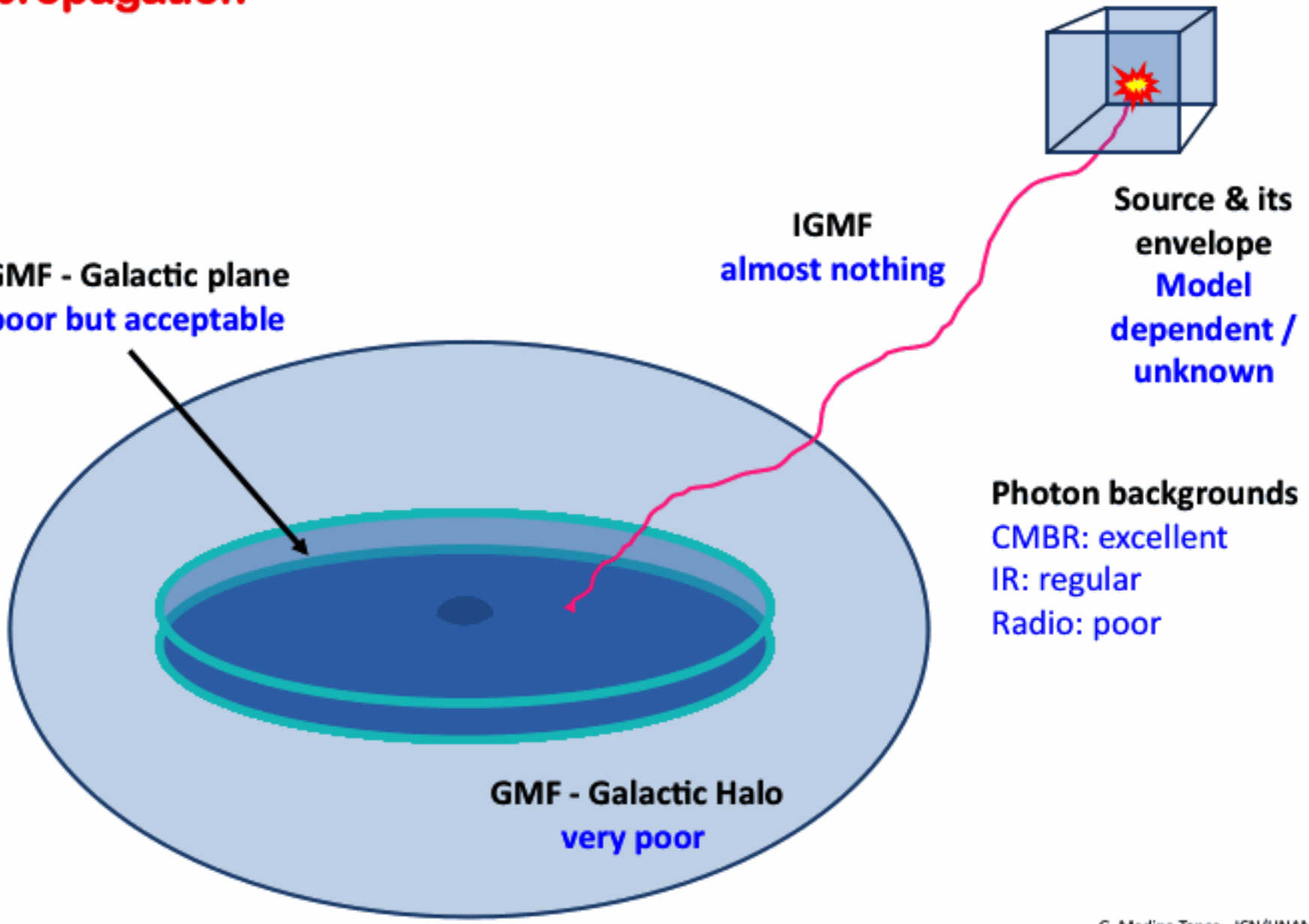

Changes in propagation regime inside the Galaxy

R_L, galactic scales & confinement:

$$R_{Lpc} \approx \frac{10^{-6}}{Z} \times \left(\frac{E_{GeV}}{B_{\mu G}} \right)$$

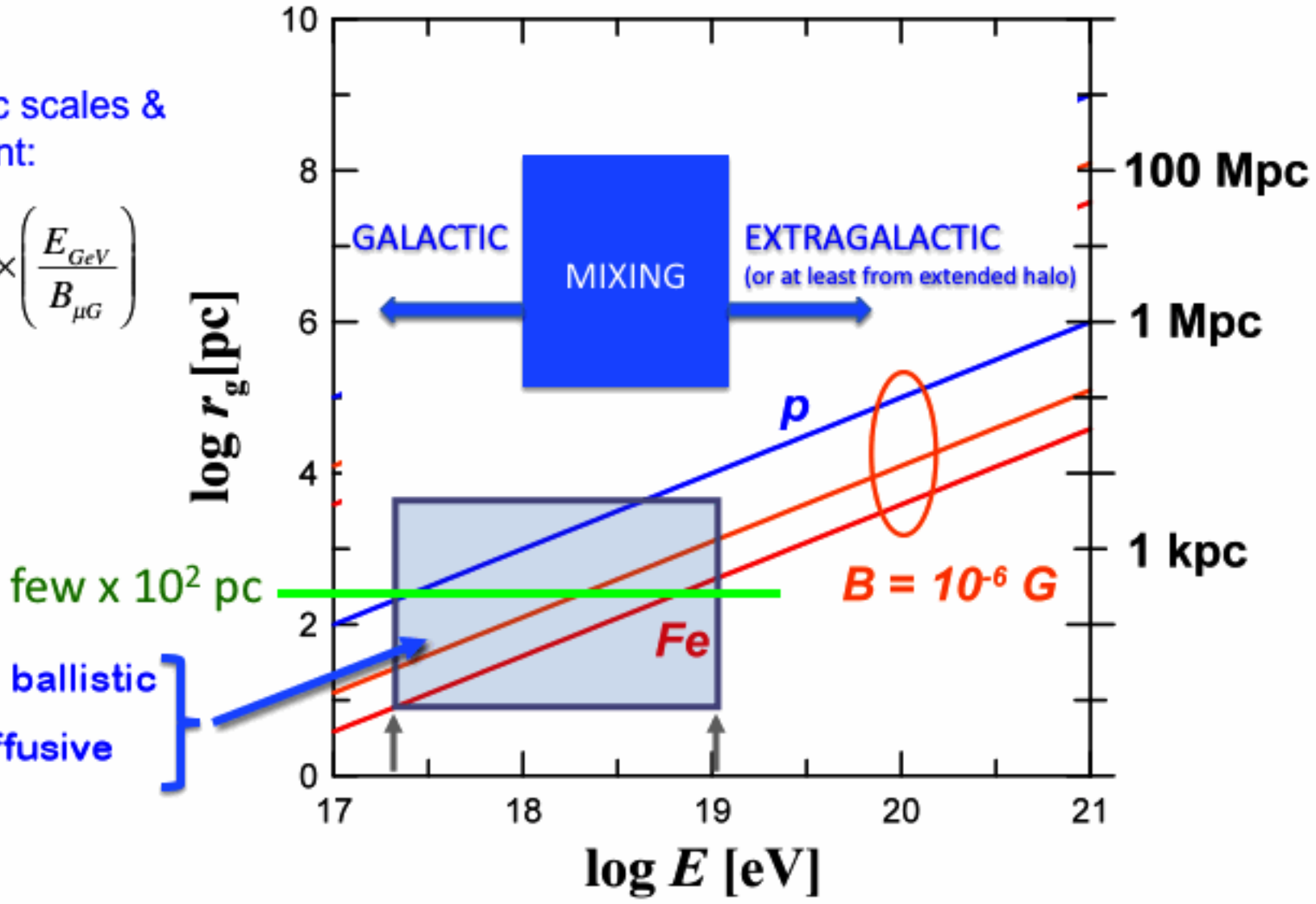

Changes in propagation regime inside the Galaxy

Wave particle interactions are resonant at $\lambda \sim r_L$

MHD turbulence + particle coupling if:

$$R_{Lpc} \leq \frac{10^3}{Z} \times \left(\frac{E_{GeV}}{B_{\mu G}} \right) \approx L_c^{GMF}$$

$$\left. \begin{array}{l} L_c^{GMF} \cong 100\,pc \\ B \approx 5\mu G \end{array} \right\} \Rightarrow E_{EeV}^{Transition} \approx 0.5 \times Z$$

That is, somewhere between the 2nd knee and ankle depending on composition of Galactic CRs.

Changes in propagation regime in the IGM

Wave particle interactions are resonant at $\lambda \sim r_L$

MHD turbulence + particle coupling if:

$$R_{L,Mpc} \approx \frac{1}{Z} \times \left(\frac{E_{EeV}}{B_{nG}} \right) \leq L_c^{IGMF} \equiv L_{\max}$$

$$\left.\begin{array}{l} L_c \approx 1\,Mpc \\ B \approx 1\,nG \end{array}\right\} \rightarrow E_{EeV} \approx 1.0 \times Z$$

But, if:

$$\left.\begin{array}{l} L_c \approx 1\,Mpc \\ B \approx 0.1\,\mu G \end{array}\right\} \rightarrow E_{EeV} \approx 100 \times Z$$

& propagation could be diffusive from p to Fe in all the observed energy range

IGMF effects

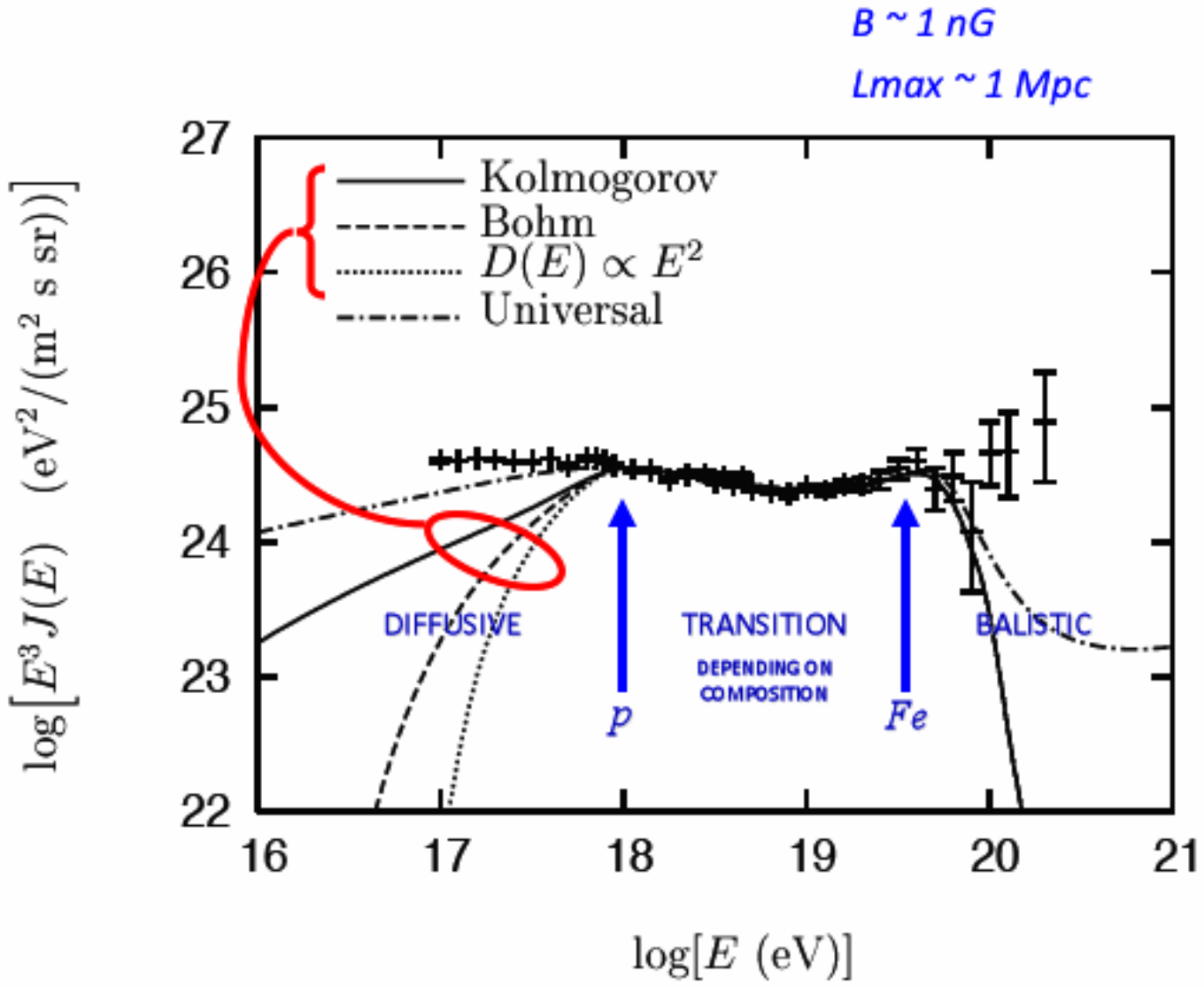

Aloisio & Berezinsky (2005)

Matching spectra: the fine-tuning of Nature ?

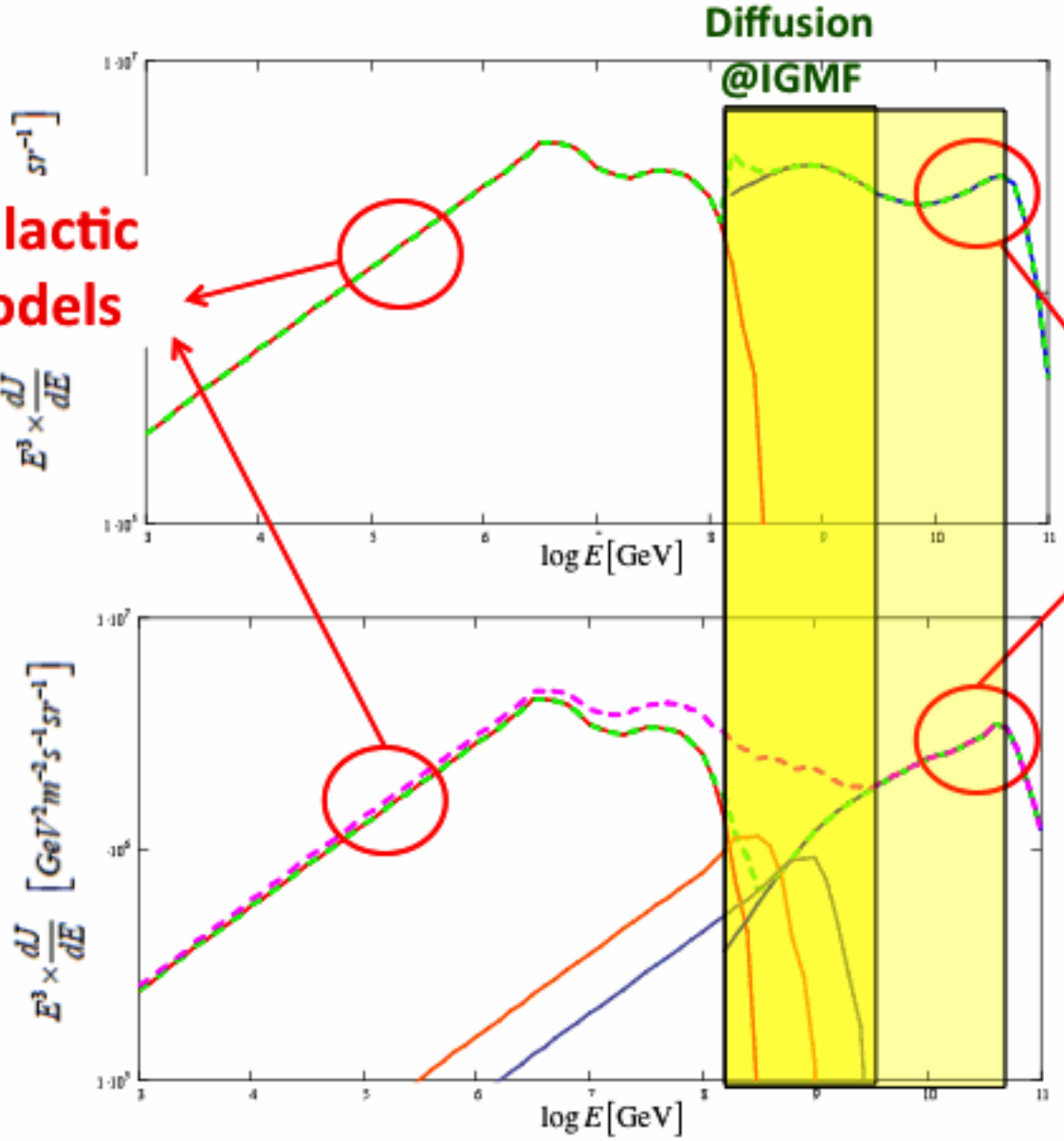

Proton injection at the sources

Extragalactic models

Normalized by Auger

Mixed injection at the sources

Dedonato & Medina Tanco (2009)

Effects of IGM propagation on heavy nuclei

Yamamoto, Mase, Takeda, Sakaki, Teshima (2003)

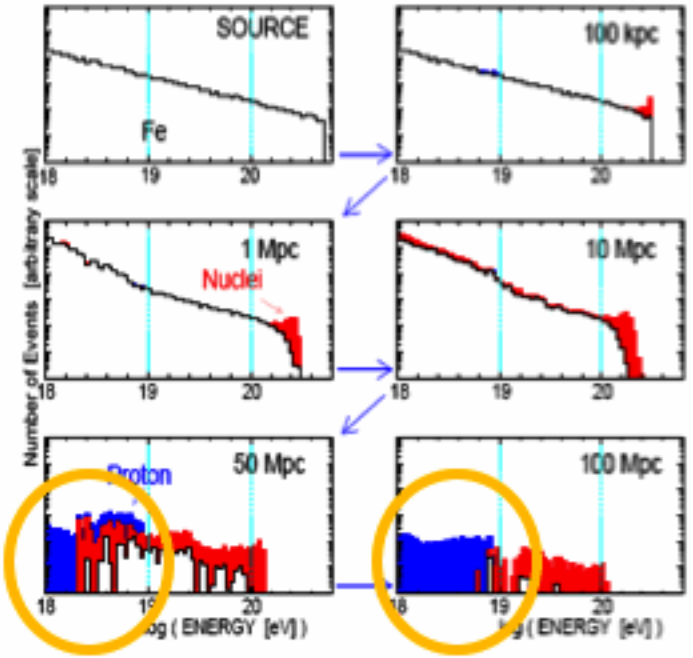

Fig. 4. Variation of energy distribution of particles that began as *Fe* after propagation over various distances from a single source. The distances from the source are indicated in each panel. The number of particles (arbitrary scale) are shown as a function of energy. Primary nuclei (*Fe*), secondary lighter nuclei, and protons are indicated by white, light shade and dark shade in the histograms respectively. The differential source spectrum is assumed to be a power law, $\propto E^{-2}$, with energy cut-off at $Z \times 2 \times 10^{19}$ eV (upper left panel). At 100 Mpc from the source, most of the *Fe* disappear because of their low rigidity.

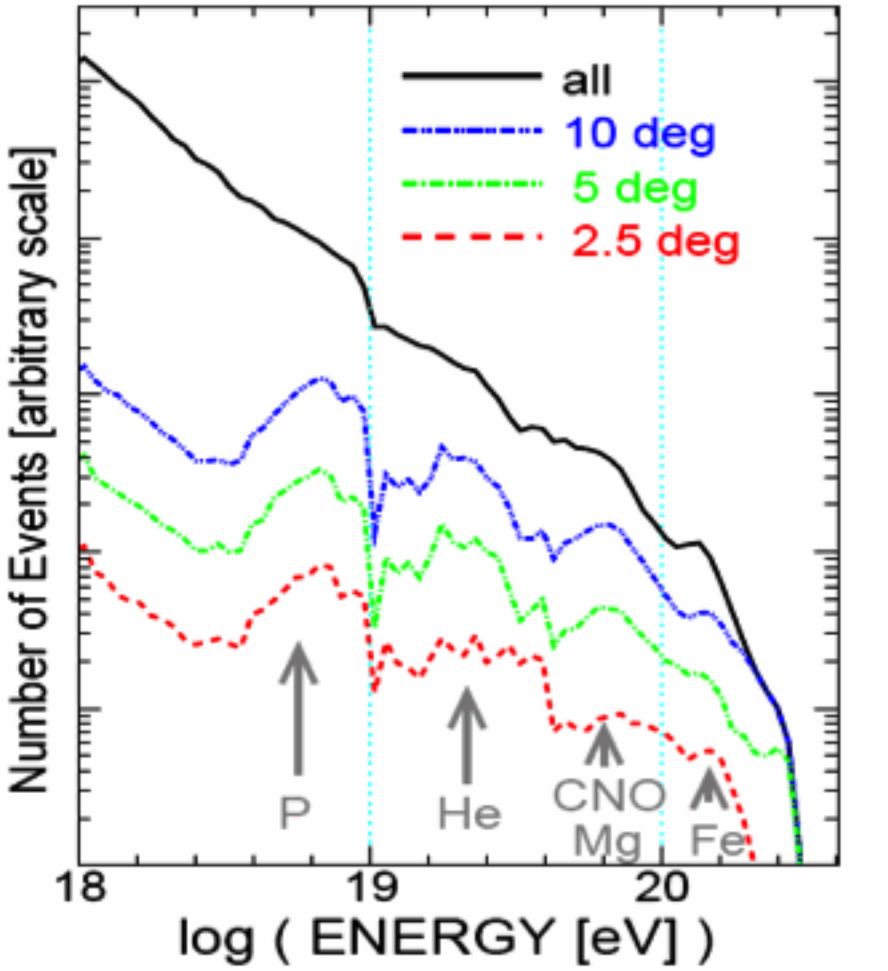

Fig. 6. The expected energy distribution of particles after propagation under the assumption that point sources are distributed uniformly in the universe. The solid line shows the energy distribution with no deflection angle cut. The other (dashed dots) lines show the energy distributions of the particle with deflection angles smaller than 10, 5, and 2.5 degrees. Particles with lower rigidity are scattered by the magnetic field. Larger rigidity particle are disintegrated by the photon field due to their large Lorentz factor.

Modification factor of nuclei vs. protons

$$\sigma_i = \sigma_i\left(E_{nuc}\right) = \sigma_i\left(E_{Tot} / A\right)$$

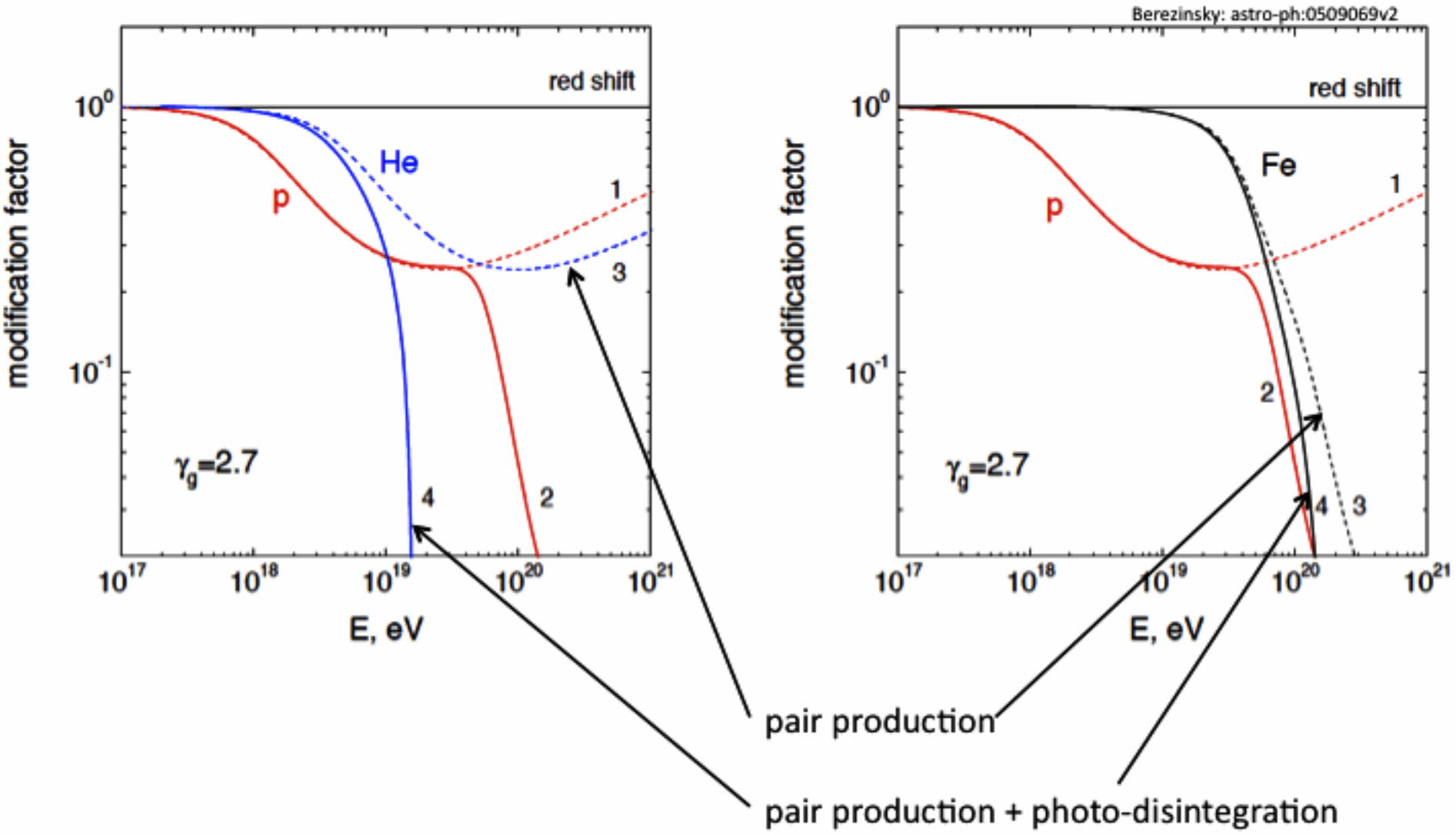

Propagation in the Intergalactic medium

R_L, intergalactic scales & astronomy:

$$R_{L,kpc} \approx \frac{1}{Z} \times \left(\frac{E_{EeV}}{B_{\mu G}} \right)$$

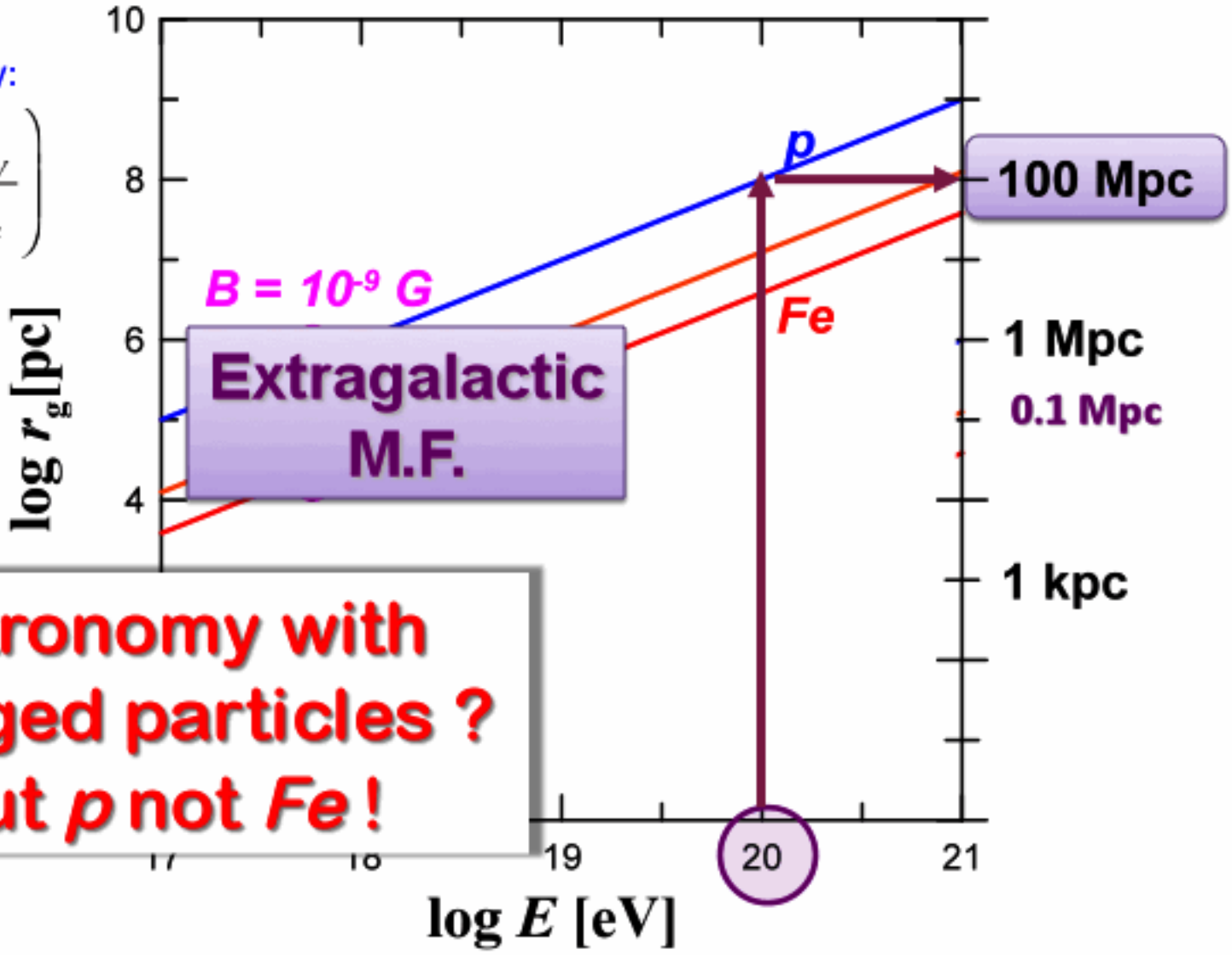

Astronomy with charged particles ?
But *p* not *Fe* !

How to distribute de IGMF and with what intensity?

LCDM universe

($\Omega_0 = 0.3$, $\Lambda = 0.7$, $H_0 = 70$ km/s/Mpc)

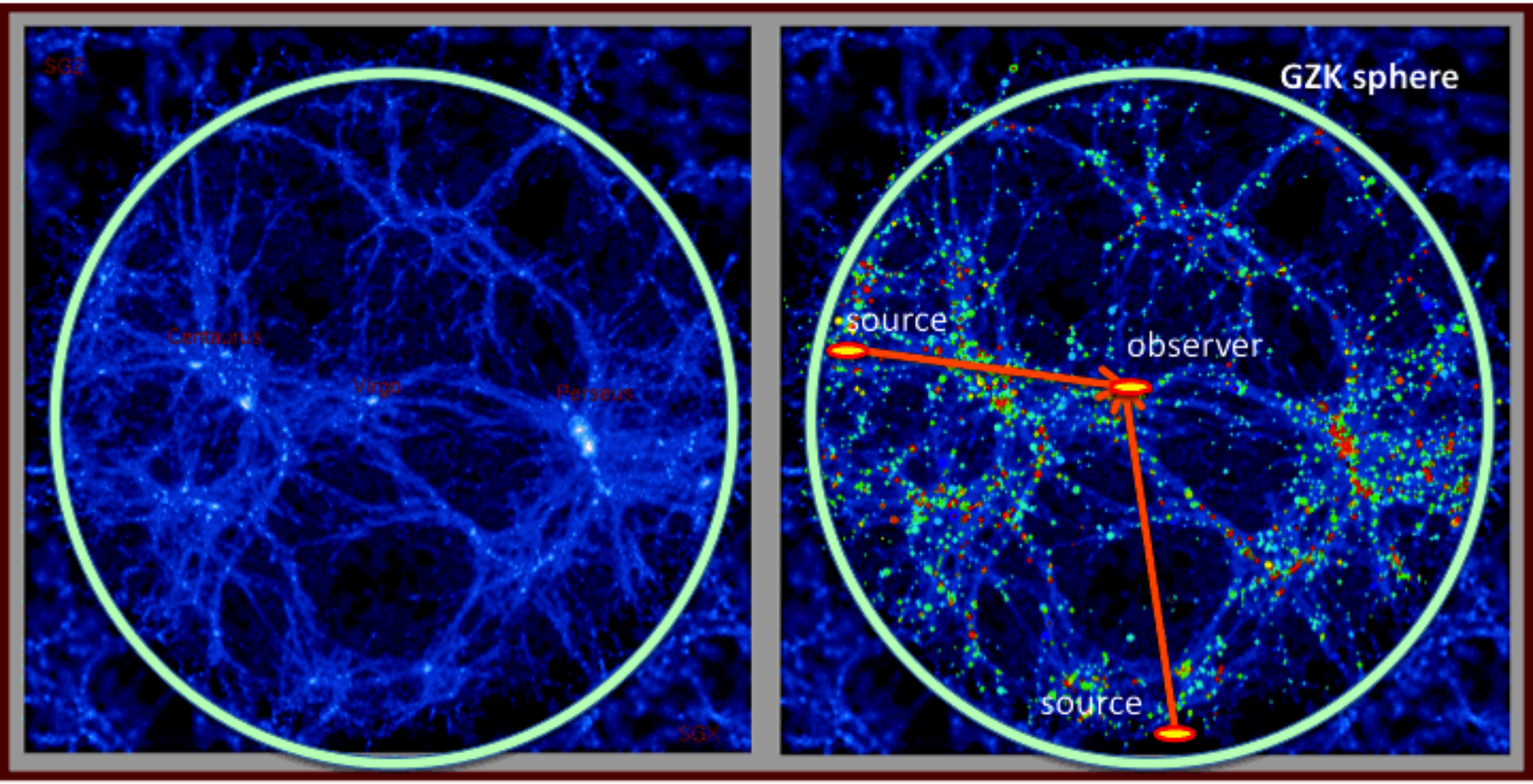

IGMF: what is the available information?

- Most of what we know about astrophysical magnetic fields has been detected via radio astronomical observations.

- Most of the cosmic broad-band ("continuum") radio emission is synchrotron radiation by relativistic electrons which spiral around magnetic field lines. These electrons are probably accelerated in the remnants of supernova explosions, together with other particles of the cosmic ray population.

- The observed synchrotron luminosity allows us to measure the total field Strength.

- Synchrotron radiation is linearly polarized -- up to 75% in a fully regular magnetic field.

- The polarization plane yields the orientation of the regular field in the plane of the sky. The degree of linear polarization tells us the field's degree of ordering.

- Faraday rotation of the polarization plane provides information on the field component along the line of sight. Hence, a three-dimensional picture of cosmic magnetic fields can be derived from radio waves.

IGMF: what is the available information?

Our knowledge of galactic magnetic fields rests on four observational pillars:

Faraday rotation

Zeeman splitting

→ magnetic field perpendicular to the plane of the sky, integrated along the line of sight. Direction sensitive: contributions from oppositely directed fields tend to cancel each other.

Polarized synchrotron continuum

Polarized emission and absorption by magnetically aligned dust grains

→ Line of sight integrated magnetic field components in the plane of the sky.
Sensitive to orientation, not direction, but 90° swings in orientation also cancel.

In addition to line of sight averaging, finite angular resolution of the telescope causes plane of sky averaging.

Faraday rotation measurements (RM) constraints:

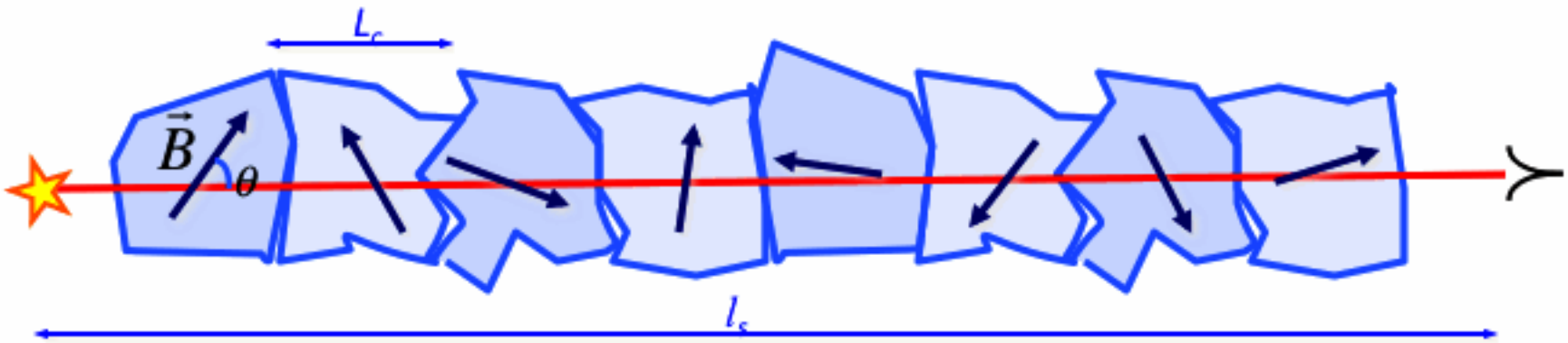

$$RM \propto \int n_e B_{||} dl \sim \sum_{i-1}^{N} n_e \left(B \times cos(\theta)\right) L_c \sim \sum_{i-1}^{N} n_e B \underbrace{\left(L_c \times cos(\theta)\right)}$$

random walk with path L_c

where: $N = \frac{l_s}{L_c}$

$$RM \propto \langle n_e \rangle \langle B \rangle \sqrt{N} L_c = \langle n_e \rangle \langle B \rangle \sqrt{\frac{l_s}{L_c}} L_c = \langle n_e \rangle \langle B \rangle \sqrt{l_s} \sqrt{L_c}$$

$$\langle B \rangle \sqrt{L_c} \propto \frac{RM}{\langle n_e \rangle \sqrt{l_s}}$$

G. Medina Tanco

Faraday rotation measurements (RM) constraints:

Actually what is done is to combine rotation measure with dispersion measure in order to eliminate n_e and to estimate *B as*:

$$\langle B \rangle \approx \langle B_{\parallel} \rangle \approx \frac{\int_0^{l_s} n_e B_{\parallel}\, dl}{\int_0^{l_s} n_e\, dl}$$

Faraday rotation and redshift

If β is the rotation angle of the polarization plane:

$$\beta = \frac{e^3}{2\pi m^2 c^2 \nu^2} \int_0^D n_e B_{\parallel} \, ds$$

$$\beta = \frac{c^2 \times RM}{\nu^2} = \frac{c^2 \times RM}{\nu_0^2 (1+z)^2}$$

$$\Rightarrow \quad \beta \propto (1+z)^{-2}$$

It is difficult to observe magnetic field structure at high redshift.

In particular, it becomes progressively more difficult to disentangle the Galactic contribution to the observed RM.

This is a great limitation on the usefulness of observations of Ly_{α} forests.

Faraday rotation measurements (RM) constraints:

$$B \times L_c^{1/2} \leq 10^{-9} \ \mathrm{G} \times \mathrm{Mpc}^{1/2}$$

Available measurements:

Very few localized determinations (mainly for high density regions)

Center of a few galaxy clusters → **1 μG**

One bridge between galaxy clusters → **0.1 μG**

Synchrotron emission constraints

$$J(\nu, E) \propto B_\perp \left(\frac{\nu}{\nu_c}\right)^{1/3} f\left(\frac{\nu}{\nu_c}\right)$$

$$\nu_c \equiv \nu_L \left(\frac{E}{mc^2}\right)^2 \quad ; \quad \nu_L = \frac{eB_\perp}{2\pi mc}$$

$$f(x) \quad : \quad lim_{x\to 0} f(x) = 1 \wedge f(x \gg 1) \to 0$$

$$n_e(E)dE = n_{e,0}\left(\frac{E}{E_0}\right)^{-\gamma} dE$$

$$j_\nu \equiv \int J(\nu, E) n_e(E) dE$$

$$j_\nu \propto n_{e,0} \nu^{\frac{1-\gamma}{2}} B_\perp^{\frac{1+\gamma}{2}}$$

$$n_e(\nu_c) \propto \frac{j_{\nu_c}}{\nu_c B_\perp}$$

$$\epsilon_{re} = \int N(E)dE = \int_{\nu_L}^{\nu_U} E n_e(\nu_c) d\nu_c \propto B^{-3/2}\Theta^2 S_\nu(\nu_0)$$

$$\epsilon_{tot} = (1+k)\epsilon_{re} + \epsilon_B$$

$$(a)\text{equipartition} \to (1+k)\epsilon_{re} \sim \epsilon_B$$

$$(b)\text{minimization of } \epsilon_{tot} \text{ w/respect to} B$$

$$B_{eq} \propto S_\nu^{2/7}\Theta^{-4/7}$$

$$B_{min} \propto S_\nu^{2/(\gamma+5)}\Theta^{-4/(\gamma+5)}$$

Magnetic fields in supercluster scales

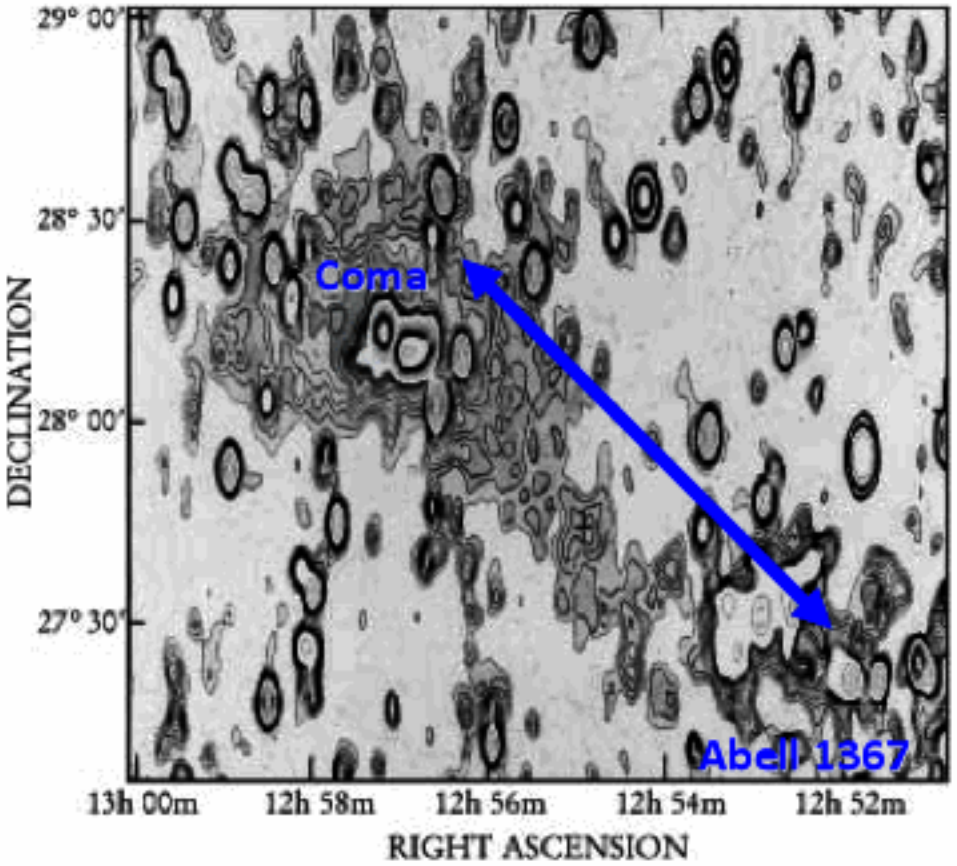

Kronberg, P. P., Phys. Today, 55-12, 40 (2002)

The Coma cluster of galaxies and its vicinity, imaged in synchrotron radiation at 326 MHz with the Westerbork Synthesis Radio Telescope in the Netherlands.

The extensions (left and lower right) strongly hint at a substantial magnetic field of at least 100 nG well beyond the Coma cluster.

$$\text{Projected distance: } \sim 1.5 \times h_{75}^{-1}\text{Mpc}$$
$$\text{3D distance: } \sim 40 \times h_{75}^{-1}\text{Mpc}$$
$$\text{Inferred B: } \sim 0.2 - 0.6\mu\text{G}$$

This region of sky contains part of the "Great Wall"--a roughly linear concentration of galaxies that stretches across the cosmos for perhaps 300 Mpc. The Coma cluster is, in fact, the largest concentration of galaxies on the Great Wall.

Magnetic fields in supercluster scales: possible scenarios for IGMF injection

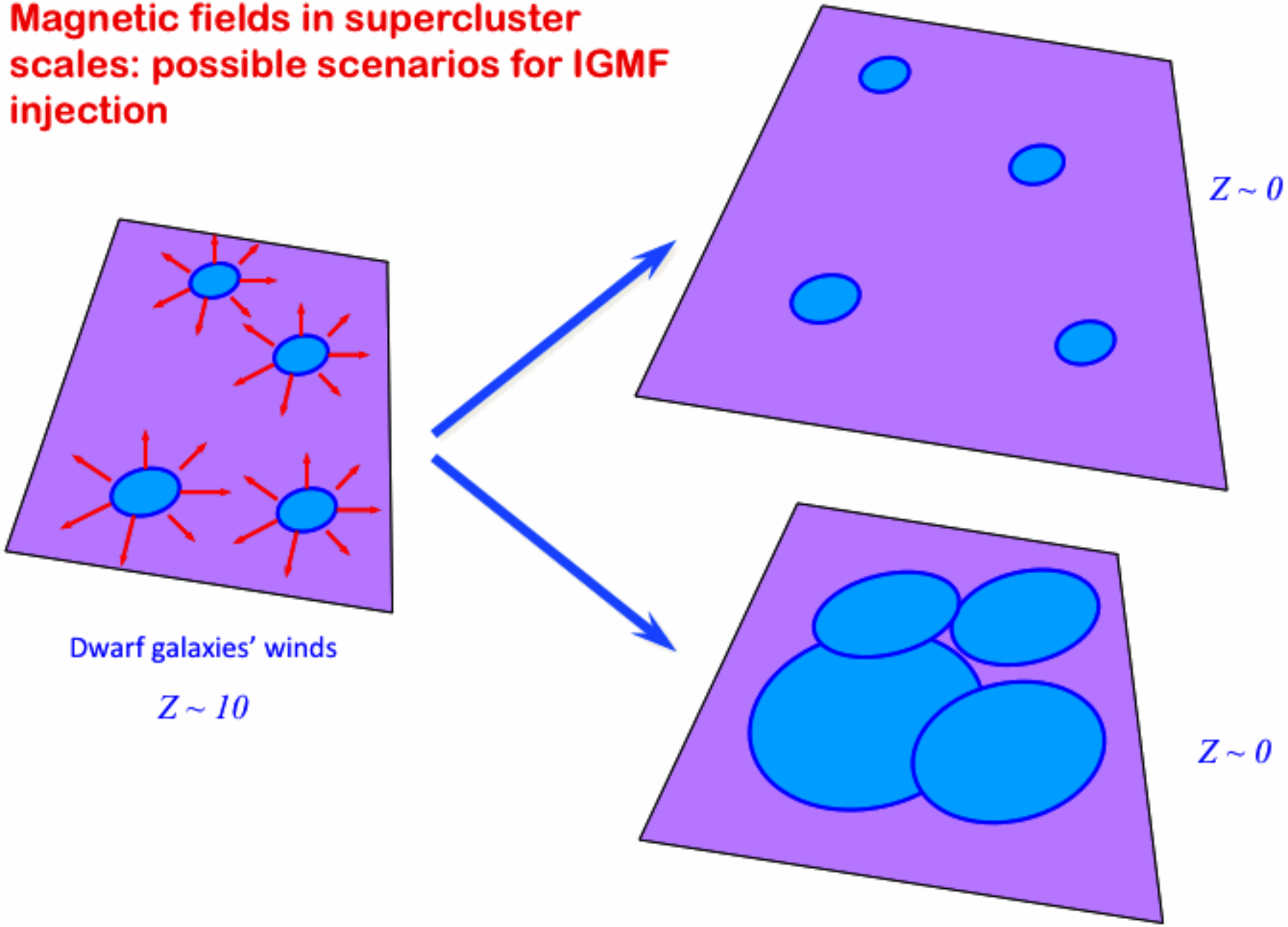

G. Medina Tanco - gmtanco@nucleares.unam.mx

IGMF filling factor is uncertain…

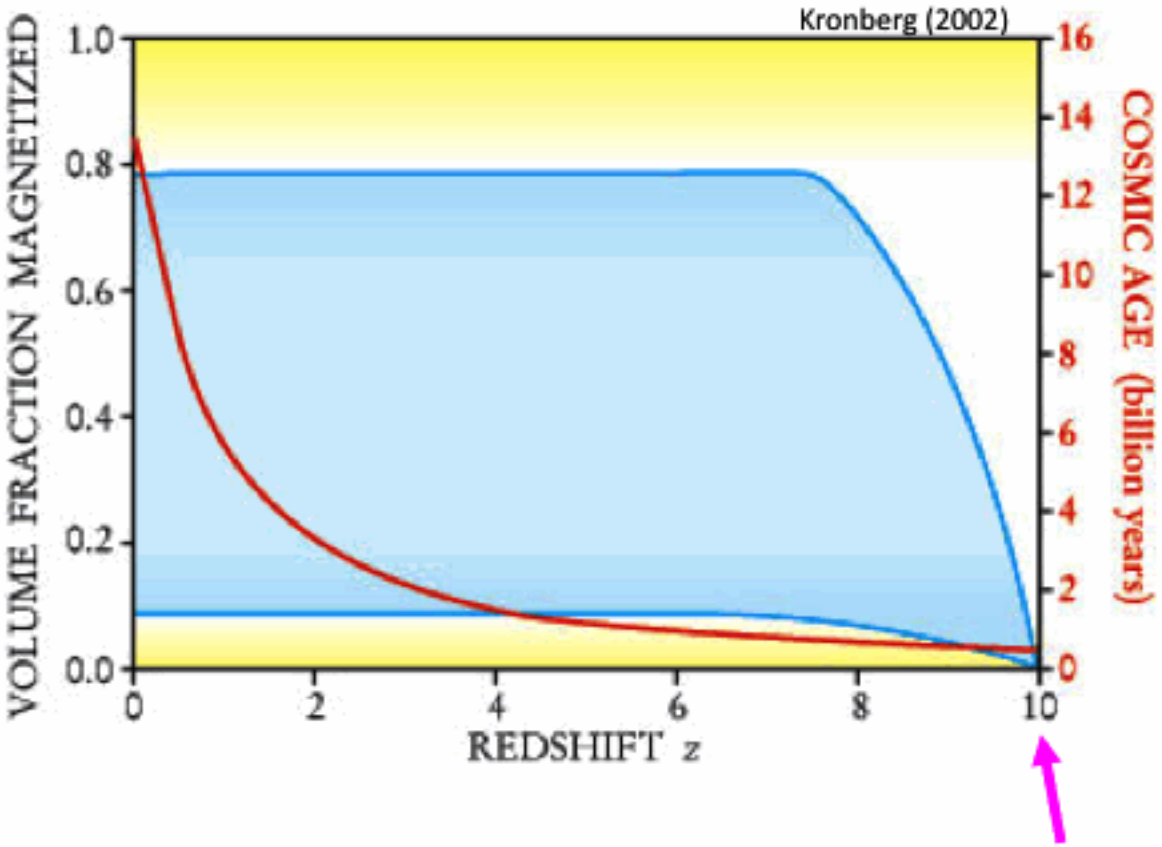

the filling is assumed to begin with primeval dwarf galaxies at redshift 10

IGMF large scale structure

LAMINAR STRUCTURE

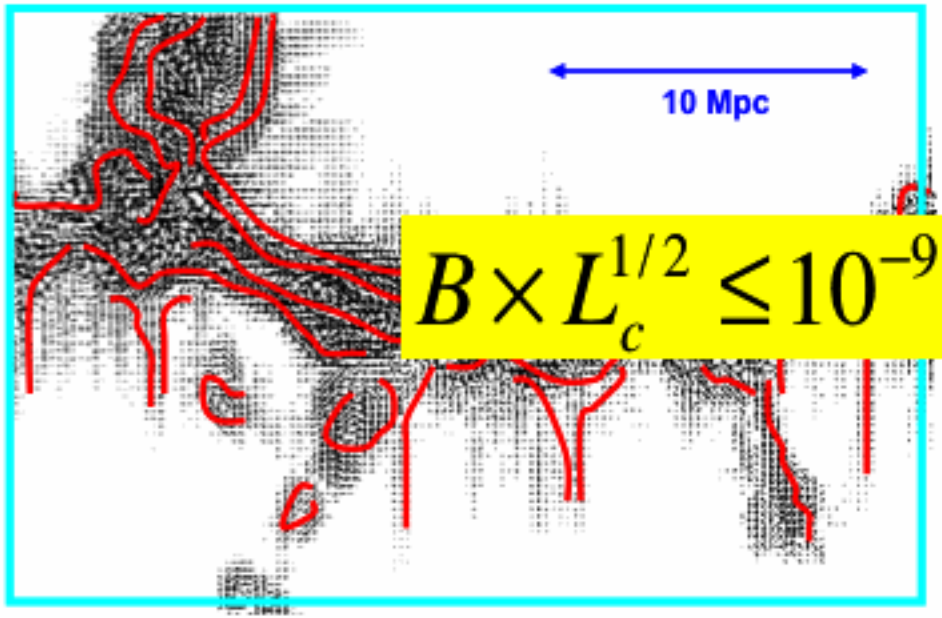

CELLULAR STRUCTURE

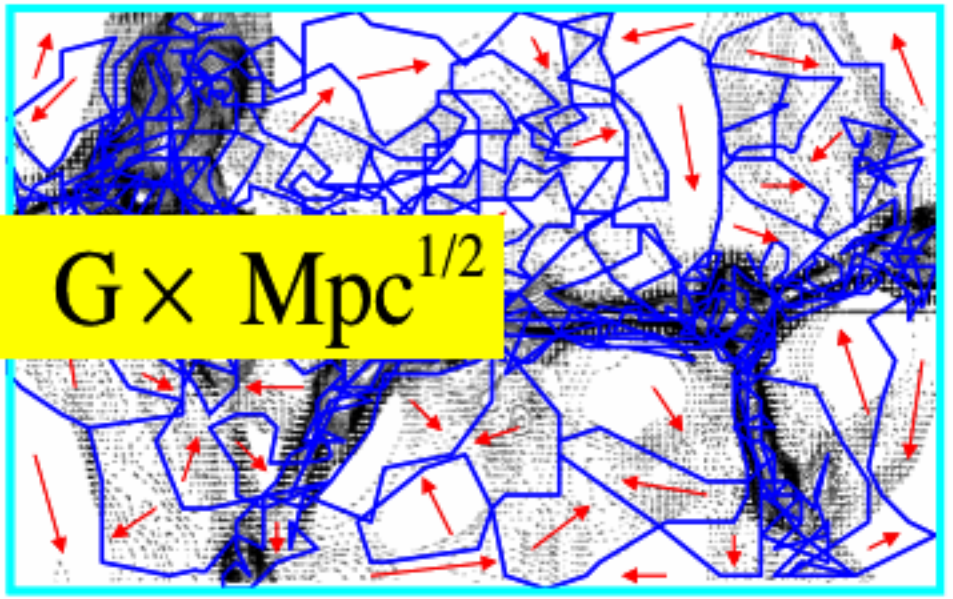

$$B \times L_c^{1/2} \leq 10^{-9} \ \mathrm{G} \times \mathrm{Mpc}^{1/2}$$

Numerical simulations in the background:
Ryu, Kahn & Biermann (1998)

IGMF large scale structure & propagation

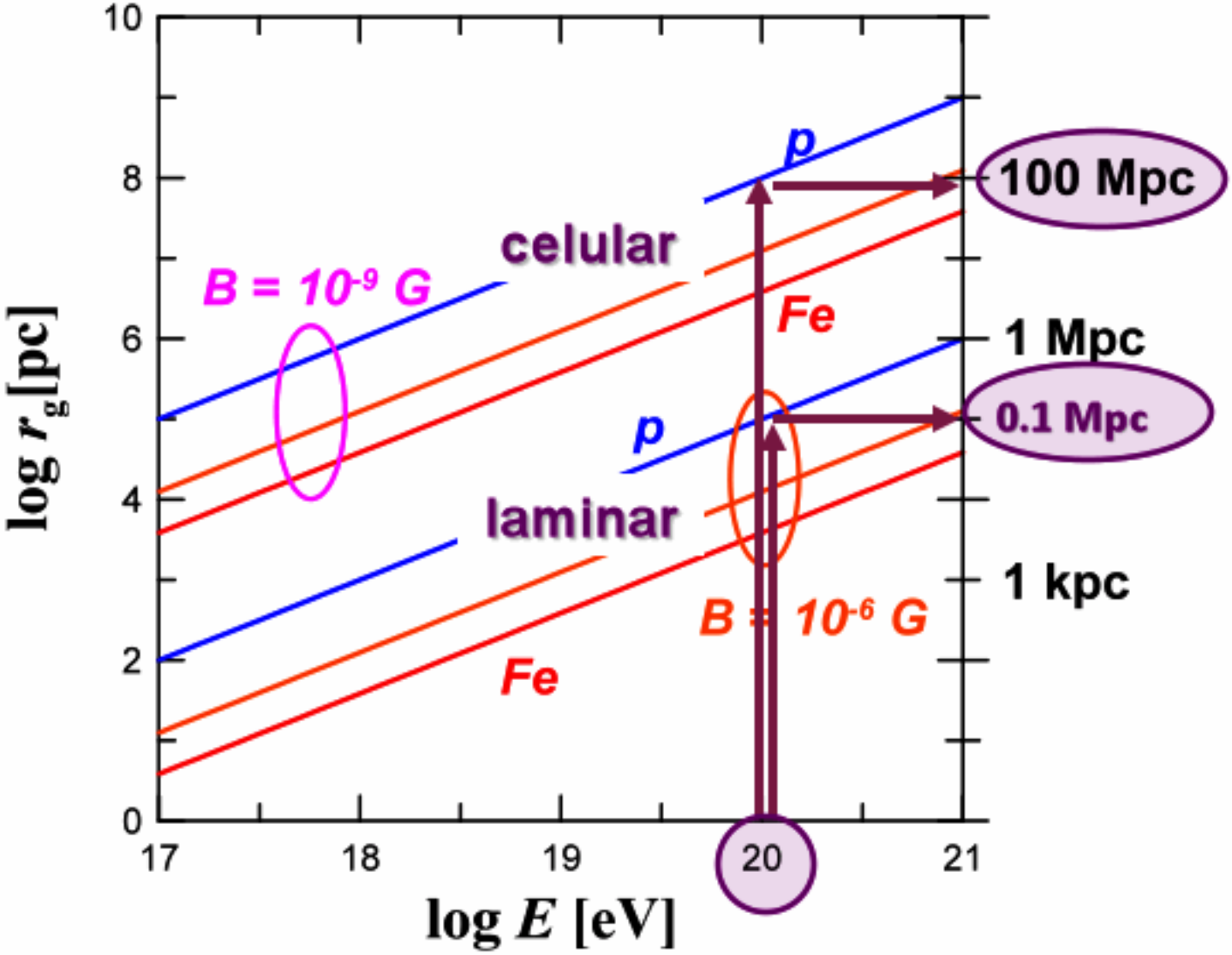

Laminar structure & propagation

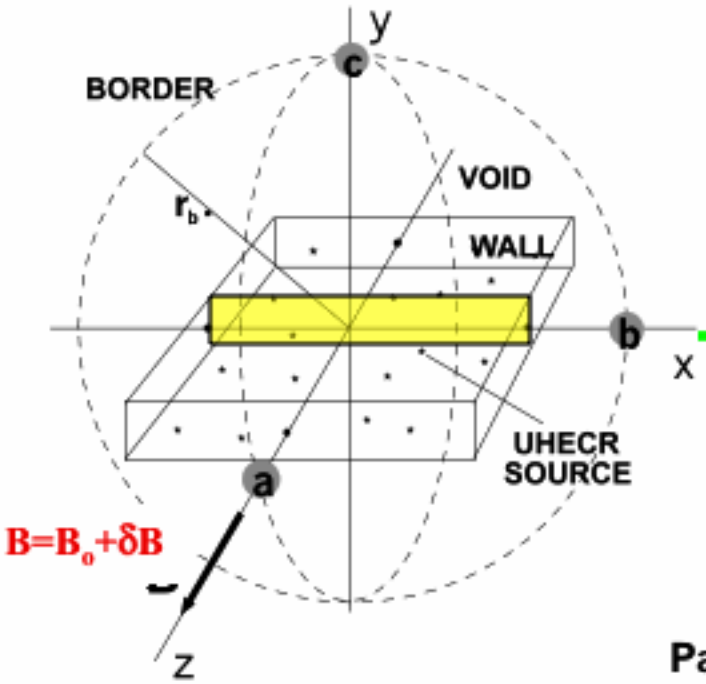

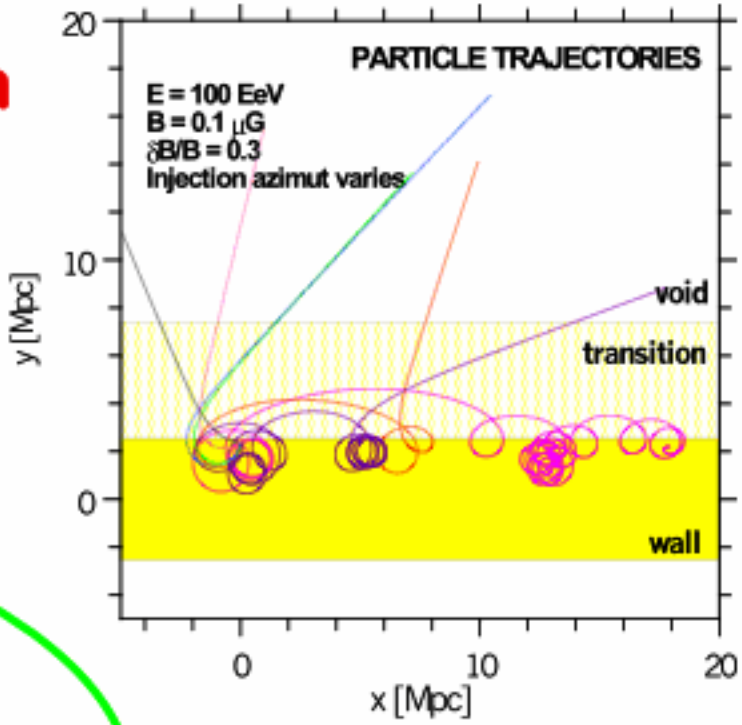

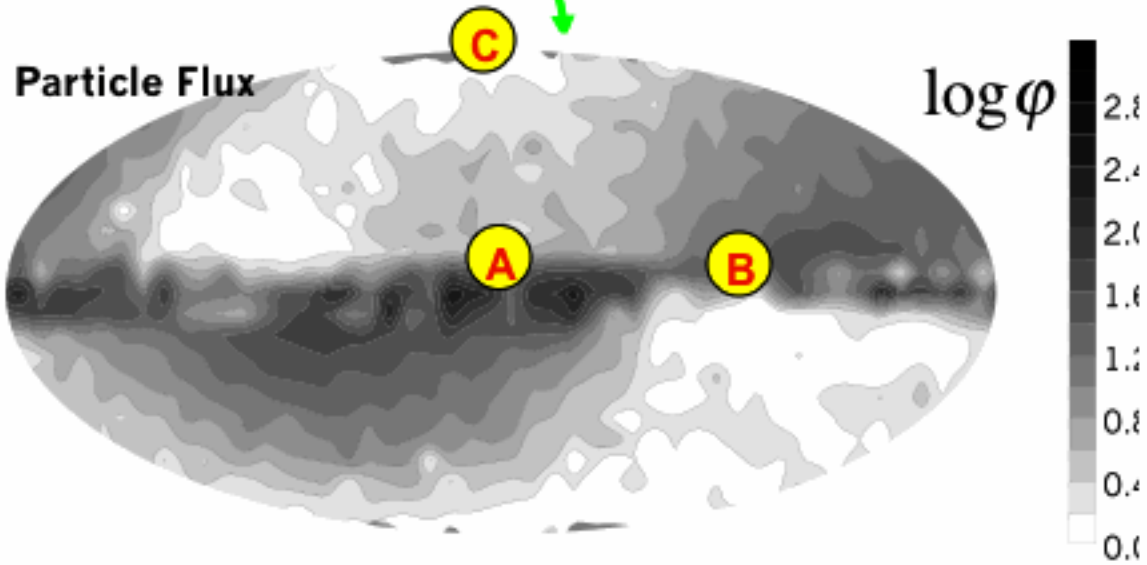

Aitoff projection of the logarithm of tl
UHECR flux over the spherical bord

G. Medina Tanco , ApJ Lett. 1999

Diffusive propagation of UHECR

Assuming Kolmogorov spectrum for IGMF: $B(k) \approx Bk^{-11/6}$ / $B@\lambda = L_c \sim 0.1 - 10\,Mpc$

Larmor radius:

$$R_L \cong 110 \frac{E_{20}/Z}{B_{\mu G}}\ kpc$$

Two diffusion regimes:

$R_L << \lambda$ ➔ Kolmogorov
$R_L \sim \lambda$ ➔ Bohm

$$R_L \ll \lambda \Rightarrow \frac{E}{Z} < 10^{21} B_{\mu G} \lambda_{Mpc}\ eV$$

$$E_{Max}^{diff} \sim 100\,EeV \Rightarrow B_{\mu G}\lambda_{Mpc} > \frac{0.1}{Z}$$

$$D(E) \approx 0.25 \left(\frac{E_{20}\lambda_{Mpc}^2}{B_{\mu G}} \right)^{1/3}\ Mpc^2/Myr$$ Kolmogorov

$$D(E) \approx 3R_L c \approx 0.1 \left(\frac{E_{20}}{B_{\mu G}} \right) Mpc^2/Myr$$ Bohm

Therefore, either approximation can be used at the current level of uncertainty at the highest energies

Diffusive propagation of UHECR

$$n(r,t) = \frac{n_0}{(8\pi Dt)^{3/2}} e^{-r^2/[4D(E,B)t]}$$

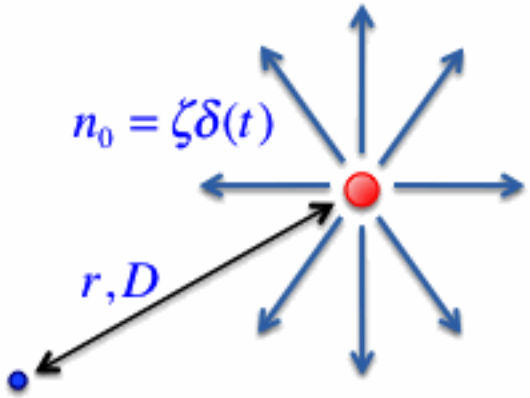

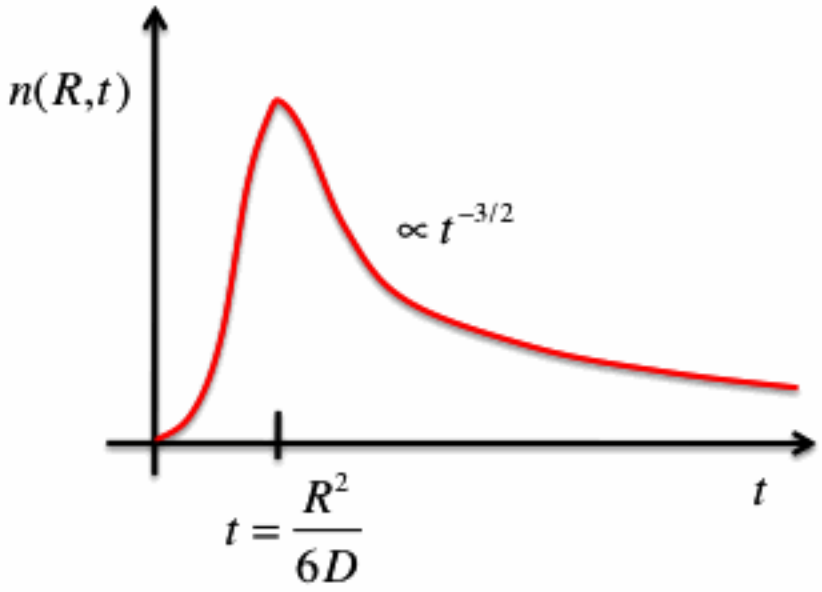

Diffusion front arrival

Since *D=D(E) (monotonically increasing)*, the diffusion front arrives first at the highest energies.

If there is a dominant source, in order to avoid unobserved structure in the spectrum, the diffusion front must have arrived already for all observed extragalactic energies (3-100 EeV)

Diffusive propagation of UHECR

Since D=D(E), the diffusion front arrives first at the highest energies and later at lower energies.
If there is a dominant source, in order to avoid unobserved structure in the spectrum, the diffusion front must have arrived already for all observed extragalactic energies (3-100 EeV)

Cen A (R~4 Mpc) : $$\tau_{CenA}^{UHECR} > 33\left(\frac{B_{\mu G}Z}{\lambda_{Mpc}^2}\right)^{1/3} Myr$$

M87 (R~15 Mpc) : $$\tau_{M87}^{UHECR} > 470\left(\frac{B_{\mu G}Z}{\lambda_{Mpc}^2}\right)^{1/3} Myr$$

Shapley (R~50 Mpc) : $$\tau_{Shapley}^{UHECR} > 5\left(\frac{B_{\mu G}Z}{\lambda_{Mpc}^2}\right)^{1/3} Gyr$$

This is valid only if one specie of nucleus is accelerated at the source. If the mechanism works at constant rigidity, then (to first order) all nuclei arrive at the same time for E/Z which, for a composition running from p to Fe, covers the whole energy spectrum. The times above (particularized for Z=1) give directly the arrival time for all nuclei.

Diffusive propagation of UHECR: anisotropy

The flux at a distance *r* is:

$$f(\theta,r,t) = \left(1+\alpha\cos\theta\right)\frac{n(r,t)c}{4\pi}$$

$$\alpha = \frac{D(E,B)}{fc}\frac{df}{dr} = \frac{r}{2tc}$$

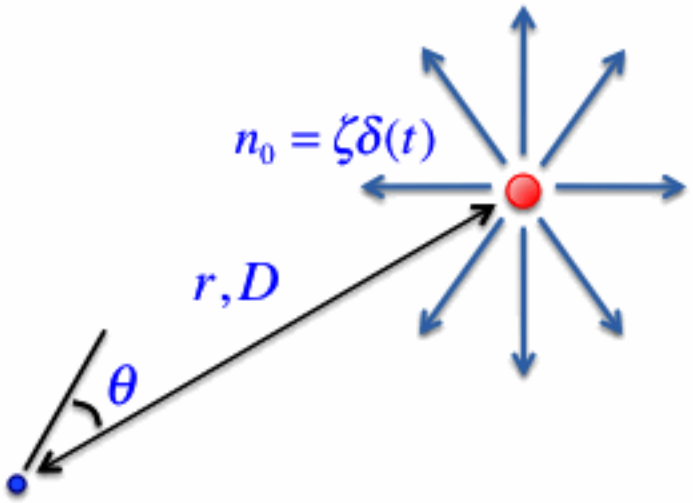

Therefore, as long as the propagation is diffusive, the emission is isotropic and *D* is spatially uniform, the anisotropy α does not depend on *D* (i.e., neither *E* nor *B*).

Diffusive propagation of UHECR: spectrum

$$n_0(t) = n_0 \times \left[H(t - t_{on}) - H(t - t_{off}) \right]$$

$$n(r,t) \approx \frac{2\dot{n}_0}{\left[8\pi D(E,B)\right]^{3/2}} \left(t_{\min}^{-1/2} - t_{\max}^{-1/2} \right)$$

$$\left.\begin{array}{l} D \propto E^{\beta} \\ n_0 \propto E^{-p} \end{array}\right\} \Rightarrow \quad n \propto E^{-\left(p + \frac{3}{2}\beta\right)}$$

$$t_{\min} = Max\left\{ \frac{R^2}{3D}, t_{off} \right\}$$

$$t_{\max} = Min\left\{ \tau_{GZK}, t_{on} \right\} \quad / \quad \tau_{GZK}(10^{20.5} eV) \sim 50\, Myr$$

If the diffusion regime is Kolmogorov
And shocks are involved $(p \tilde{>} 2)$

$$\left.\begin{array}{l} D \propto E^{1/3} \\ n_0 \propto E^{-2.2} \end{array}\right\} \Rightarrow \quad n \propto E^{-2.7}$$

Cellular structure & propagation

CELLULAR STRUCTURE:

The IGMF must be scaled with density in order to do modeling.

Is there a general scaling?
If so: How to scale?

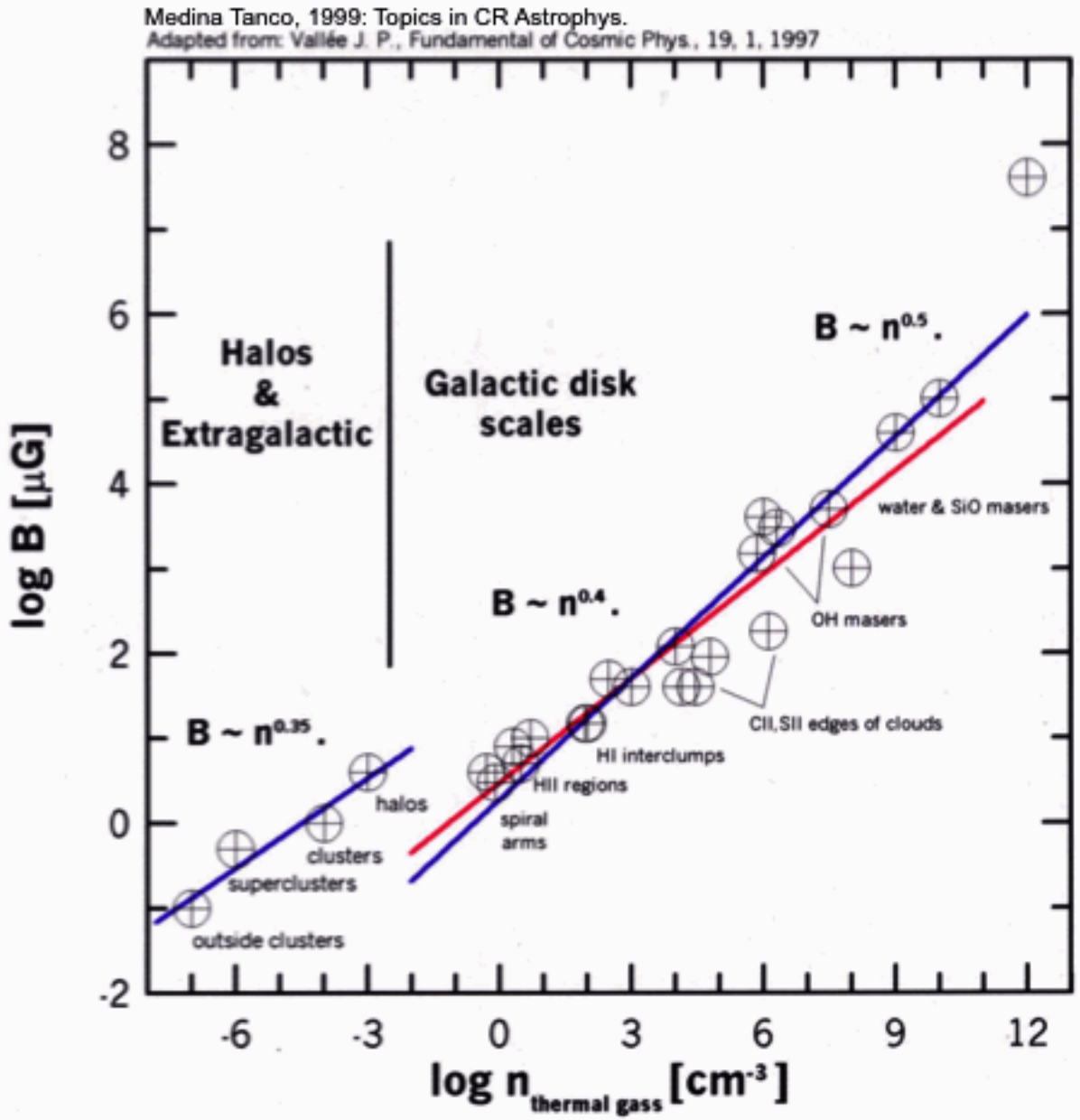

Cellular structure & propagation

$E > 4 \times 10^{19}$ eV

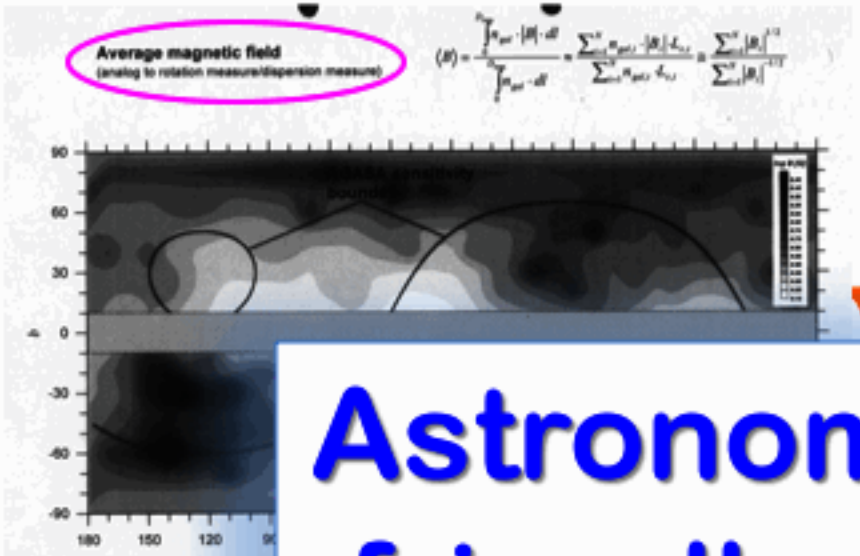

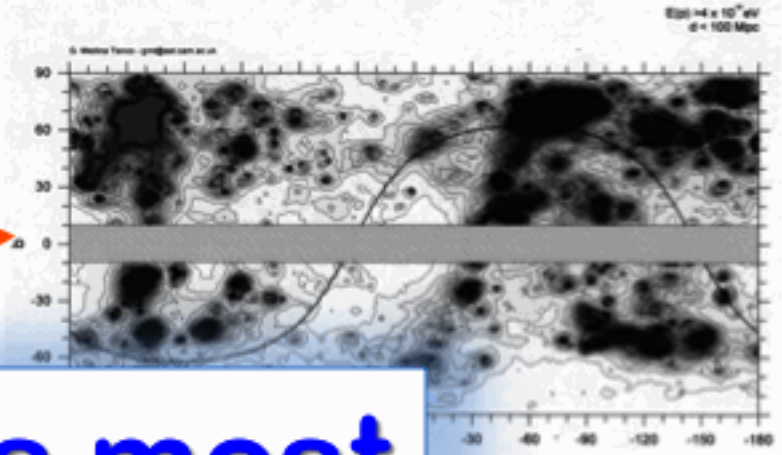

Astronomy's most friendly scenario

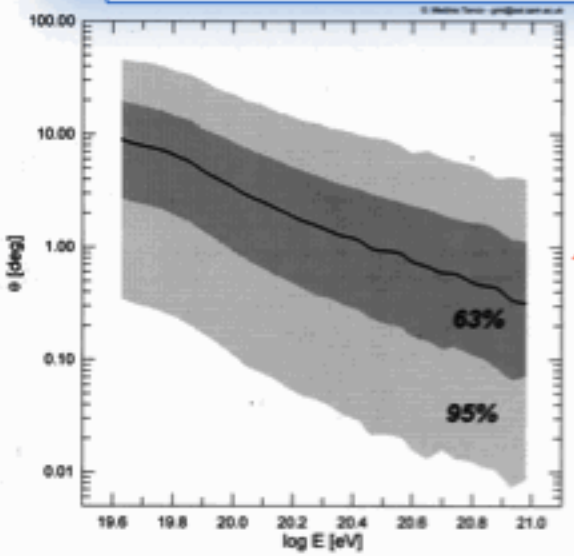

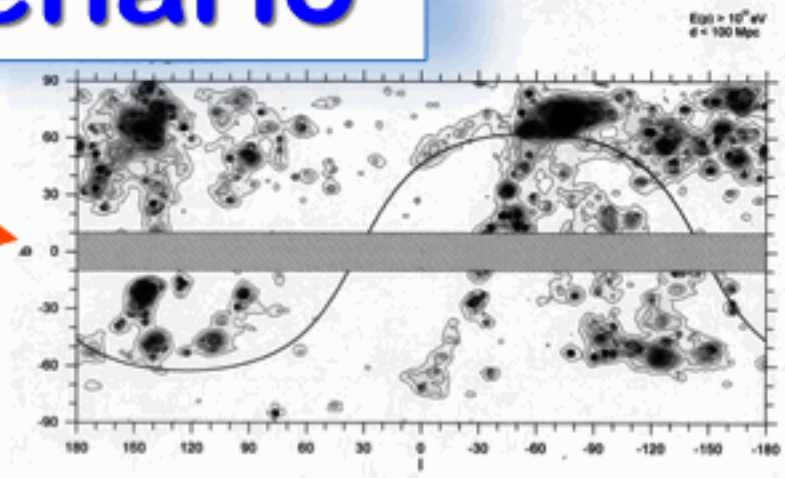

G. Medina Tanco, 1999,2001

Scattering intergalactic medium

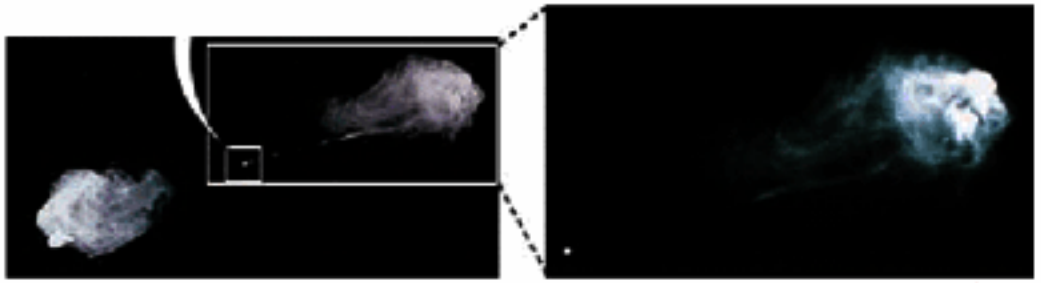

ISOTROPIZATION OF UHECR FLUX DUE TO SCATTERING BY RADIO-GHOSTS

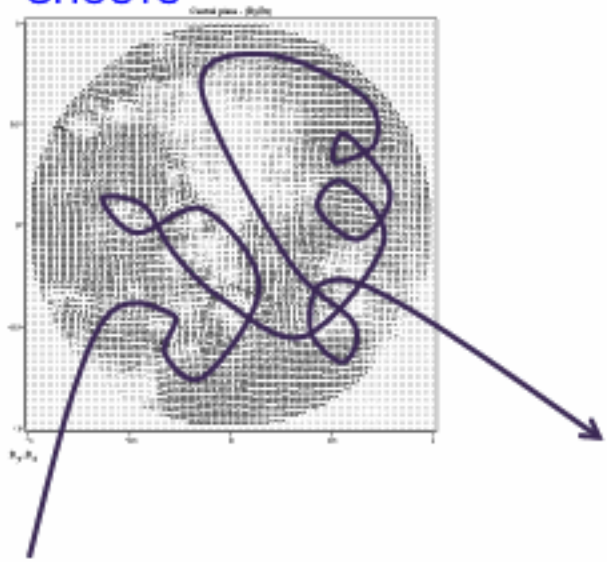

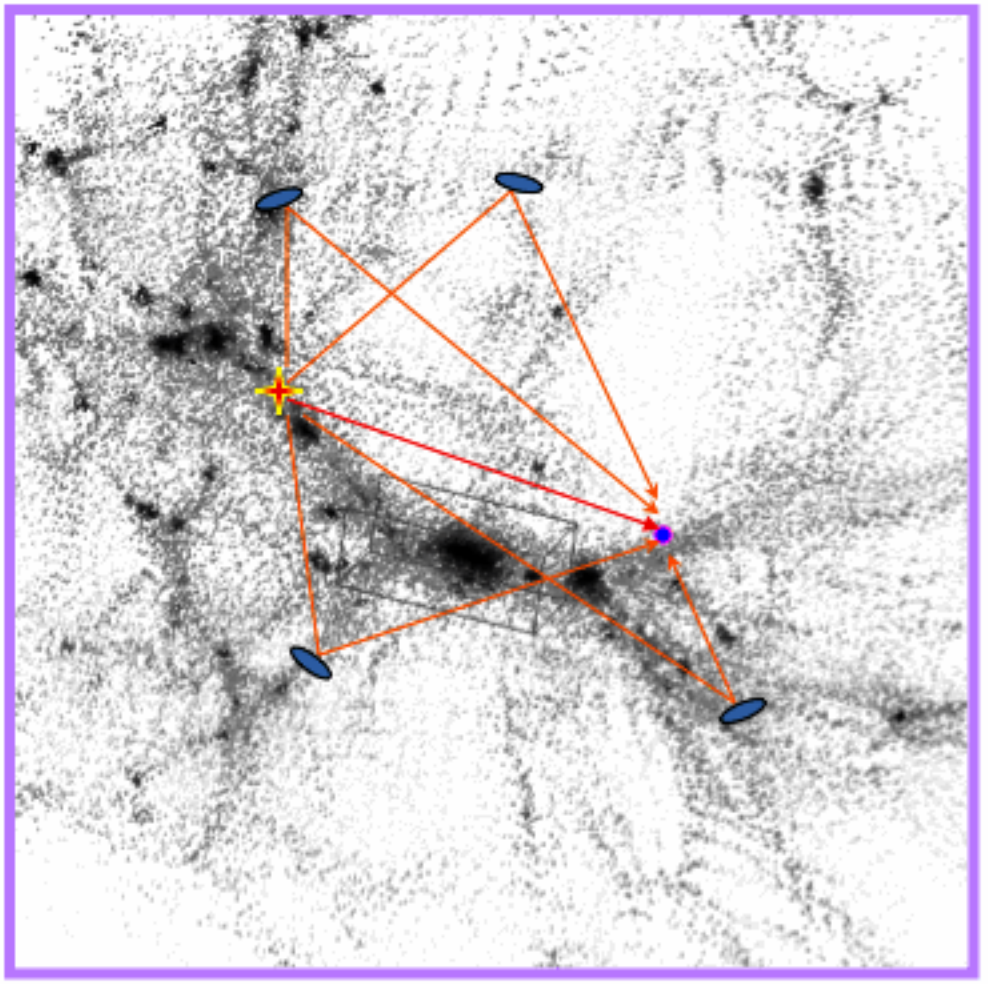

Medina-Tanco & Ensslin, APP, 2001

UHECR GMF propagation

The Galaxy

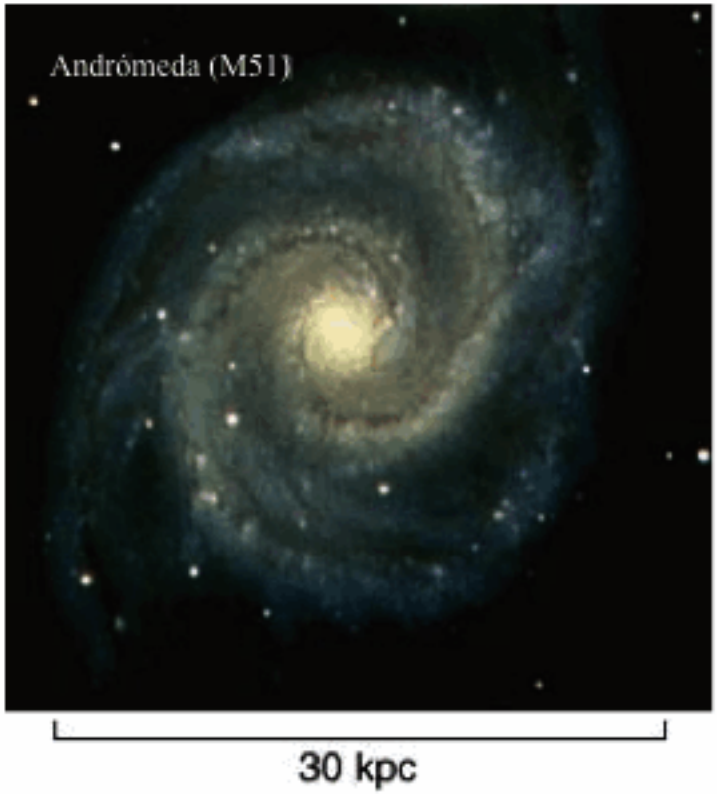

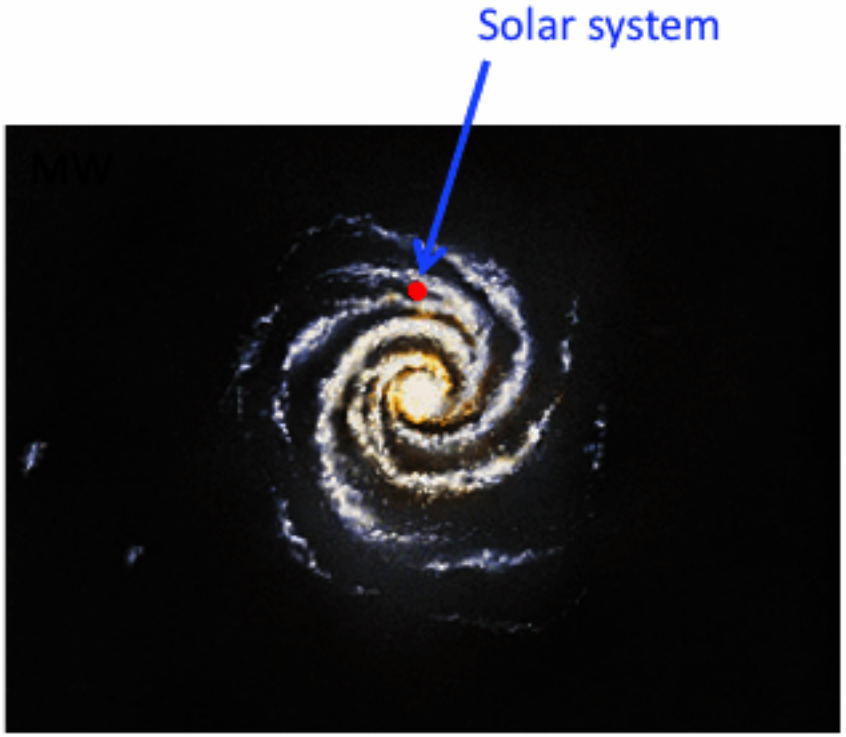

© Little green men

Structure of the Galaxy

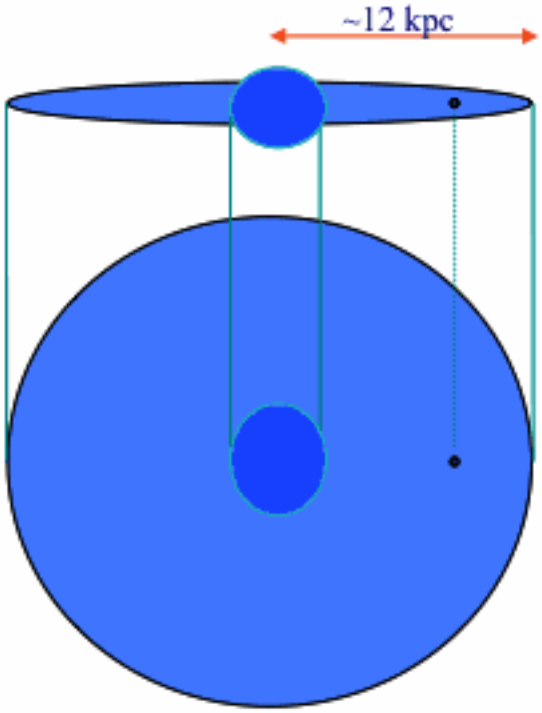

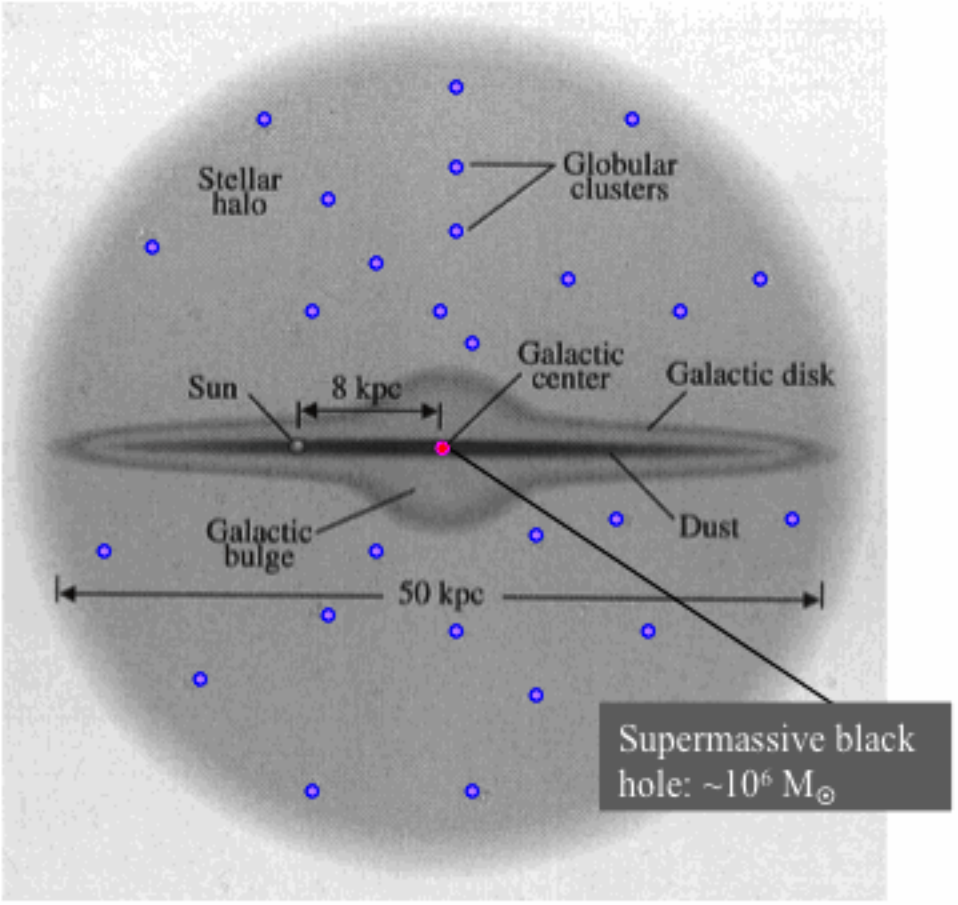

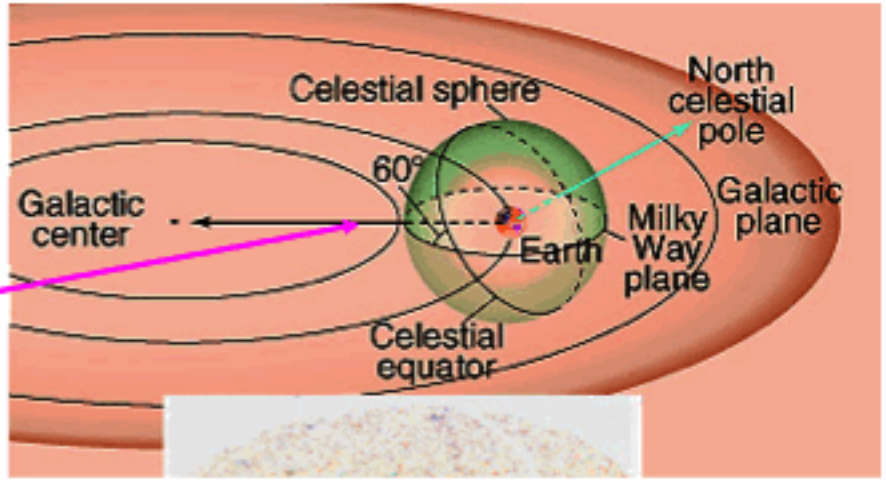

Structure and dynamics of the Galaxy

Our Galaxy has 3 basic components

Halo: stars, globular clusters, a few high velocity clouds, virtually no gas

Disk: stars, gas, molecular clouds, open clusters

Bulge: stars, dust, super-massive black hole

Different age, chemical composition and dynamics.

Halo: spherical distribution, isotropic orbits around the Galactic center, red stars, virtually no gas.

Old stars (the oldest in the Galaxy).

Old structure, remnant of the first steps of Galaxy formation.

Disk: flattened distribution, abundant gas, blue stars, *spiral structure*.

Both young and old stars.

R~15 kpc, Δz~300 pc (aspect ratio: ~1/100)

Bulge: spheroidal distribution, high gas density and star density (up to $n_\star \sim 5 \times 10^4$ stars/pc^3 $\sim 10^6$ n_{sun}), large amount of dust

Strong star formation ⇨ young and old stars

Smoothed gas distribution in the Galaxy

Hydrogen ISM density

$(H_1 + H_2)$

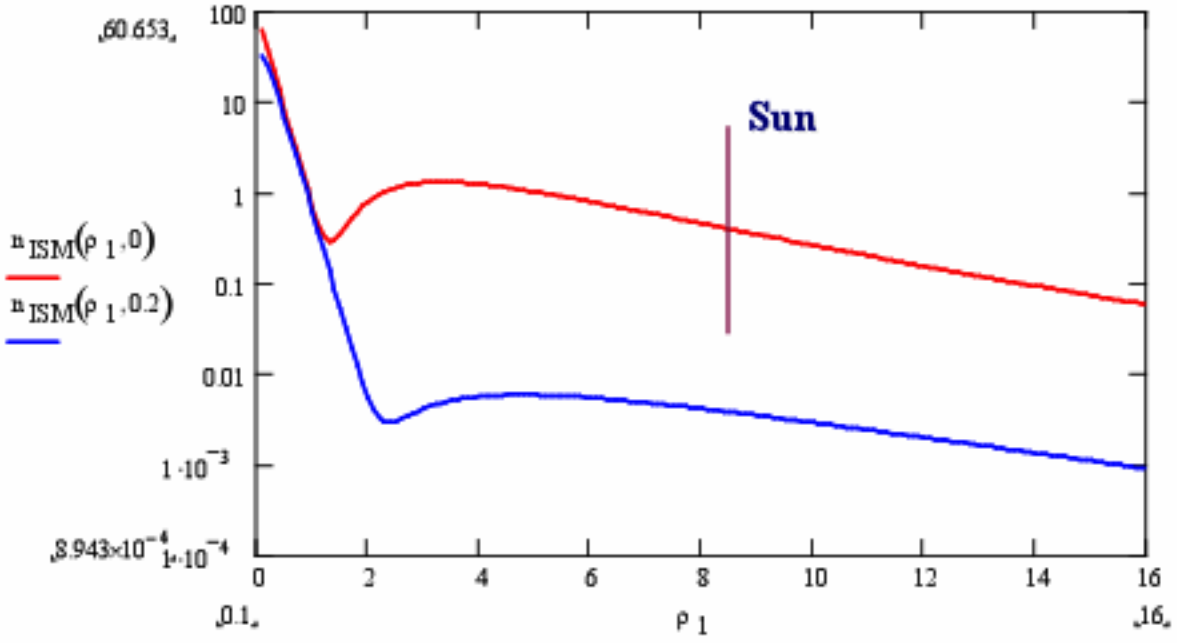

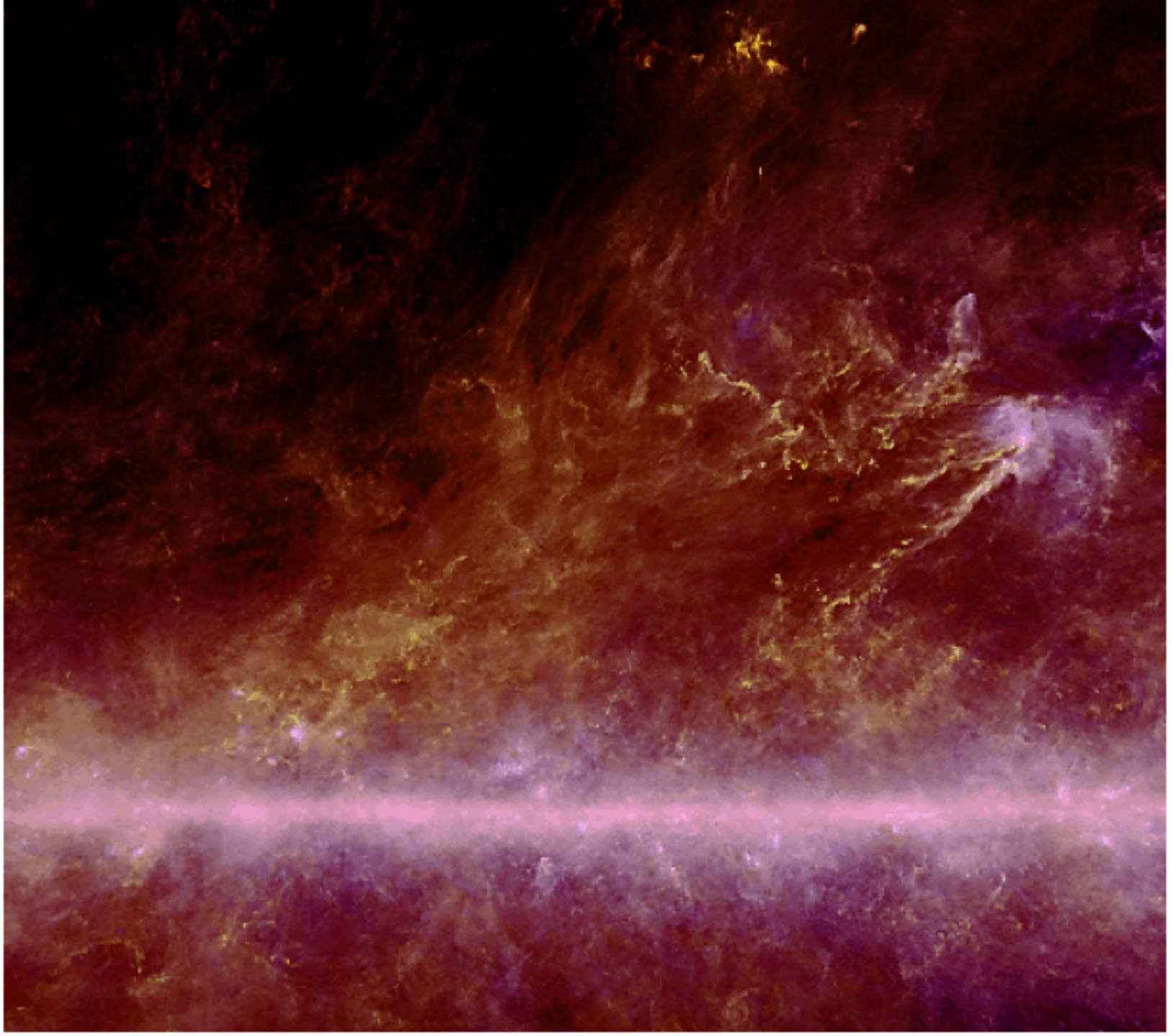

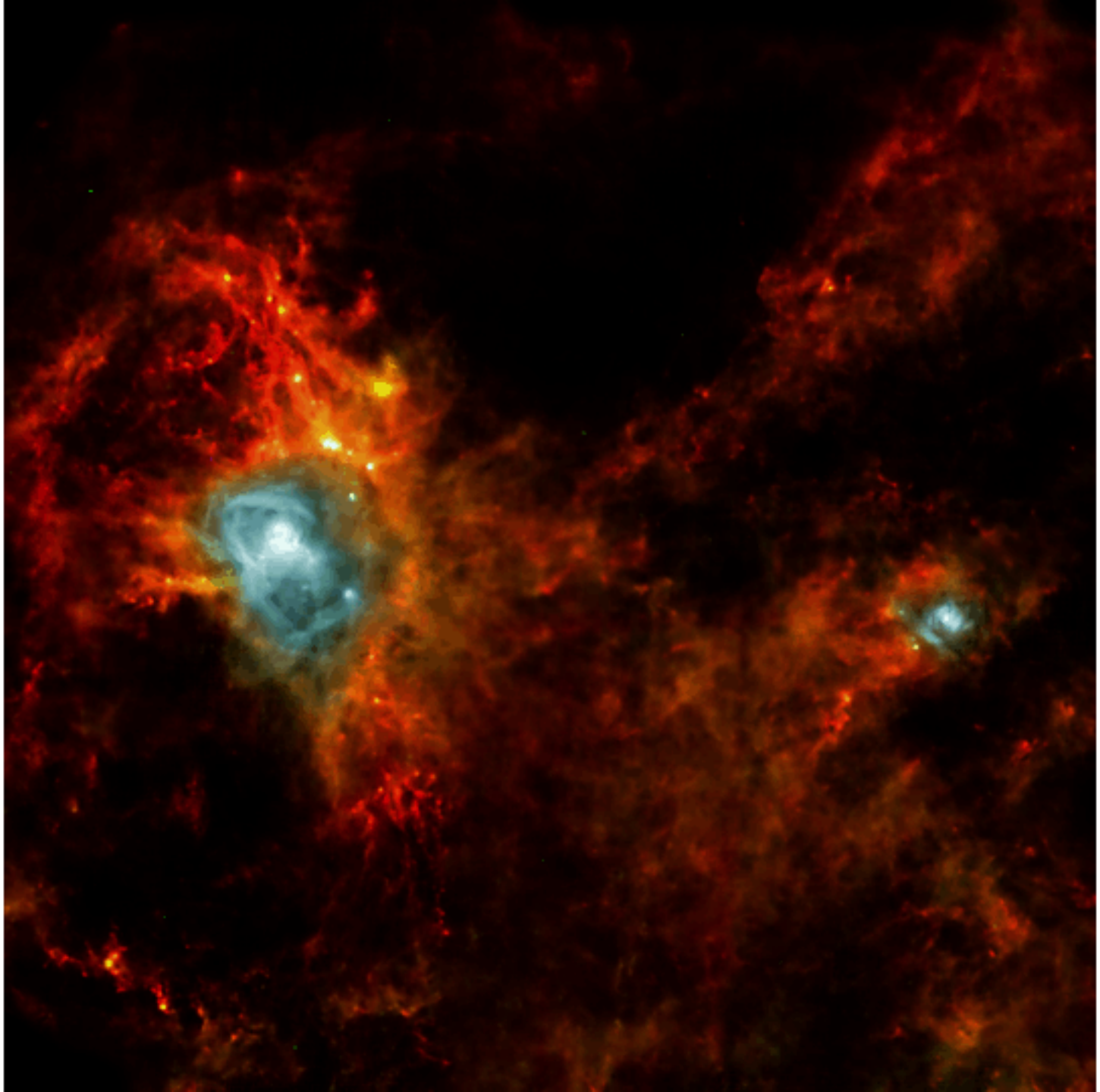

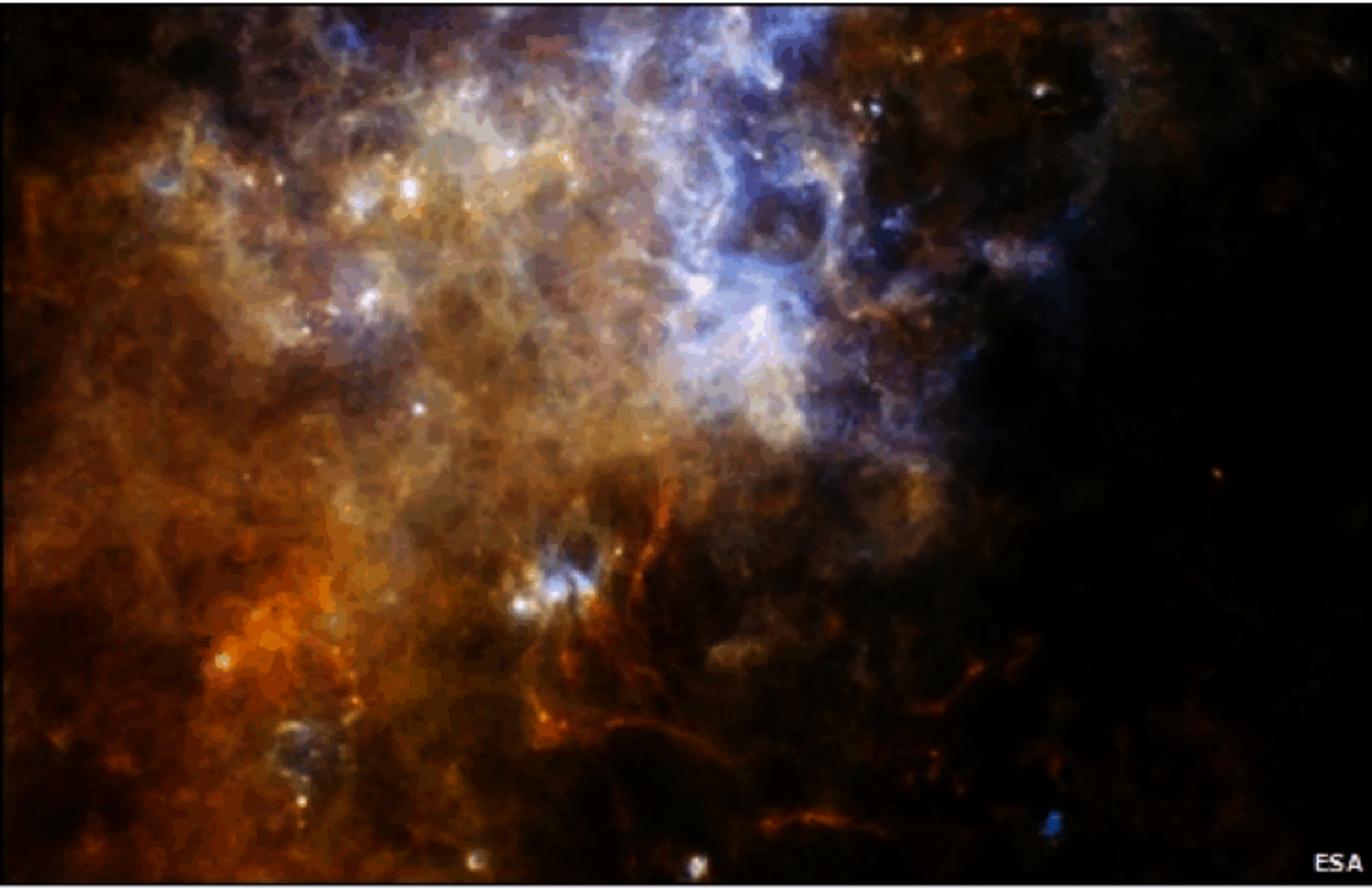
ESA

Composition of the ISM - Matter

- Interstellar Clouds
  $0.011 M_{\odot}/pc^3$, ~90% of ISM
  - Bright Nebulae, e.g. Orion (M42)
  - Dark Nebulae, e.g. Ophiuchus
  - HI 8 H-atoms/cm^3, 0.01 elec/cm^3
  - H_2 1 H-mol/cm^3
  - All other elements
  - HII ~8 elec/cm^3
- Interstellar Gas
  - Mean density between clouds
    0.1 H-atoms/cm^3, 0.035 elec/cm^3
- Interstellar Grains
  $0.0015 M_{\odot}/pc^3$, ~10% of ISM
  - Number density 0.5×10^{-12} cm^{-3}
  - Mass density ~1g/cm^3

Stanley D. Hunter

Local ISM structure

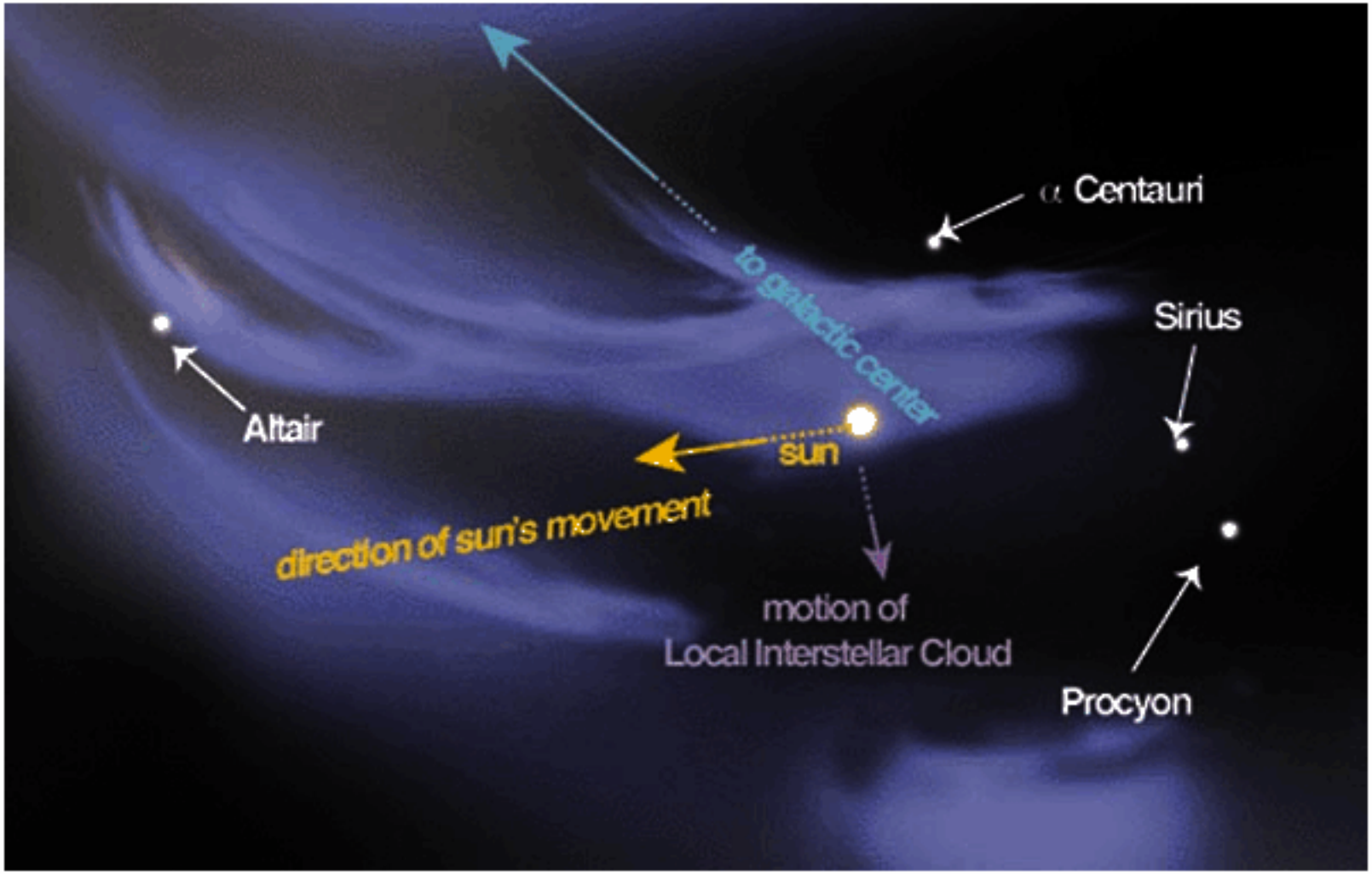

Combined observations of the Prototypical spiral galaxy M51 with the interferometric radio telescope Very Large Array (VLA) near Socorro (New Mexico/ USA) and with the 100m single disk radio telescope near Effelsberg (Germany). The contour lines trace the total radio emission at 5 GHz (6 cm wavelength) and the vectors the polarized emission. The vectors indicate that the orientation of the regular magnetic field is spiral and mostly follows the spiral arms, as evident from the background optical image obtained by the Hubble Space Telescope. The magnetic field is strong also between the spiral arms. This was not expected from the idea that the spiral arms are density waves where gas and magnetic fields should be compressed. Instead, the magnetic field must be enhanced between the spiral arms by some other mechanism which is still not understood. Outside of the optical extent of the galaxy, little radio synchrotron emission is detected at high frequencies because the relativistic electrons, responsible for the radio emission and "illuminating" the magnetic field, cannot travel far away from the regions of their origin, supernova remnants. These are embedded into the inner disk of galaxies where the star formation rate is highest.

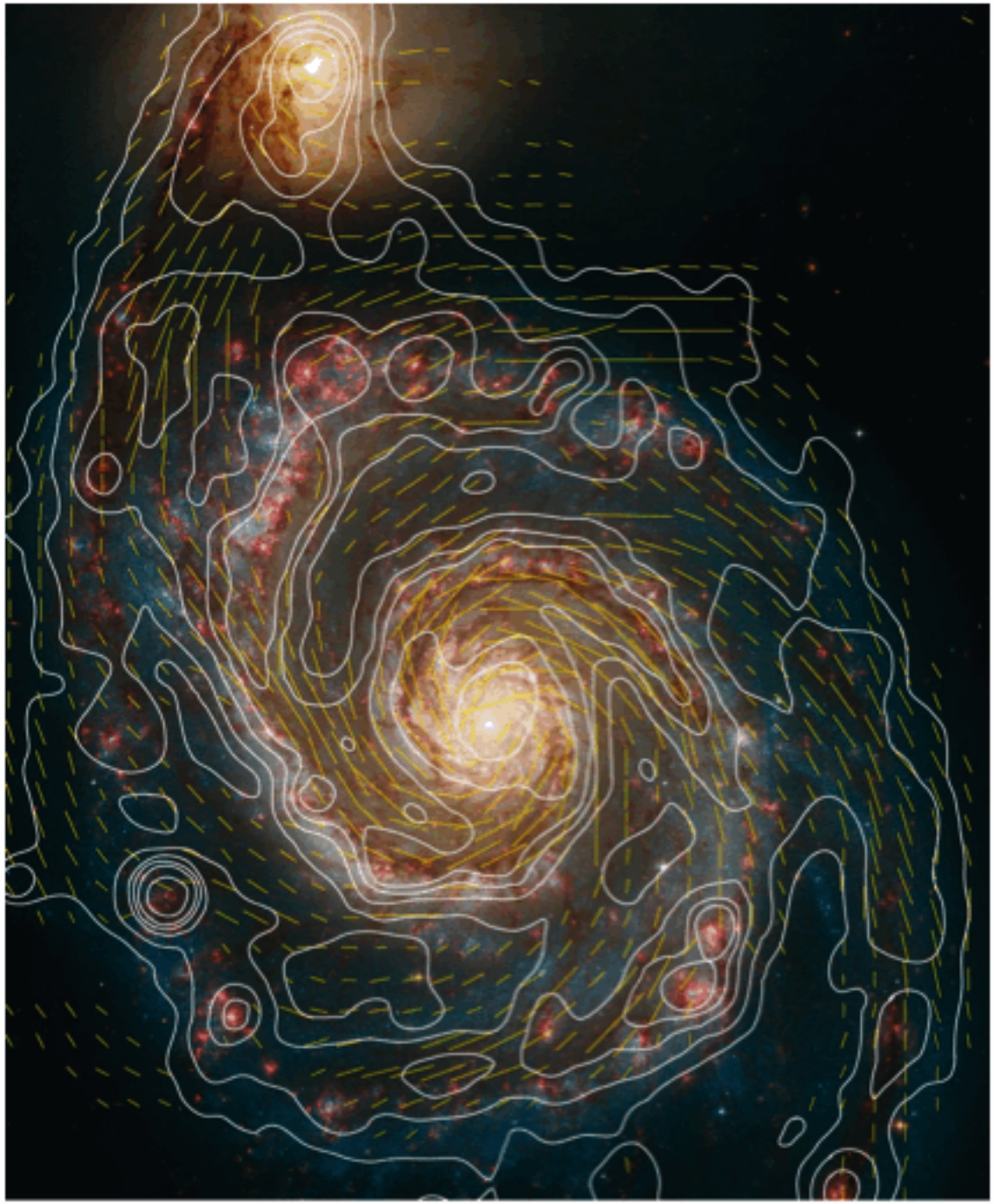

Spiral galaxy M51 (total and polarized intensity), combined from data observed with the interferometric radio telescope Very Large Array (VLA, USA) and the Effelsberg 100m single-dish radio telescope (Germany) at 5 GHz (6 cm wavelength)
Optical background image: Hubble Space Telescope (Hubble Heritage Team)
© A. Fletcher & R. Beck (MPIfR Bonn)

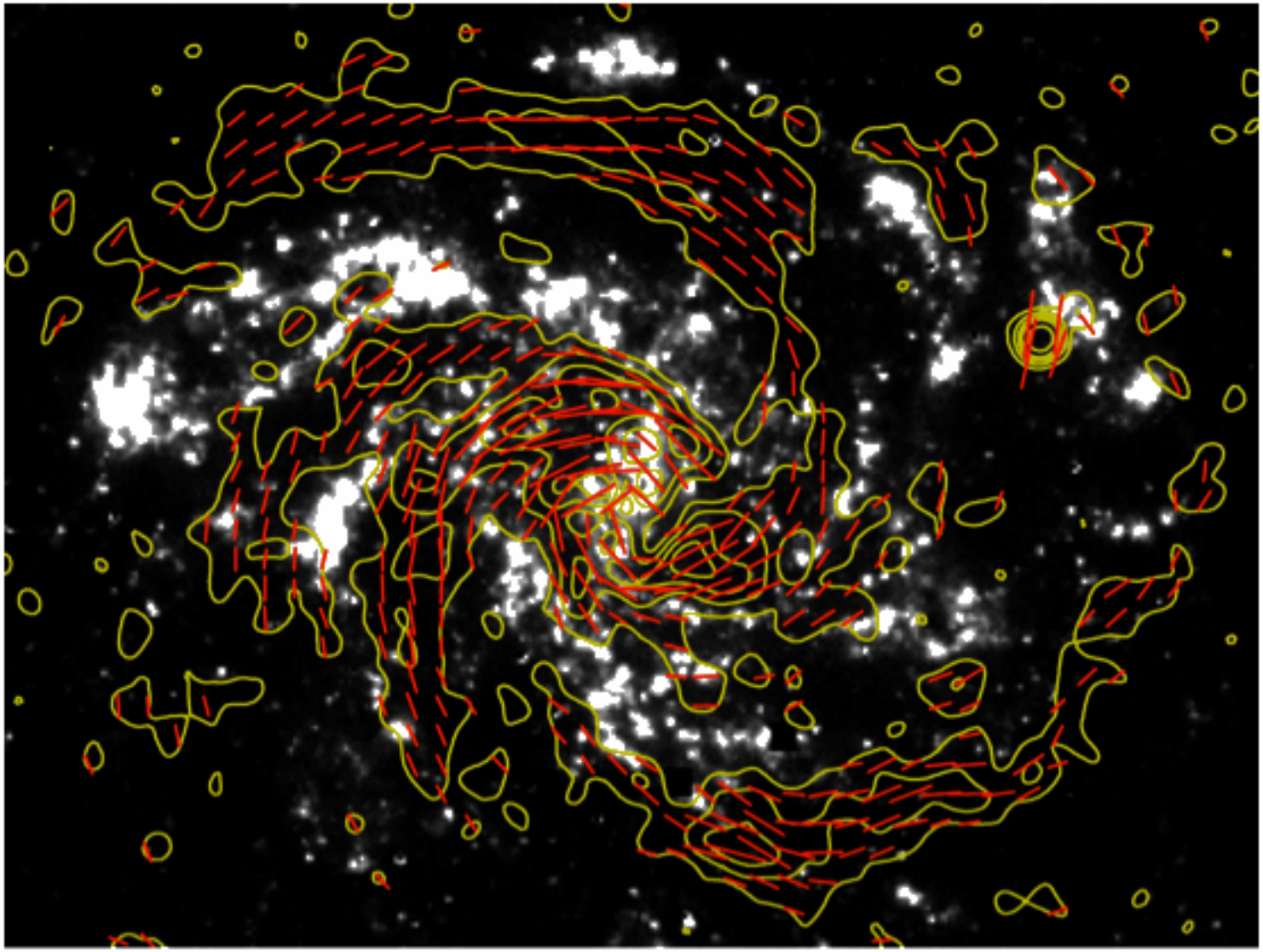

Spiral galaxy NGC 6946 (polarized intensity), combined from data observed with the VLA and the Effelsberg telescope at 5 GHz (6 cm wavelength)
© R. Beck (MPIfR Bonn)

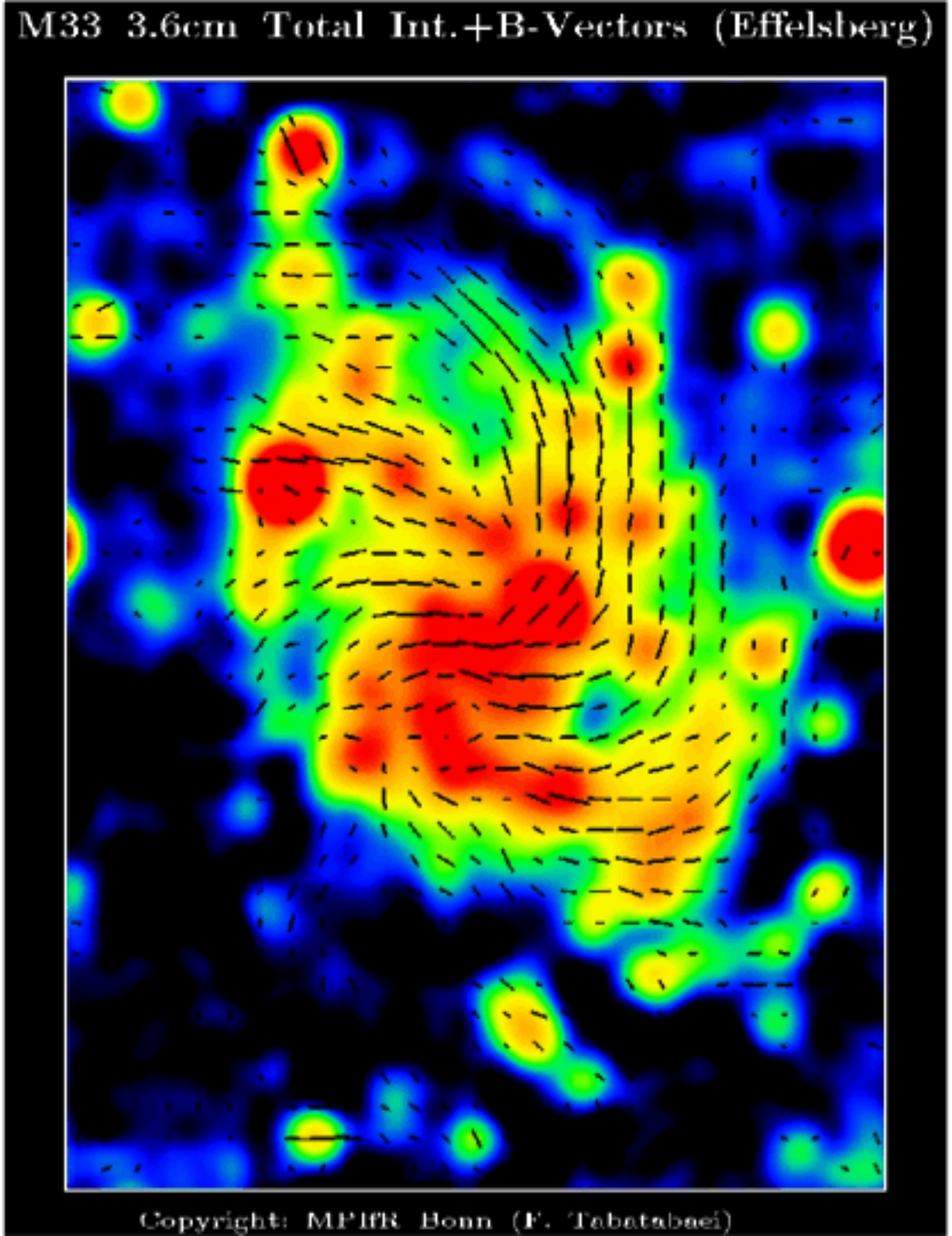

Spiral galaxy M33 (total and polarized intensity), observed with the Effelsberg telescope at 8 GHz (3.6 cm wavelength)
© F. Tabatabaei, R. Beck & M. Krause (MPIfR Bonn)

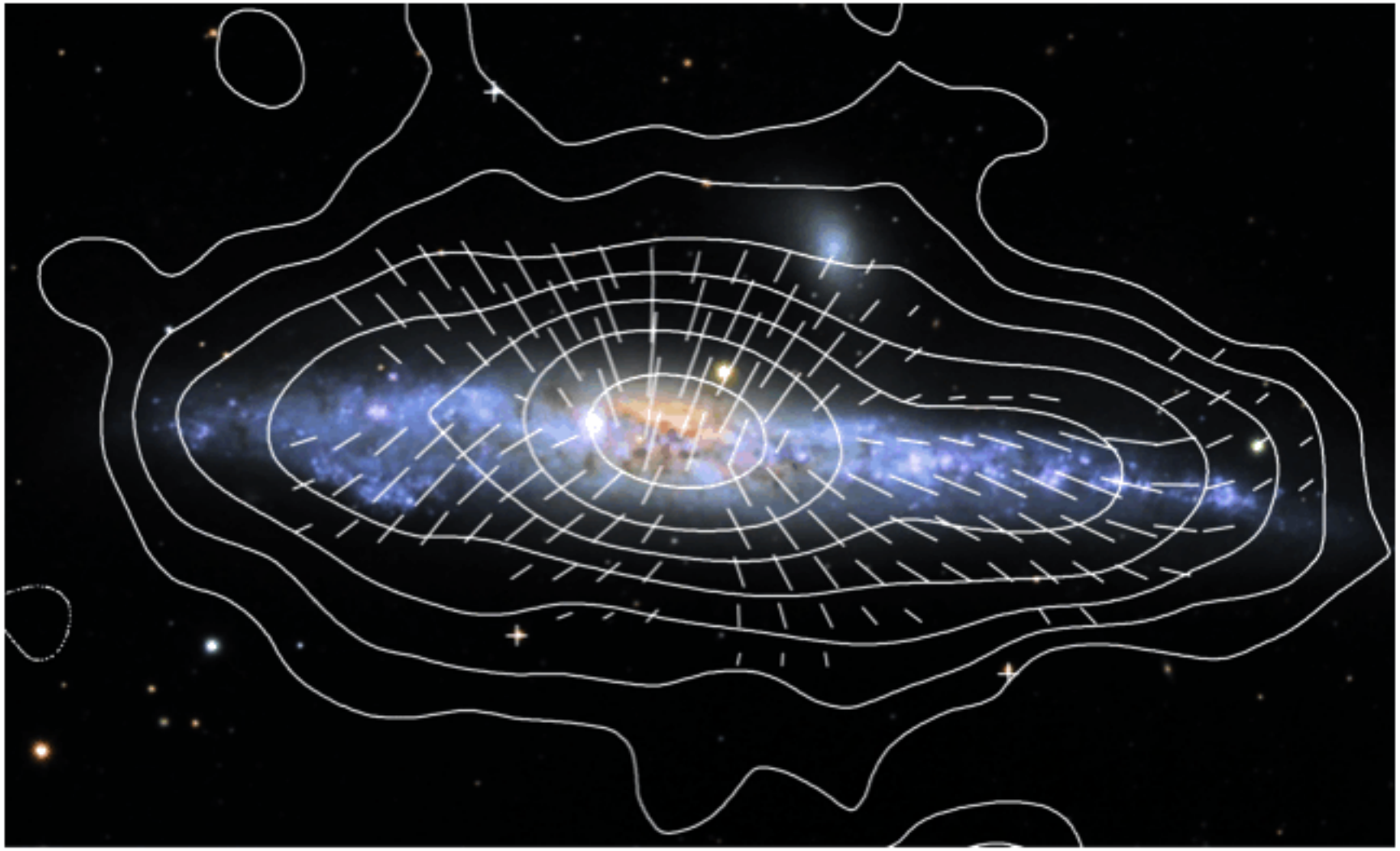

Edge-on irregular galaxy NGC 4631 (total and polarized intensity), observed with the Effelsberg telescope at 8 GHz (3.6 cm wavelength)
Optical background image: Misti Mountain Observatory
© M. Krause (MPIfR Bonn)

For the few cases in which the radio synchrotron emission at high frequencies is not restricted to the optical extent the emission is related to interactions between galaxies.

For example, huge radio lobes were discovered on two sides of the galaxy NGC 4569 which is located in the dense Virgo cluster of galaxies where interactions are frequent.

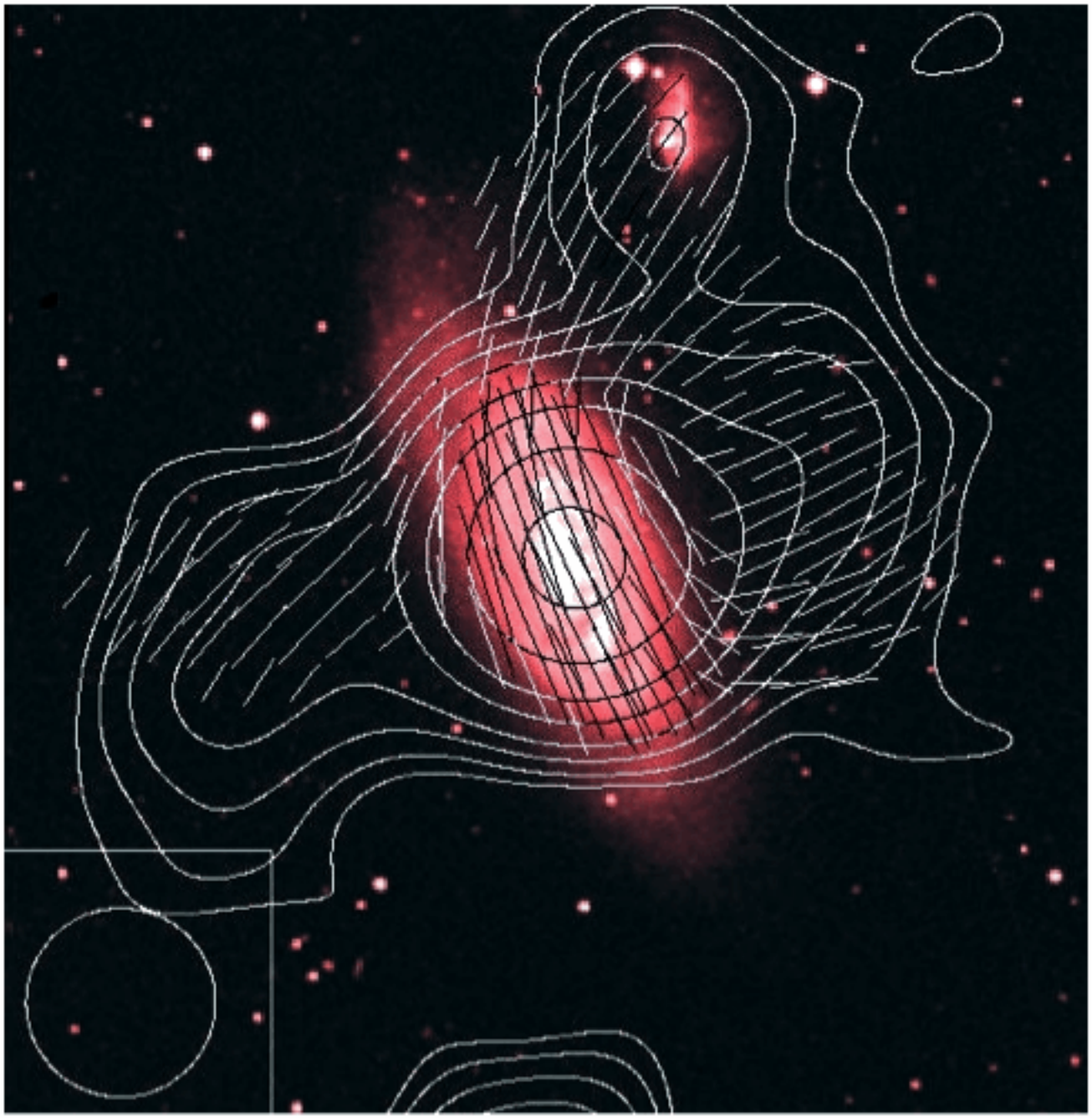

Interacting galaxy NGC 4569 in the Virgo Cluster (total and polarized intensity), observed with the Effelsberg telescope at 5 GHz (6 cm wavelength)
© C. Chyzy (Jagiellonian Univ. Kraków)

Magnetic fields in other spiral galaxies

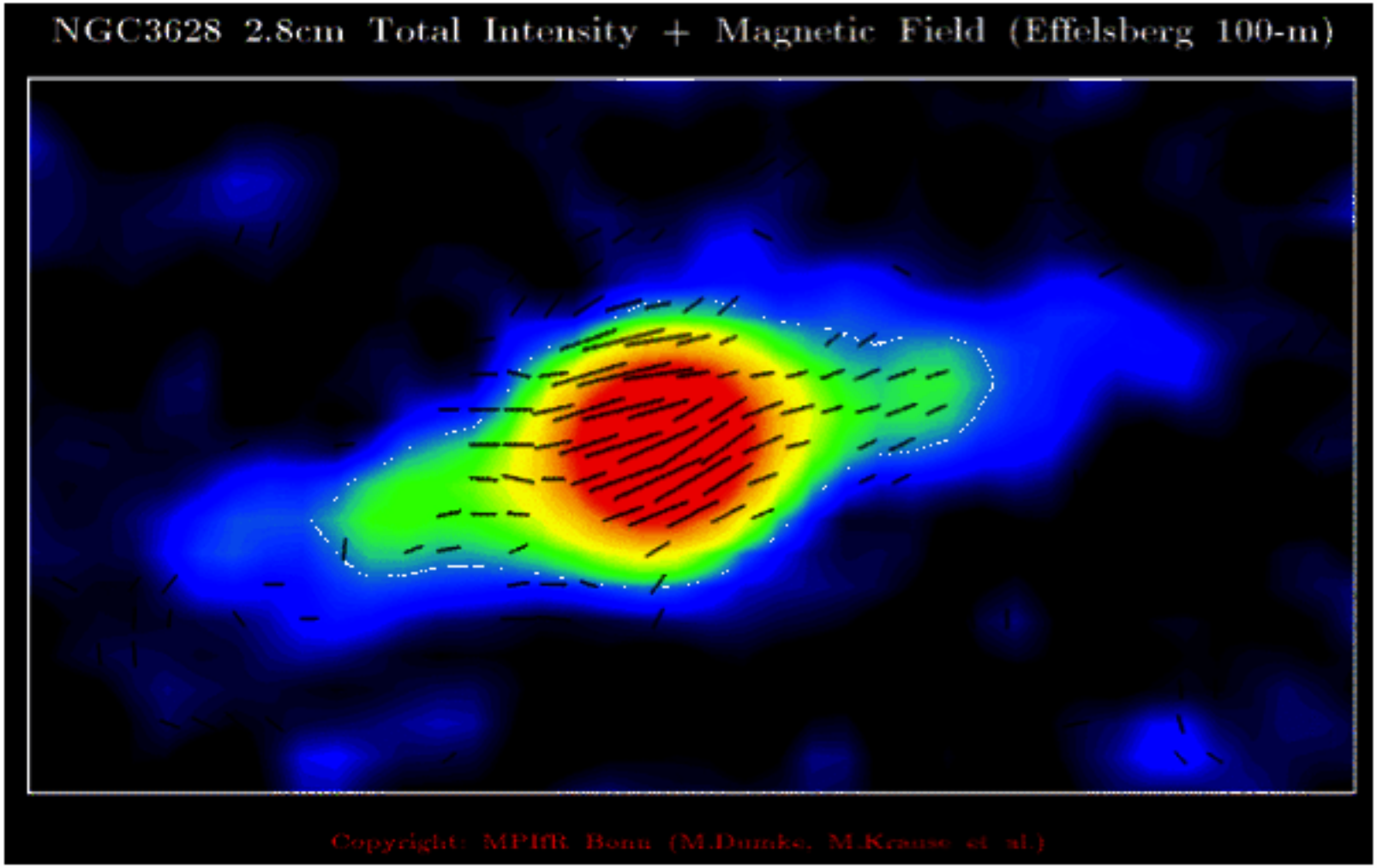

NGC 891

Believed to be very similar to the Milky Way.

The X-shaped structure of the magnetic fields indicates the action of a galactic wind.

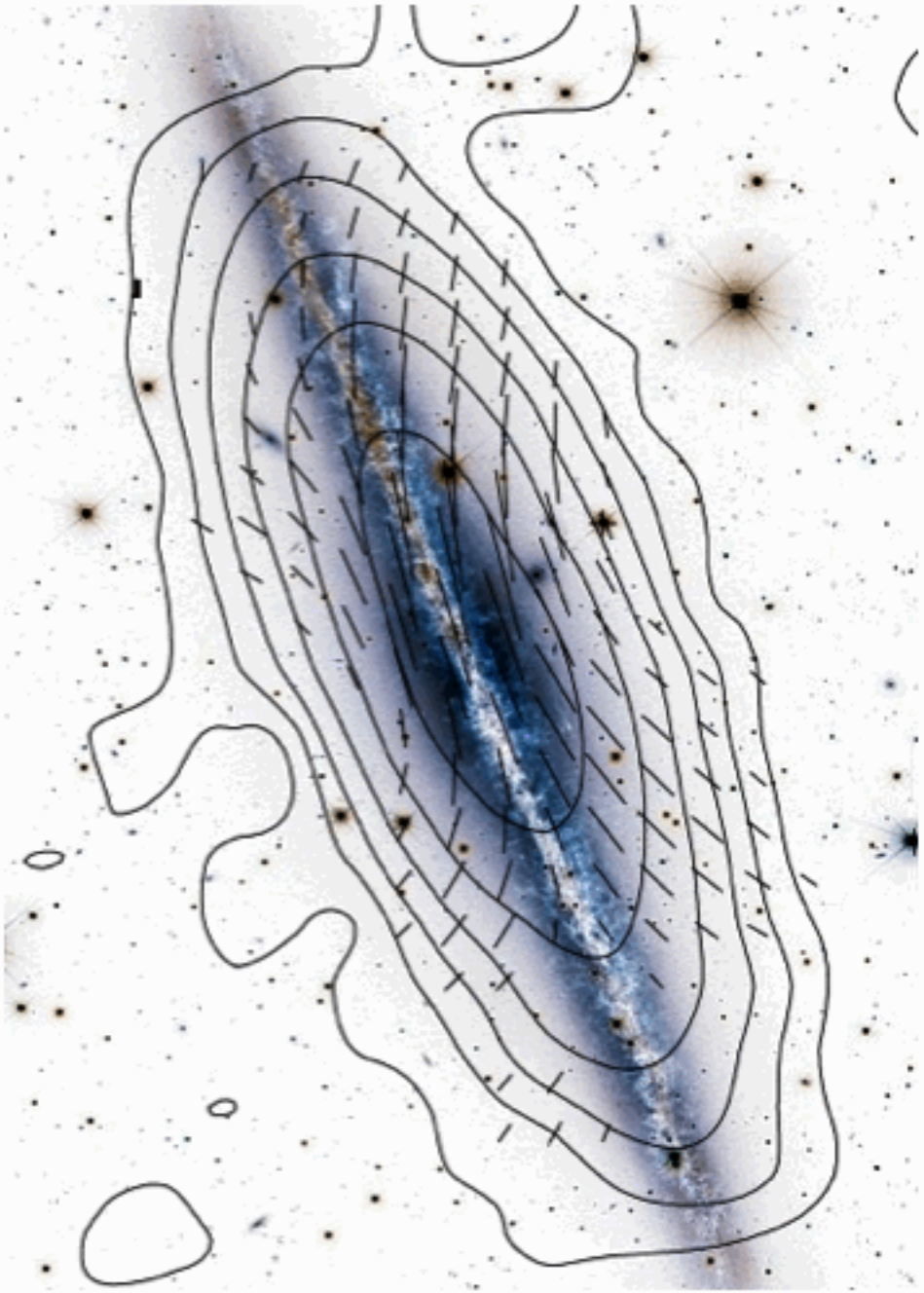

Edge-on spiral galaxy NGC 891 (total and polarized intensity), observed with the Effelsberg telescope at 8 GHz (3.6 cm wavelength) Optical background image: CFHT/Coelum

© M. Krause (MPIfR Bonn)

GMF topology

From approximately

70 spiral galaxies

Vertical structure	Azimuthal structure		
	ASS	BSS	MSS
Even	S0	S1	S0+S1
Odd	A0	A1	A0+A1
Mixed	M0	M1	M0+M1

Beck et al (1996)

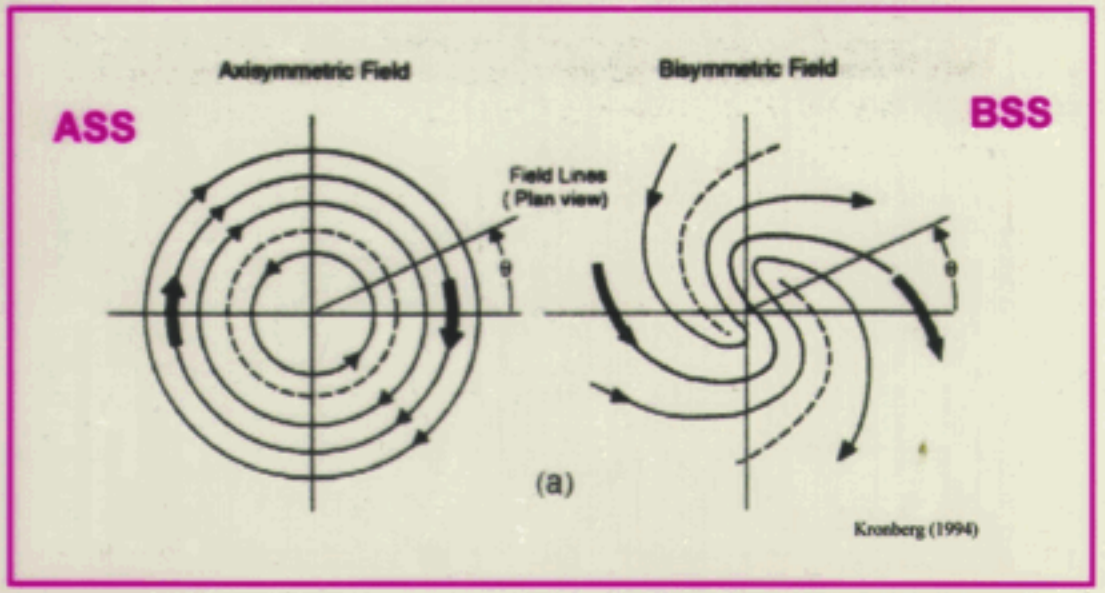

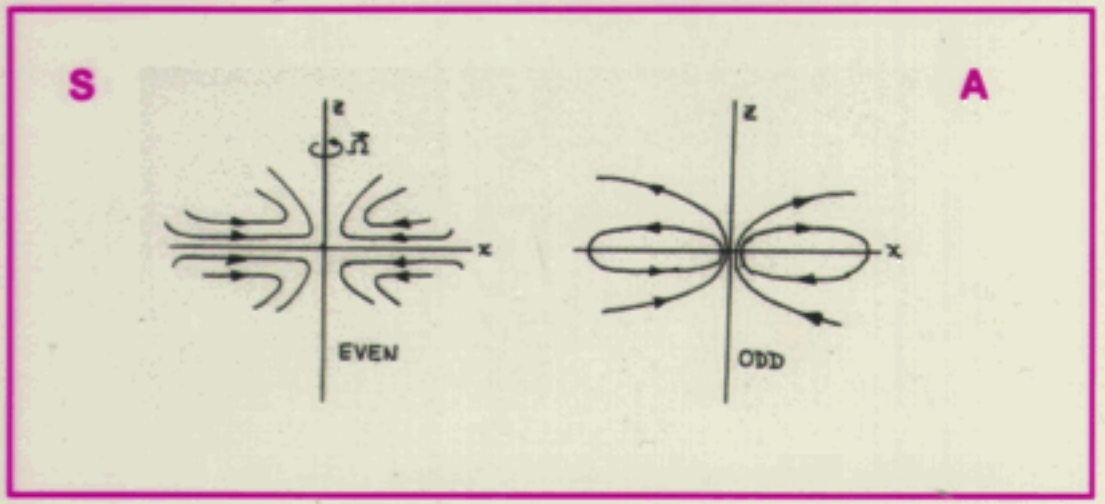

GMF topology

Axisymmetric and bisymmetric field configurations for disk systems along with the corresponding RM vs. ϕ plots. Top panels show toroidal field lines near the equatorial plane. Lower panels show RM as a function of azimuthal angle for observations at the circle (dotted line) in the corresponding top panel. Note that the pitch angle has the opposite sign for the two cases shown.

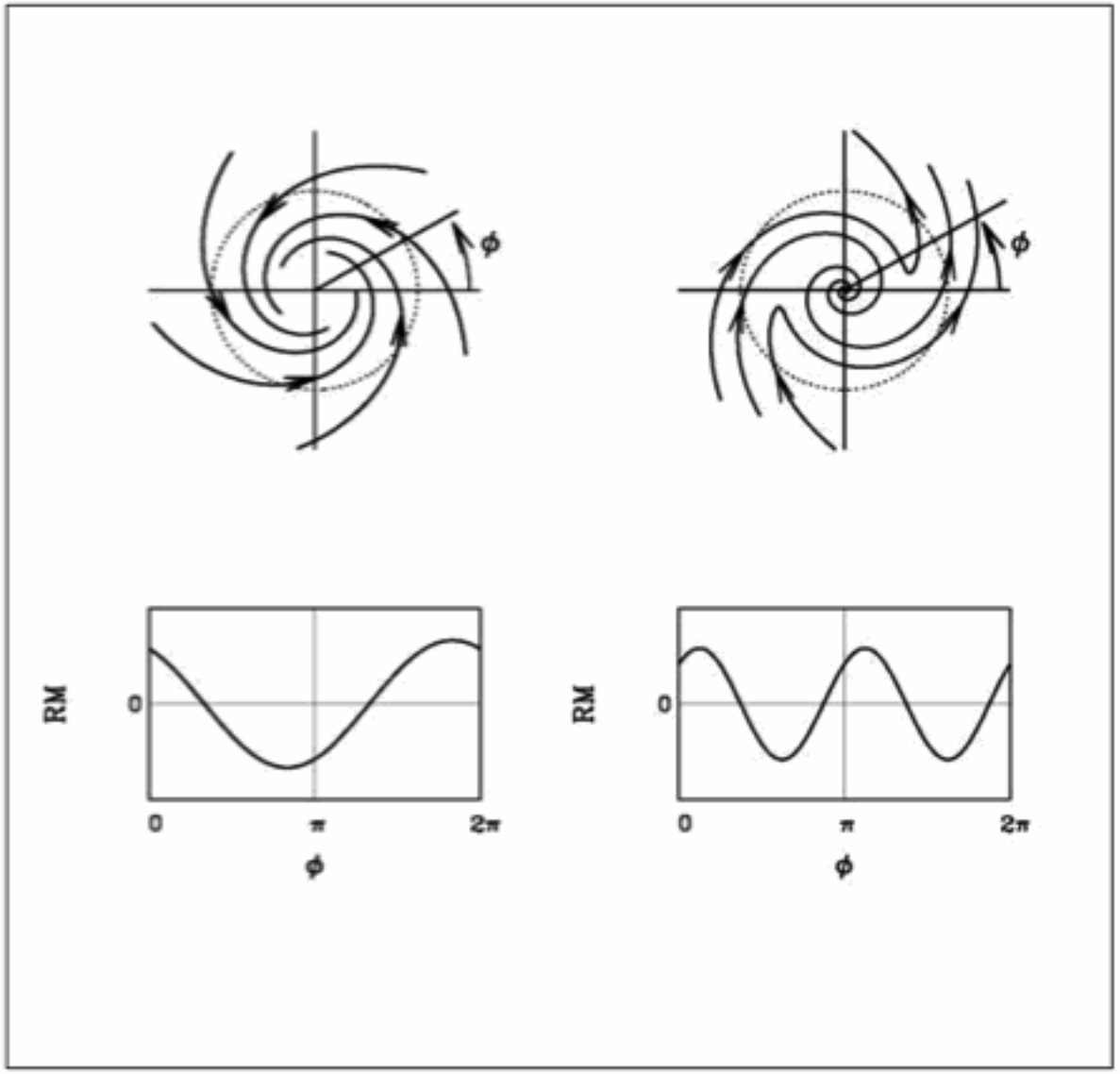

Widrow astro-ph/0207240

GMF topology

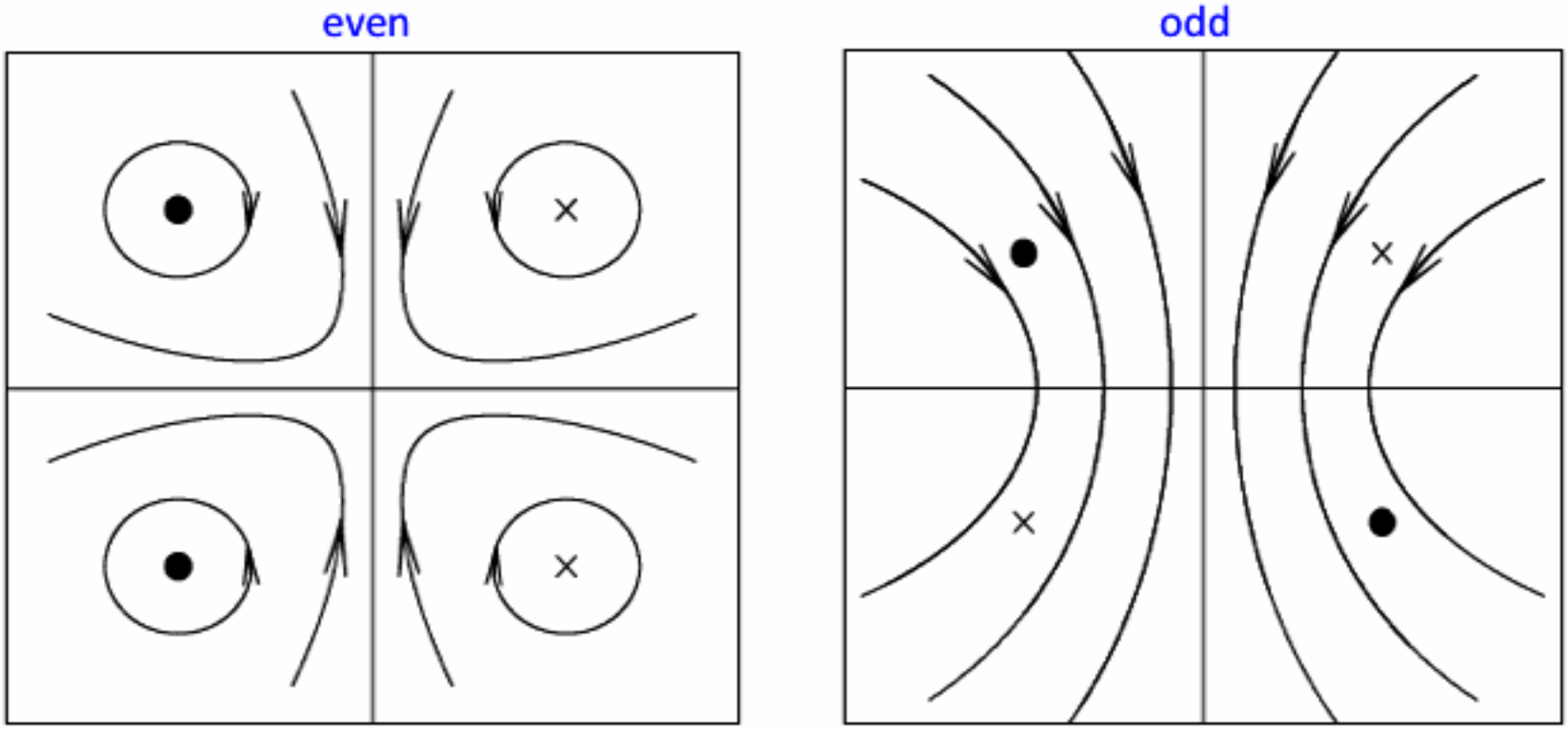

Field lines for even (left panel) and odd (right panel) configurations. Shown are cross-sections perpendicular to the equatorial plane and containing the symmetry axis of the galaxy (i.e., poloidal planes). The toroidal field is indicated by an 'x' (field out of the page) or 'dot' (field into the page).

Magnetic fields in our Galaxy

Extra galactic radio sources

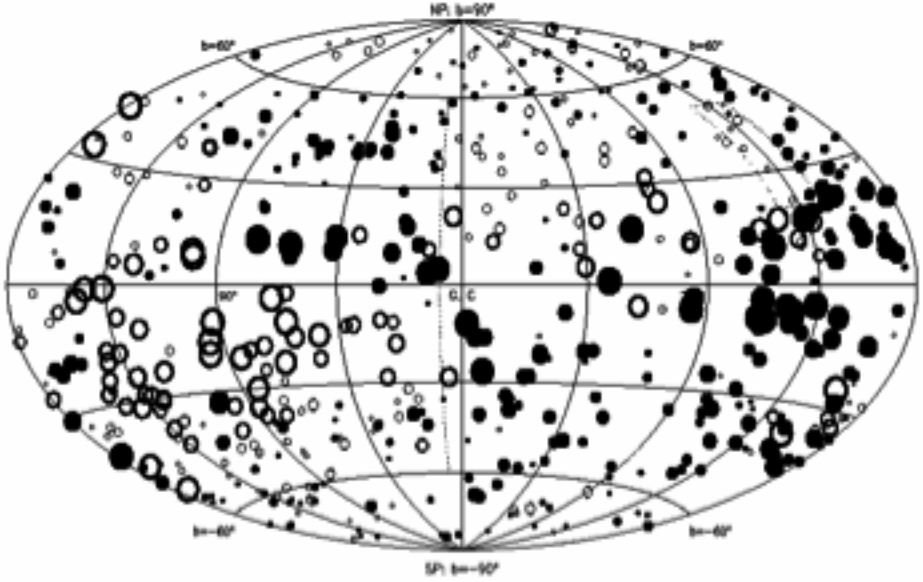

Pulsars

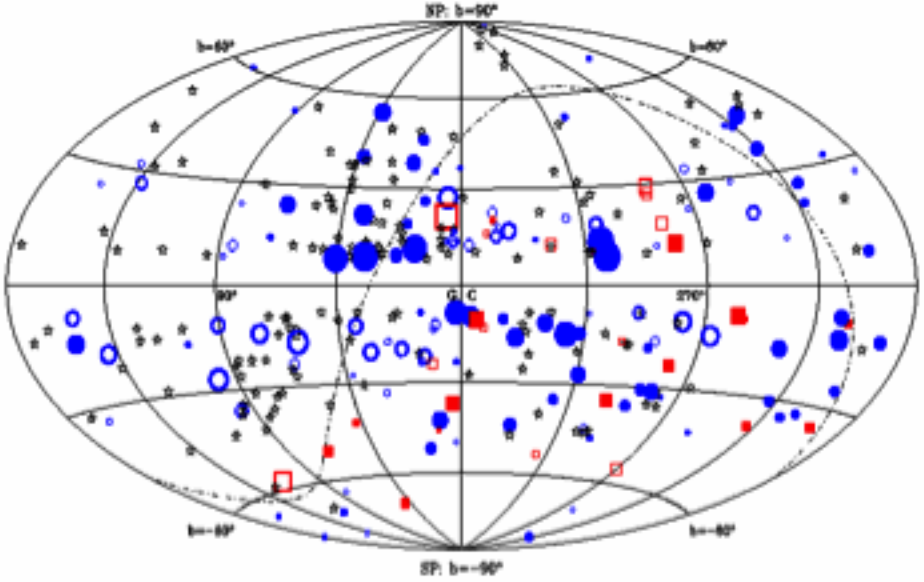

Jin Lin Han 2001

Magnetic fields in our Galaxy

From JinLin Han (2001)

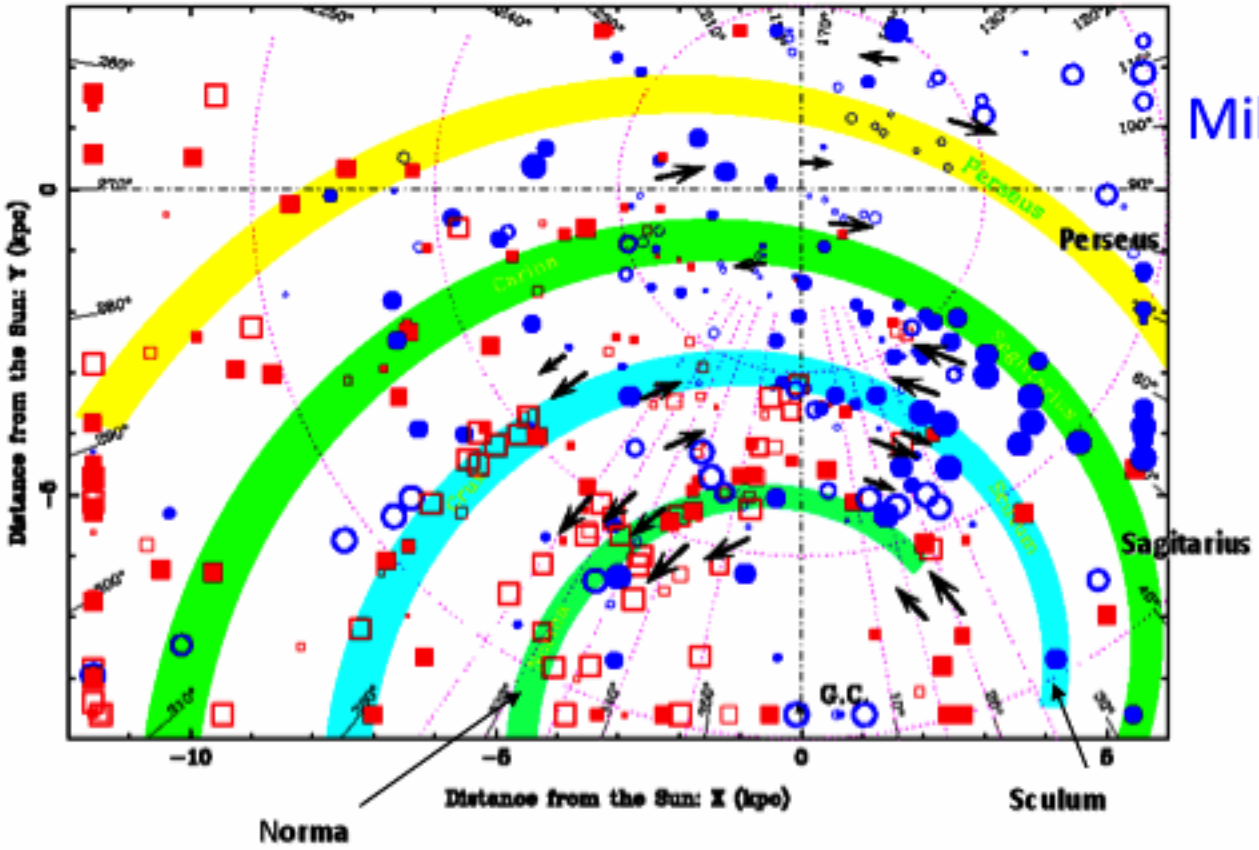

Pulsar RM projected onto the plane -- open symbols correspond to negative RM.

Magnetic fields in our Galaxy

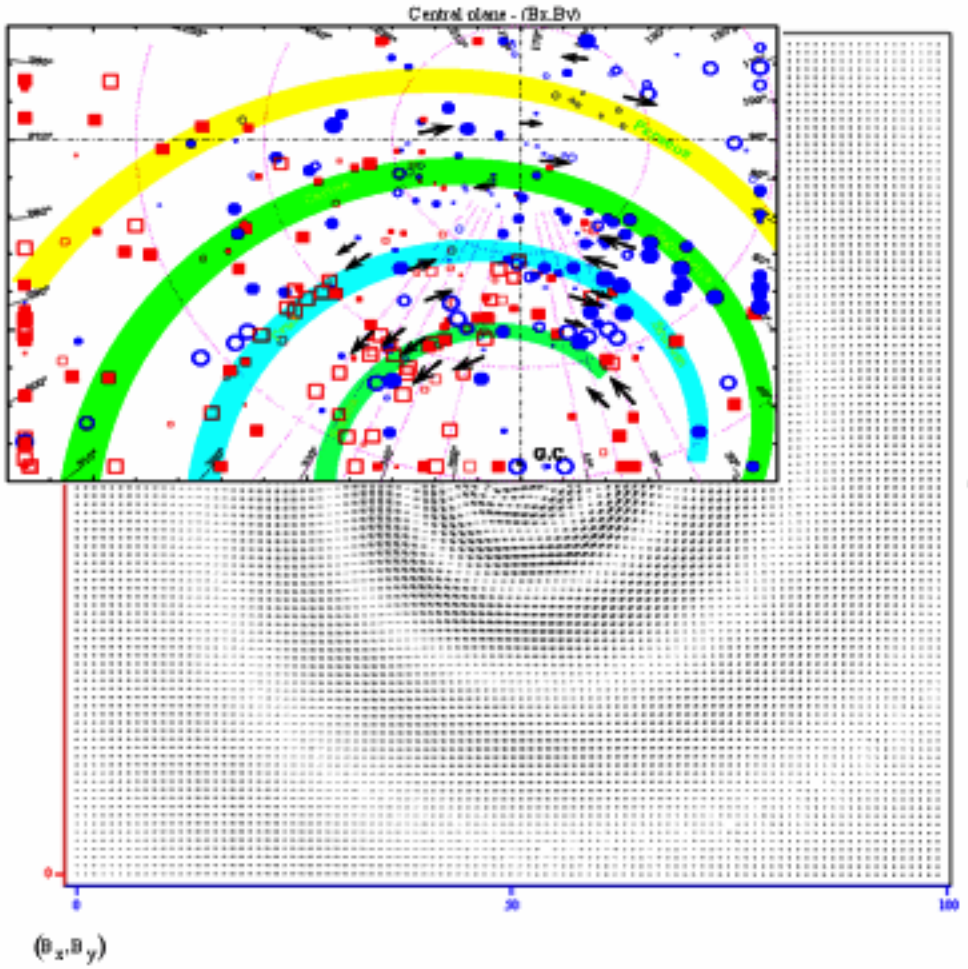

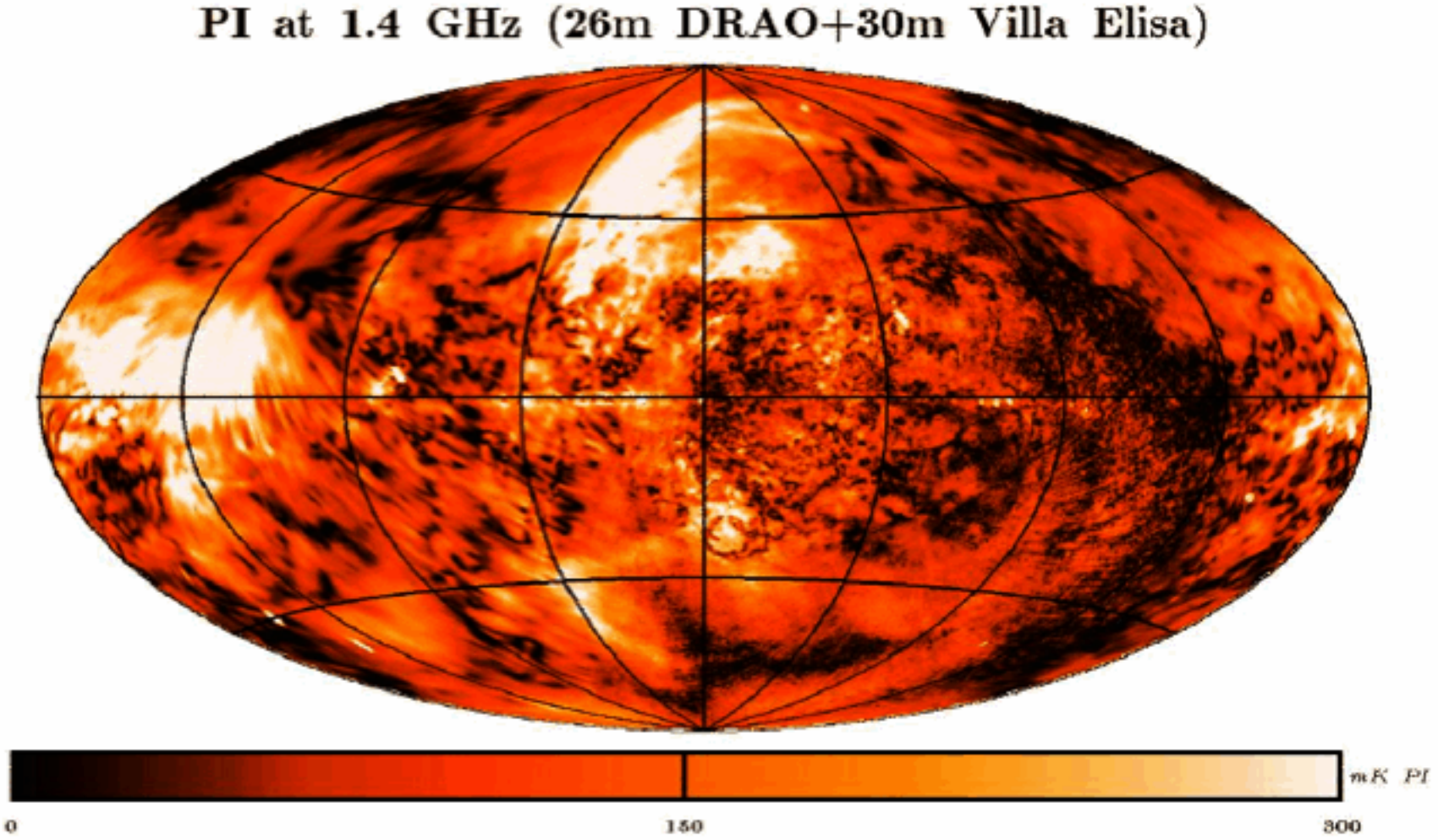

All-sky polarization survey of the Milky Way at 1.4 GHz (20 cm wavelength), observed with the 20m DRAO (Canada) and 30m Villa Elisa (Argentina) radio telescopes

© M. Wolleben (DRAO), P. & W. Reich (MPIfR Bonn) and J.C. Testori (Villa Elisa)

Global structure inferred from observations

The mean orientation of the magnetic field is parallel to the galactic plane and nearly azimuthal;

The deviation is consistent with alignment along the spiral arms (Heiles 1996).

This orientation is consistent with the effects of induction in a system with strong differential rotation and a spiral density wave pattern (Roberts and Yuan 1970).

Assuming that the galactic halo rotates more slowly than the disc, induction would act on a vertical field so as to produce a reversal in the azimuthal field across the galactic plane (so-called dipole symmetry).

The traditional view has been that the field does not reverse across the plane (Beck et al 1996), although some authors favor asymmetry (Han et al 1997; 1999, Han 2001, 2003). This important question is still open.

At least within several kpc of the Sun GMF has both mean and random components (Rand and Kulkarni 1989, Han et al 2006, Beck 2007)

The mean component is of the order 1.4–2μG and the RMS field ~ 5–6μG.

There is evidence that the mean field reverses with Galactocentric radius (bisymmetric spiral structure), but the locations and frequency of reversal are quite uncertain (see Han

There is no agreement as to the large scale structure of the GMF

At least 2 reversals → BSS model

Dynamo theory → ASS model

Reversals are not seen in other galaxies!

Symmetry in z →

- Best agreement seems to point to S (quadrupolar)
- But there are claims for odd symmetry (even if local irregularities may confuse interpretation)

Therefore, there even exist the possibility that two dynamos operate in the Galaxy:

Large scale field in the outskirts of the Galaxy ➔ S0

B_r , B_ϕ ➔ EVEN

B_z ➔ ODD

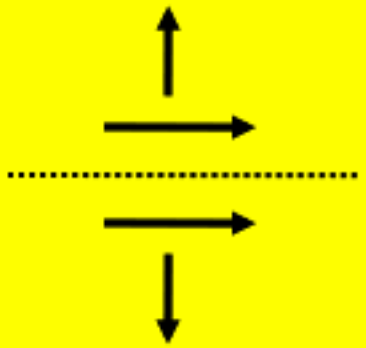

Large scale field near the Galaxy center ➔ A0 (dipole)

B_r , B_ϕ ➔ ODD

B_z ➔ EVEN

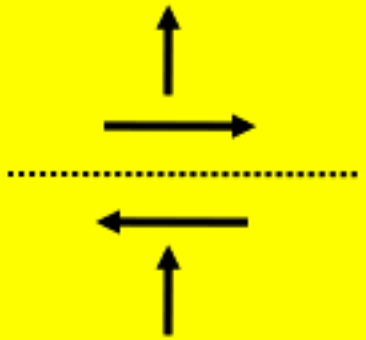

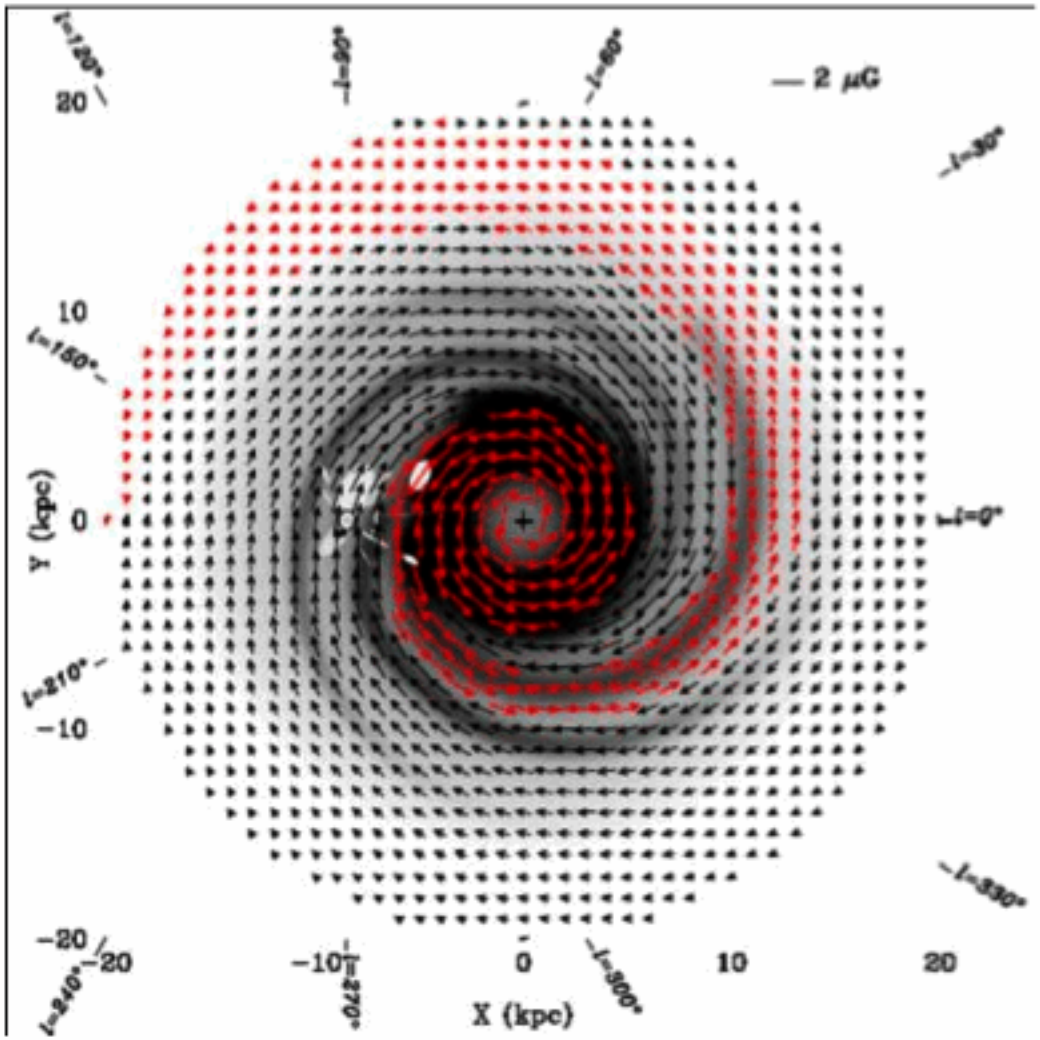

Model of the large-scale structure of the magnetic fields in the Milky Way disk, derived from radio polarization surveys at 1.4 GHz (DRAO/Villa Elisa) and 22 GHz (WMAP) and rotation measures of extragalactic sources

© X. Sun (NAO Bejing) and W. Reich (MPIfR Bonn)

And there is turbulence too...

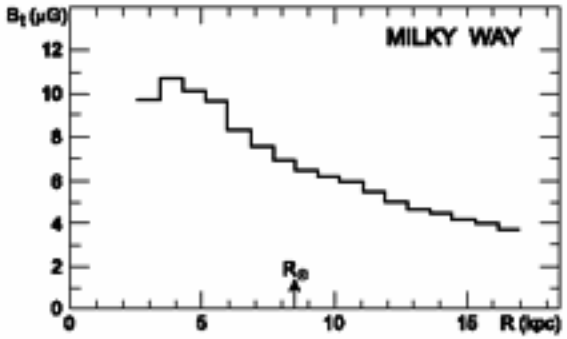

Figure 1. Strength of the total magnetic field in the Galaxy, averaged from the deconvolved surface brightness of the synchrotron emission at 408 MHz (Beuermann *et al.*, 1985), assuming energy equipartition between magnetic field and cosmic ray energy densities (Berkhuijsen, personal communication). The accuracy is about 30%. The Sun is assumed to be located at R=8.5 kpc.

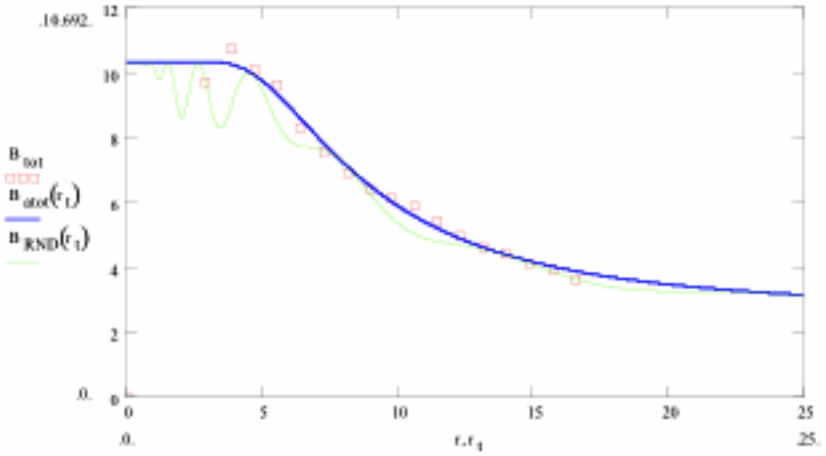

+

a model for

$\boldsymbol{B}_{\mathrm{reg}}$

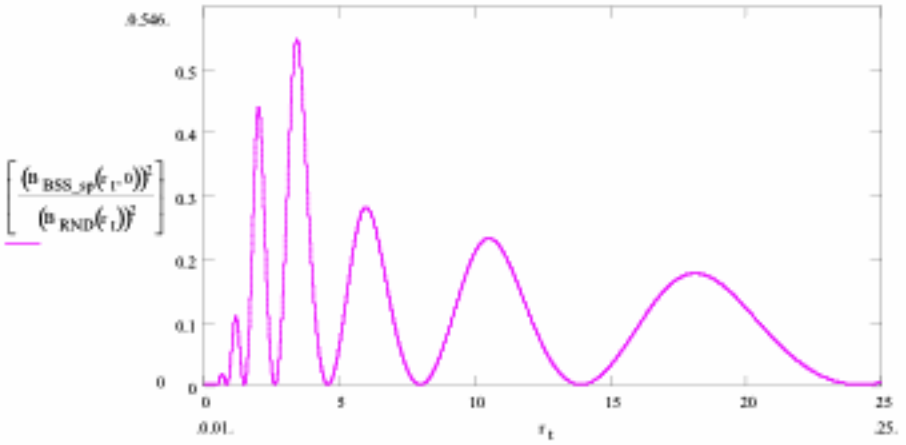

And there is turbulence too…

Regular component is predominant in the interarm region

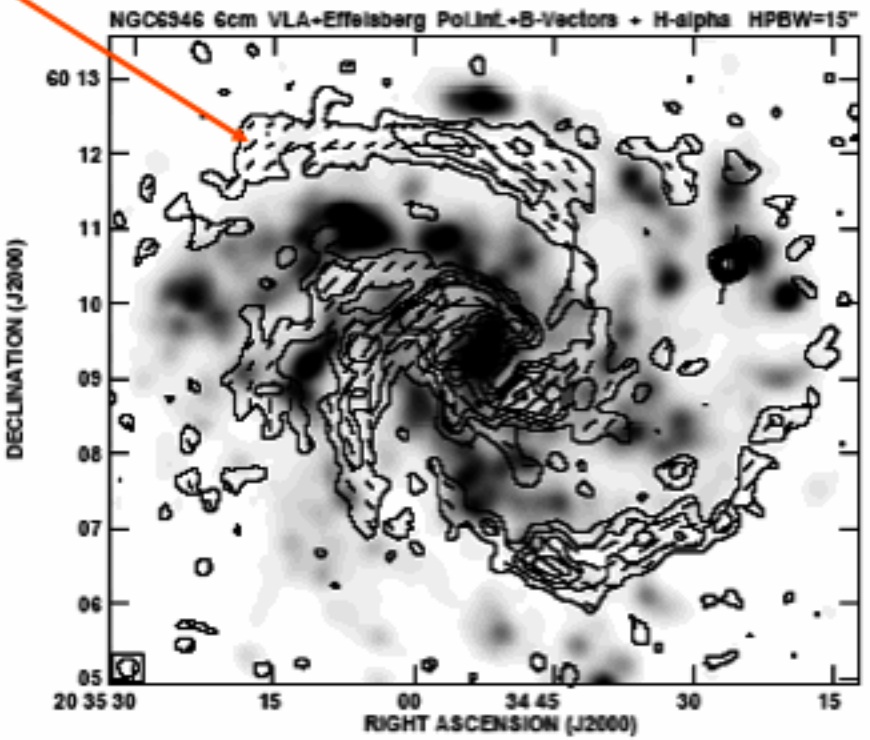

Figure 3. Polarized radio intensity (contours) and B–vectors of polarized intensity of NGC 6946 at 15″ resolution, combined from VLA and Effelsberg observations at $\lambda 6$ cm. The grey-scale image shows the Hα emission (kindly provided by A. Ferguson), smoothed to the same resolution. (From Beck & Hoernes 1996)

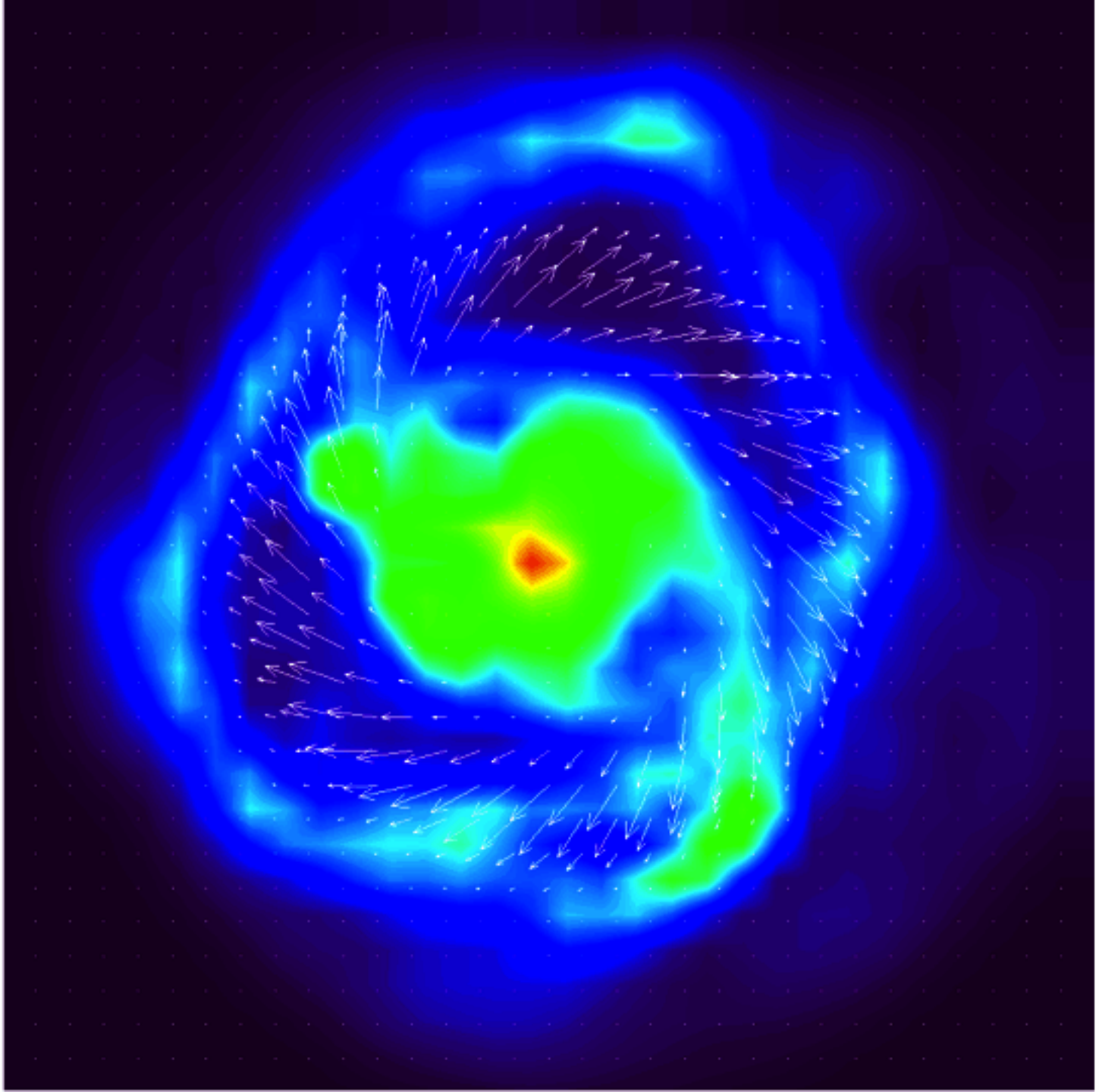

Detlef Elstner
AIP, Germany

Magnetic fields in other spiral galaxies

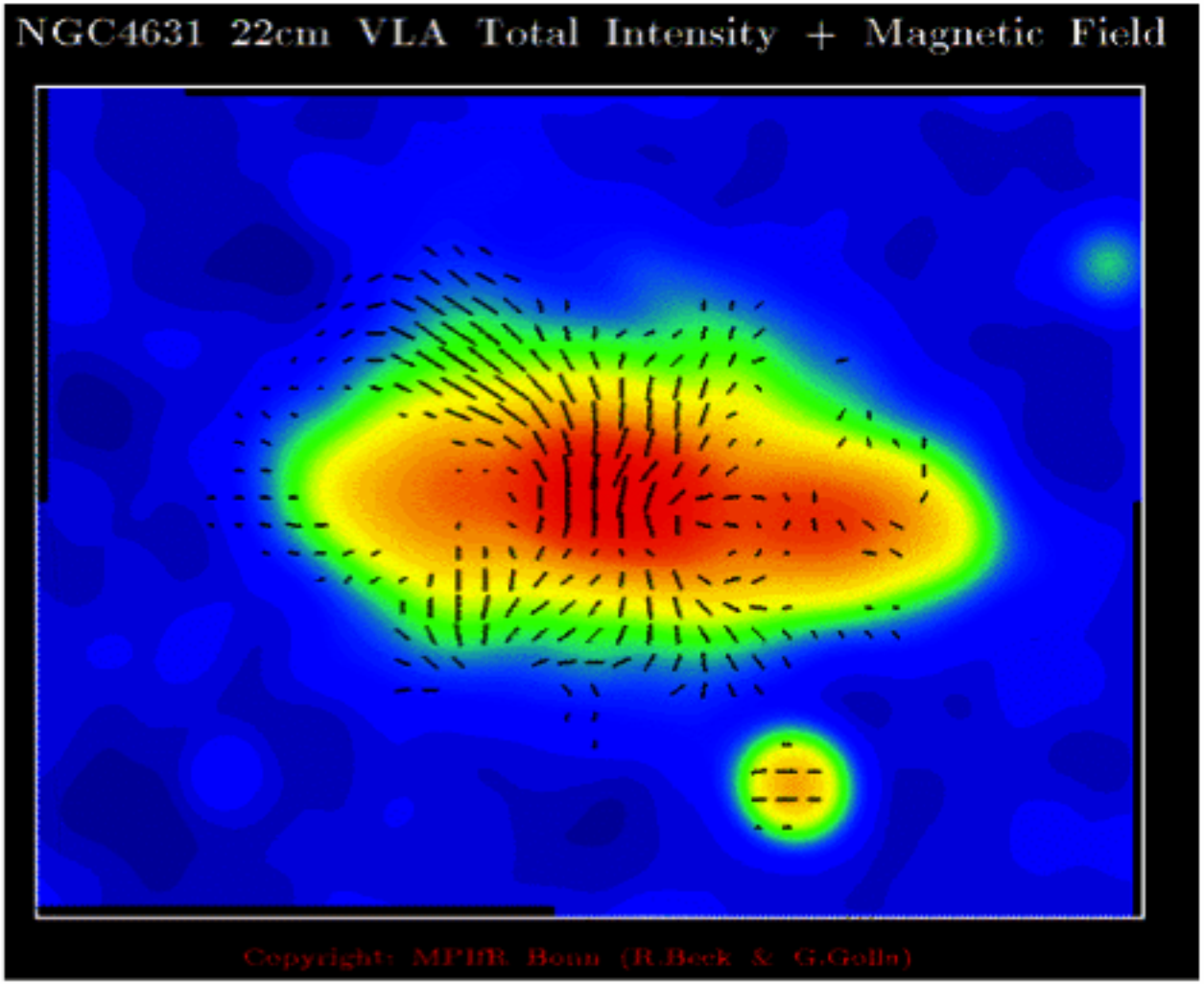

A dipolar component in a galaxy halo ?

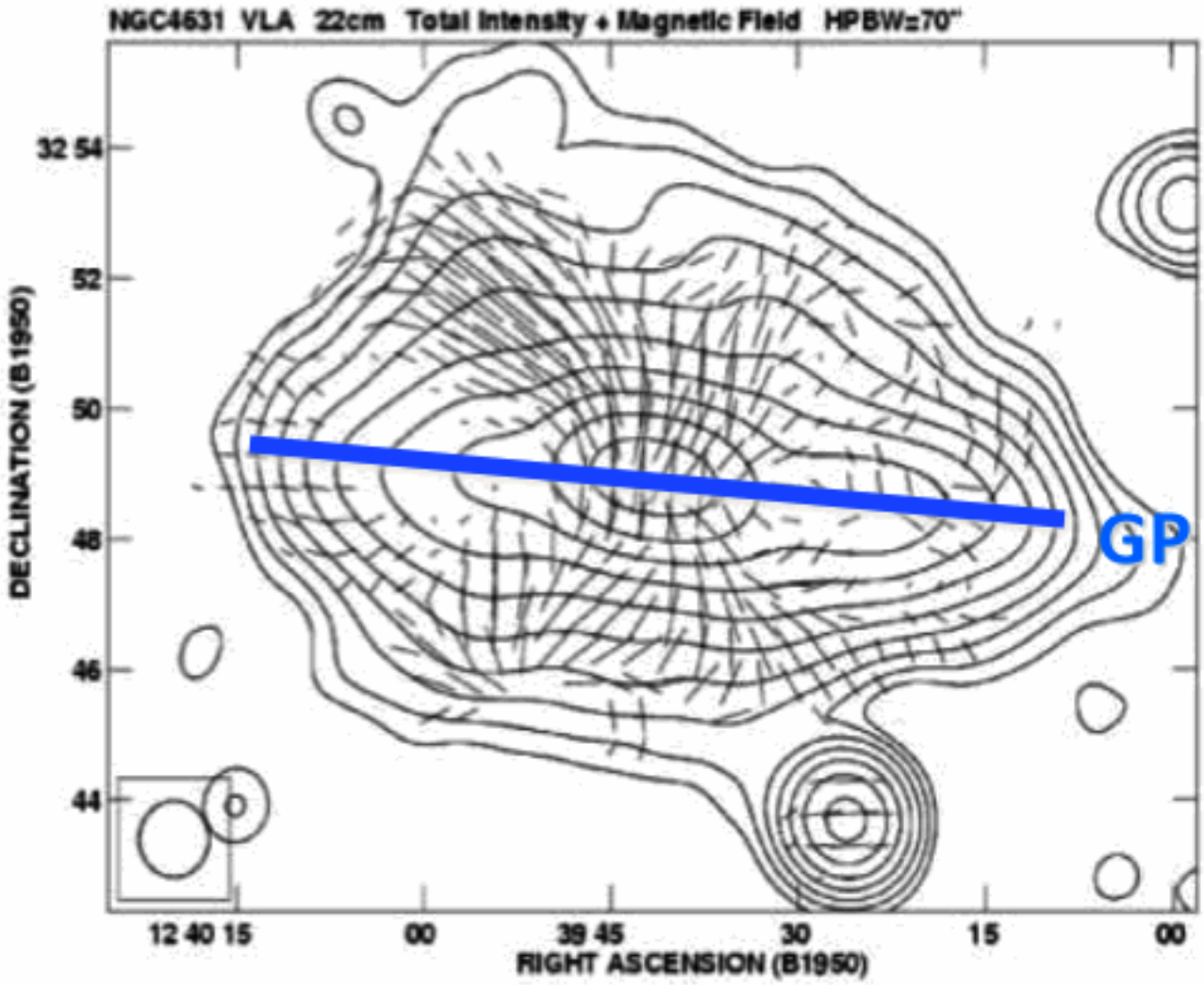

Total radio emission and B vectors of polarized emission of NGC 4631 at 22 cm (VLA, 70″ synthesized beam). The B vectors have been corrected for Faraday rotation; their length is proportional to the polarized intensity (From Krause & Beck, unpublished)

In the inner Galaxy things are more complex...

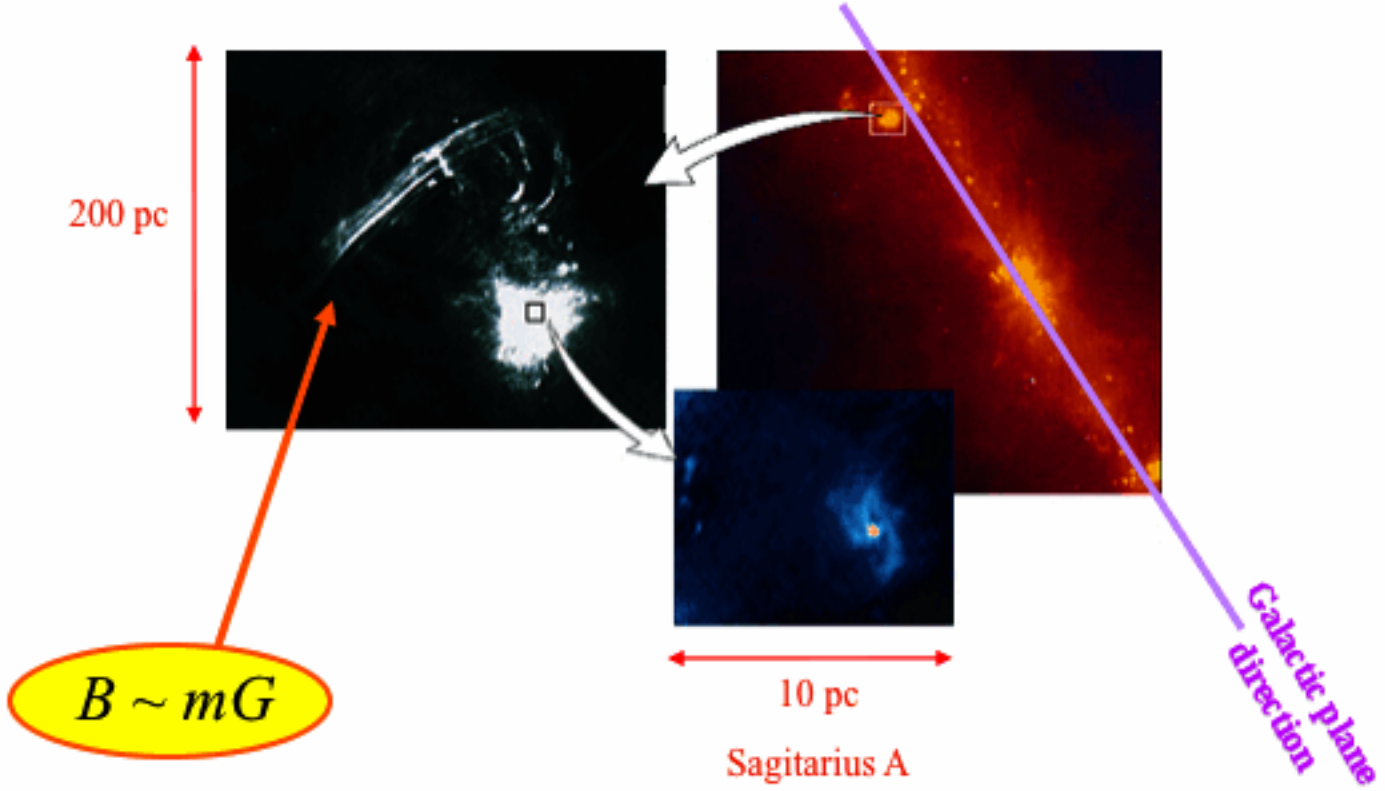

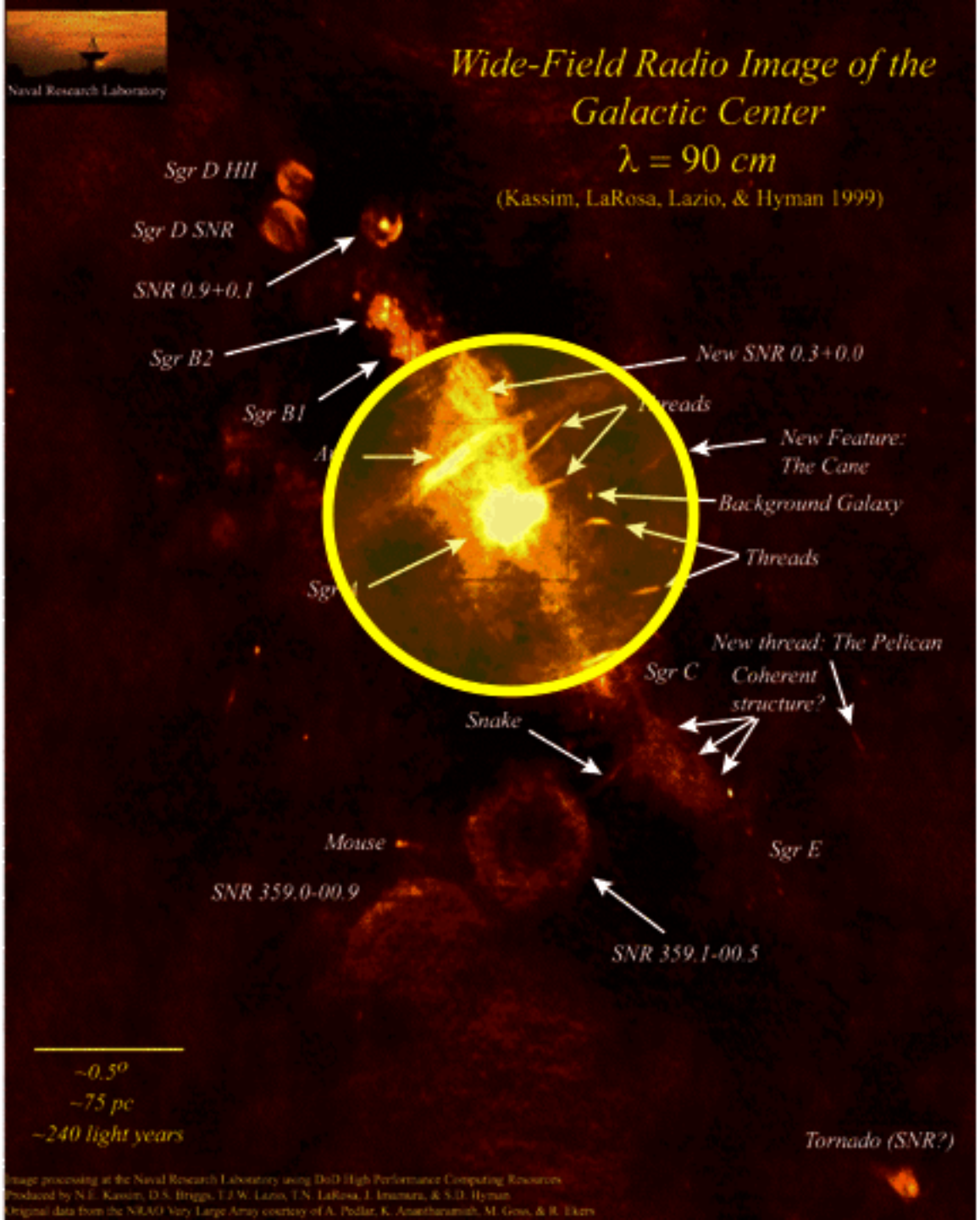
Naval Research Laboratory
Wide-Field Radio Image of the Galactic Center
λ = 90 cm
(Kassim, LaRosa, Lazio, & Hyman 1999)
Sgr D HII
Sgr D SNR
SNR 0.9+0.1
Sgr B2
Sgr B1
New SNR 0.3+0.0
New Feature: The Cane
Background Galaxy
Threads
New thread: The Pelican
Sgr C
Coherent structure?
Snake
Mouse
SNR 359.0-00.9
Sgr E
SNR 359.1-00.5
~0.5°
~75 pc
~240 light years
Tornado (SNR?)
Image processing at the Naval Research Laboratory using DoD High Performance Computing Resources
Produced by N.E. Kassim, D.S. Briggs, T.J.W. Lazio, T.N. LaRosa, J. Imamura, & S.D. Hyman
Original data from the NRAO Very Large Array courtesy of A. Pedlar, K. Ananthasubmh, M. Goss, & R. Ekers

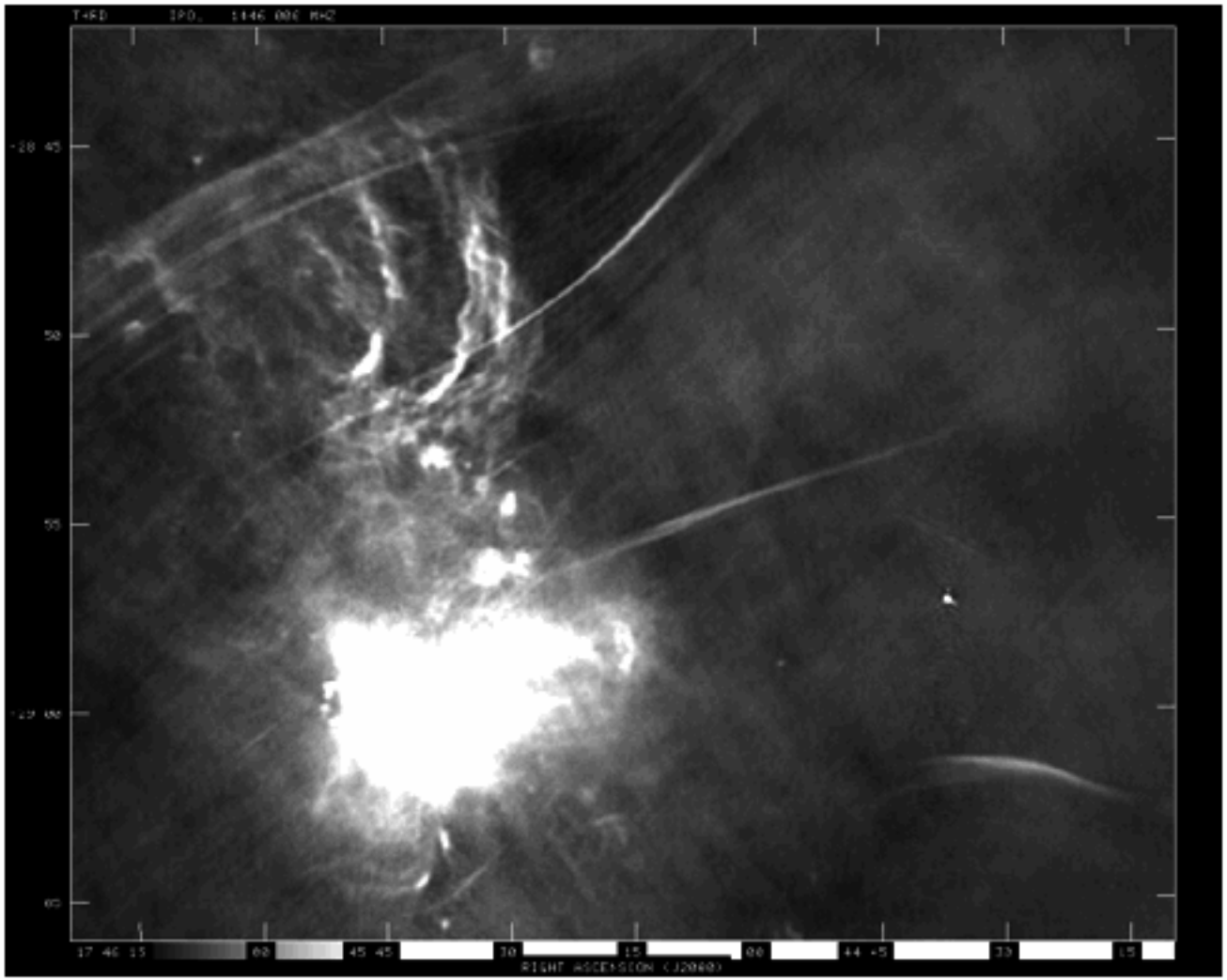
T+60 IPD, 1446.000 MHZ
-28 45
50
55
-29 00
05
17 46 15
00
45 45
30
15
00
44 +5
33
15
RIGHT ASCENSION (J2000)

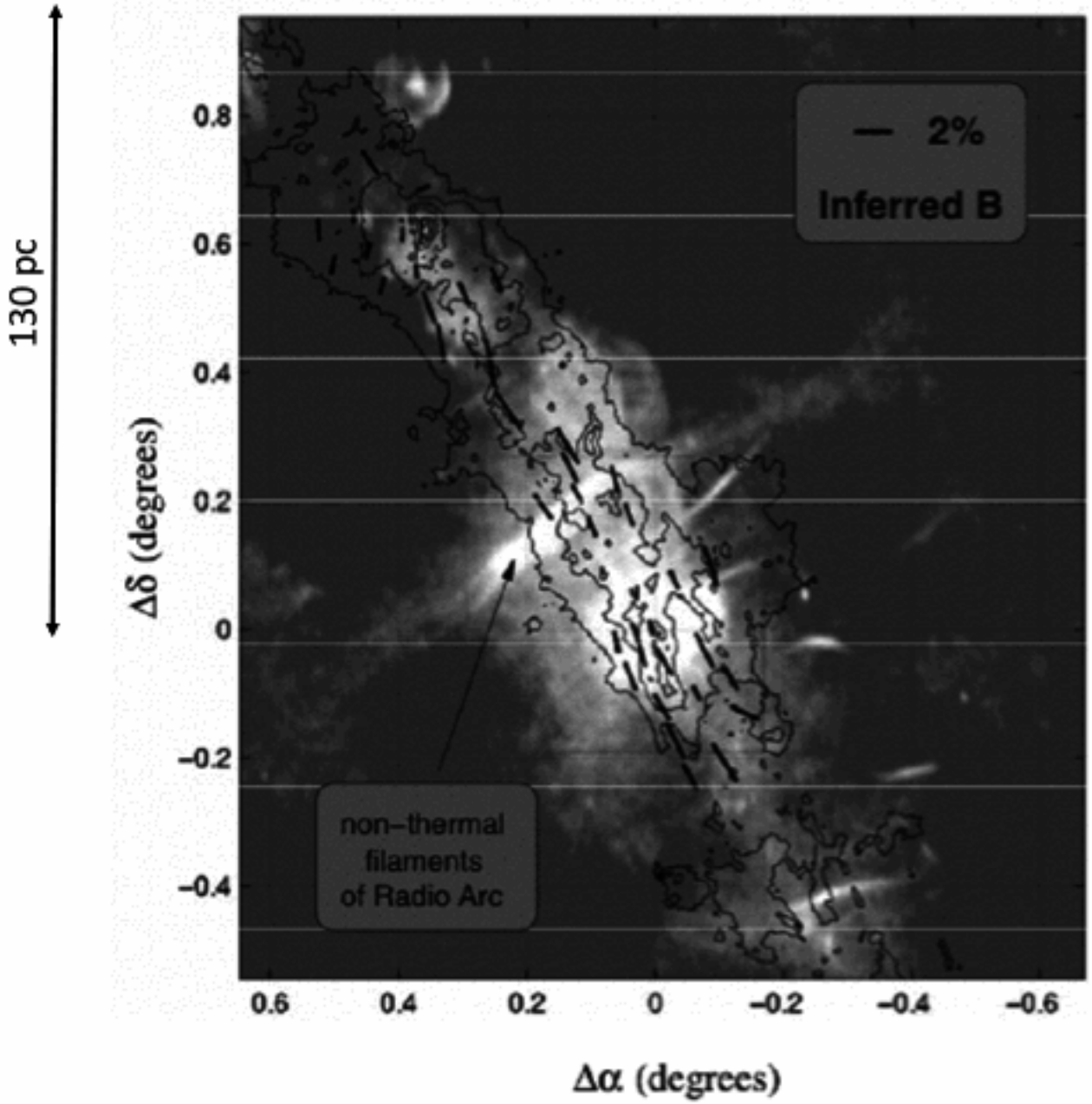

Novak et al. (2003)

Chuss et al. (2003)

Polarimetry @ 350 μm

$$\langle B(r < 30\,pc) \rangle \approx 3\,mG$$

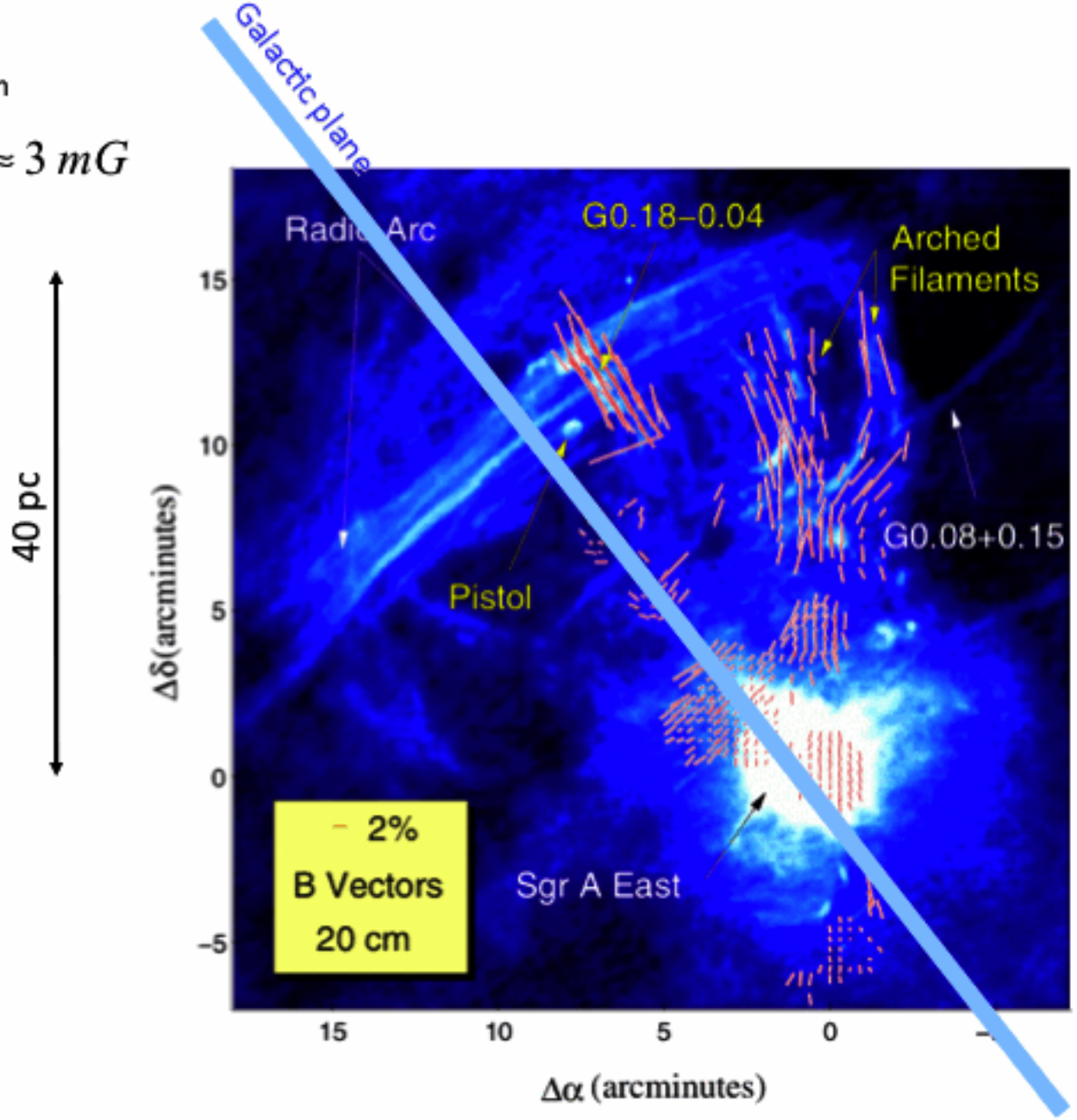

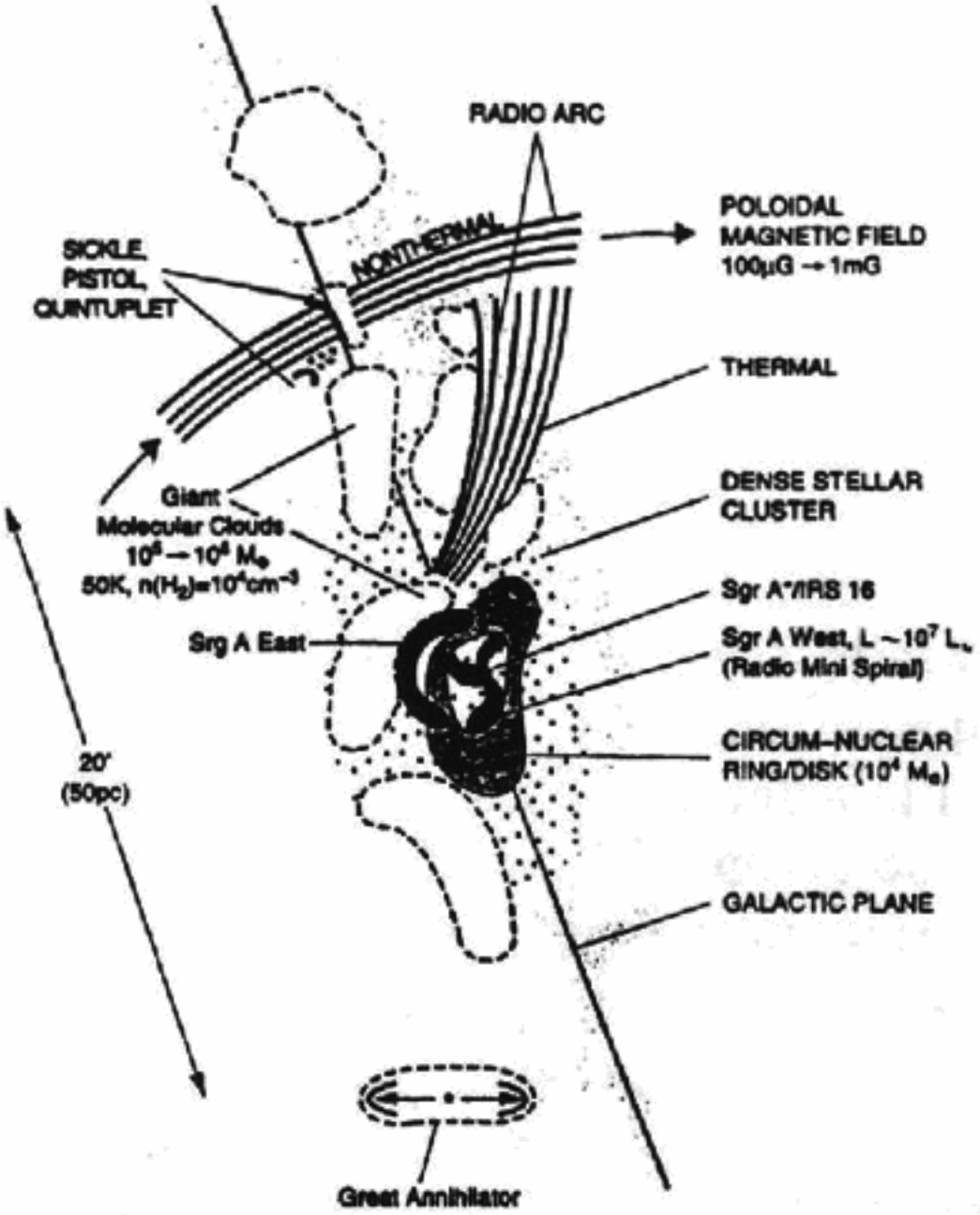
RADIO ARC
NONTHERMAL
SICKLE,
PISTOL,
QUINTUPLET
POLOIDAL
MAGNETIC FIELD
100μG → 1mG
THERMAL
DENSE STELLAR
CLUSTER
Giant
Molecular Clouds
$10^5 - 10^6$ $M_\odot$
50K, $n(H_2)=10^4 cm^{-3}$
Sgr A*/IRS 16
Srg A East
Sgr A West, L ~ 10^7 $L_\odot$
(Radio Mini Spiral)
CIRCUM-NUCLEAR
RING/DISK (10^4 $M_\odot$)
20'
(50pc)
GALACTIC PLANE
Great Annihilator

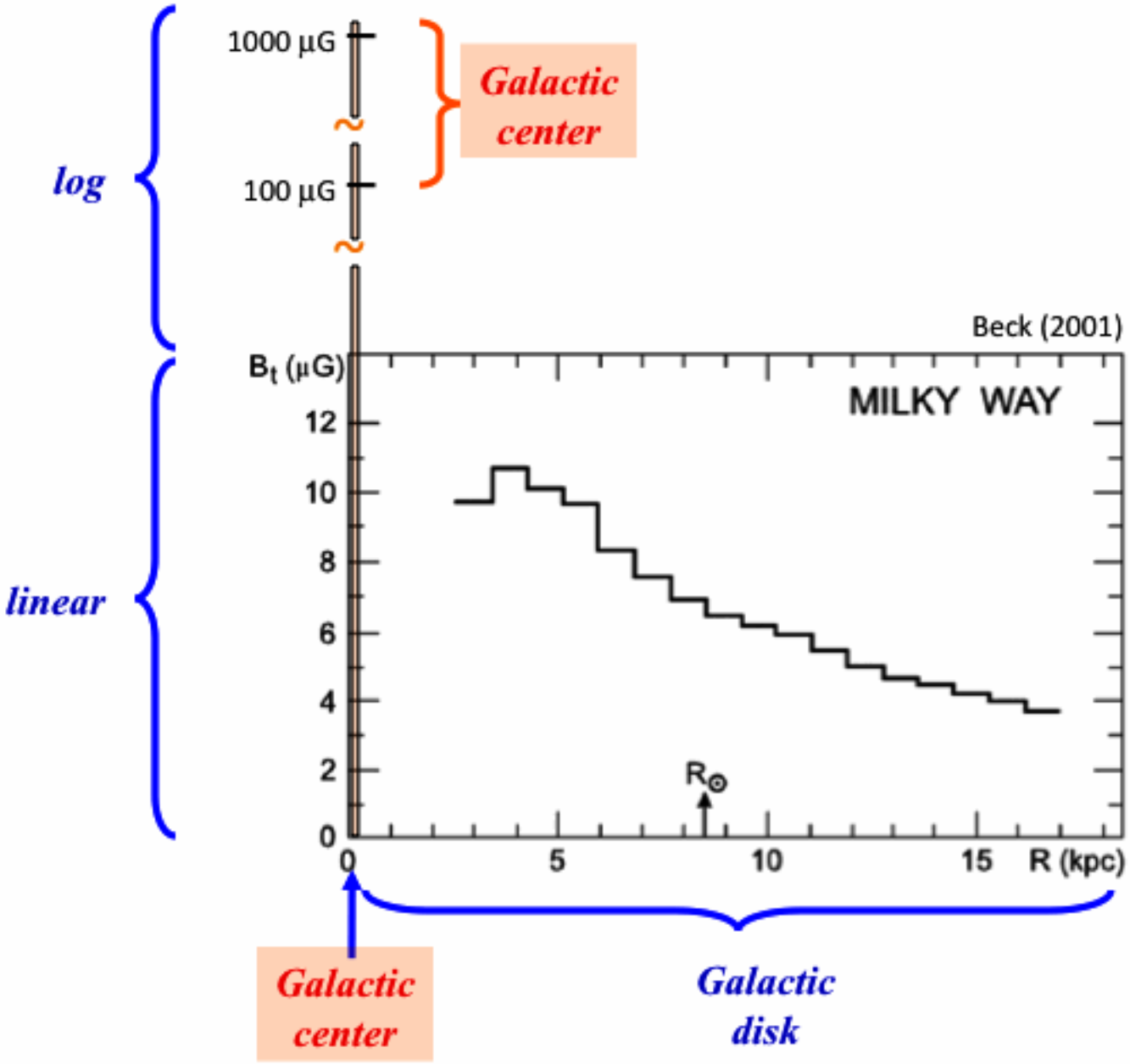
log
linear
1000 μG
100 μG
Galactic center
Beck (2001)
B_t (μG)
MILKY WAY
12
10
8
6
4
2
0
$R_\odot$
0
5
10
15
R (kpc)
Galactic center
Galactic disk

A plausible GMF model ?

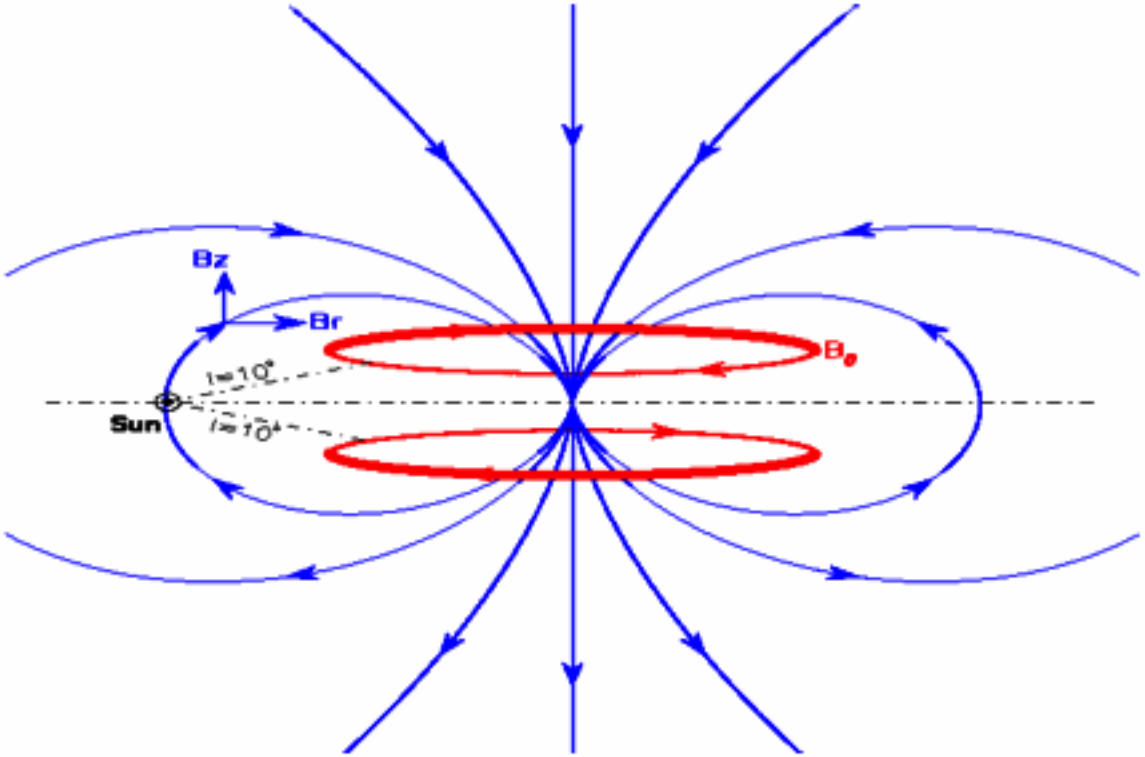

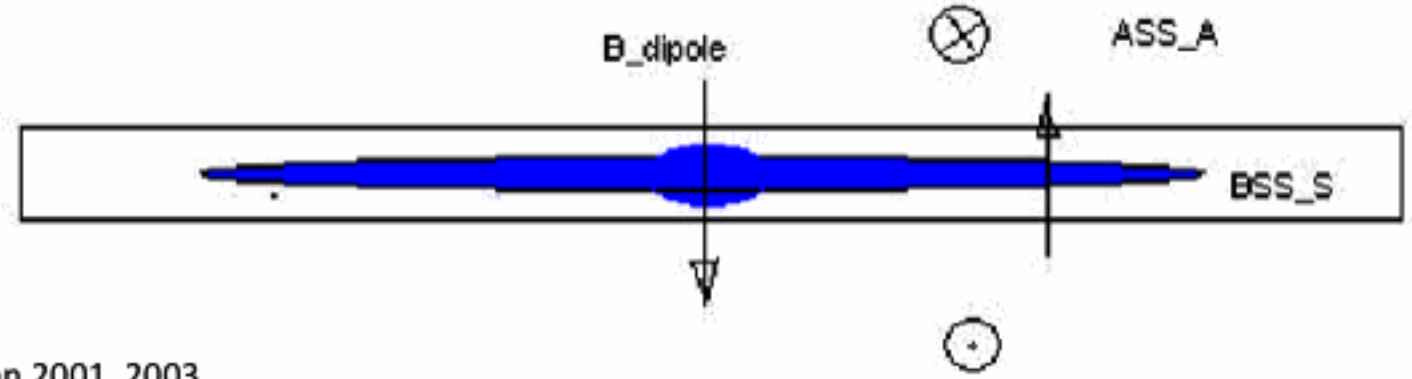

Han 2001, 2003

Galactic propagation along the transition

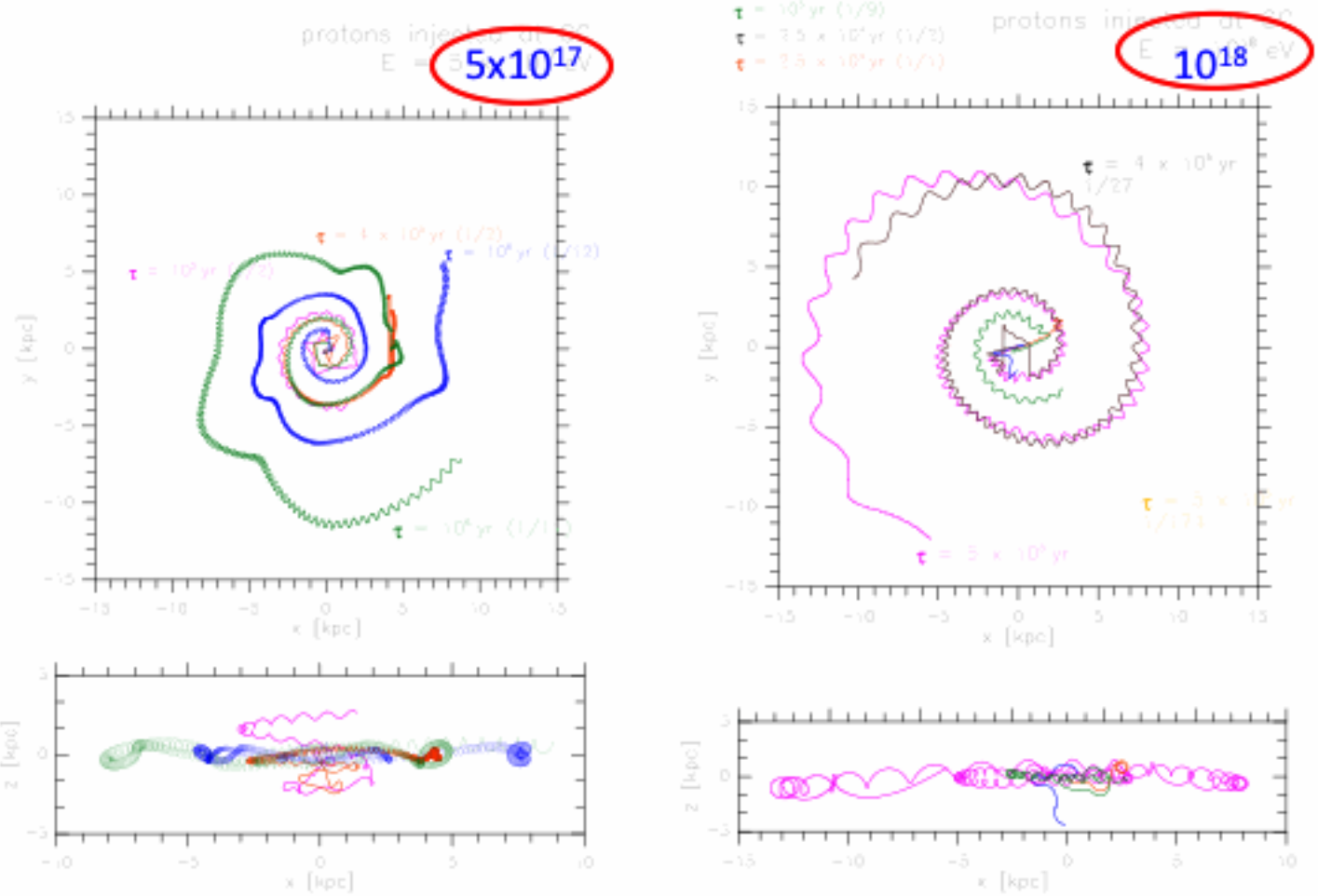

Medina Tanco & Watson (2001)

Galactic propagation along the transition

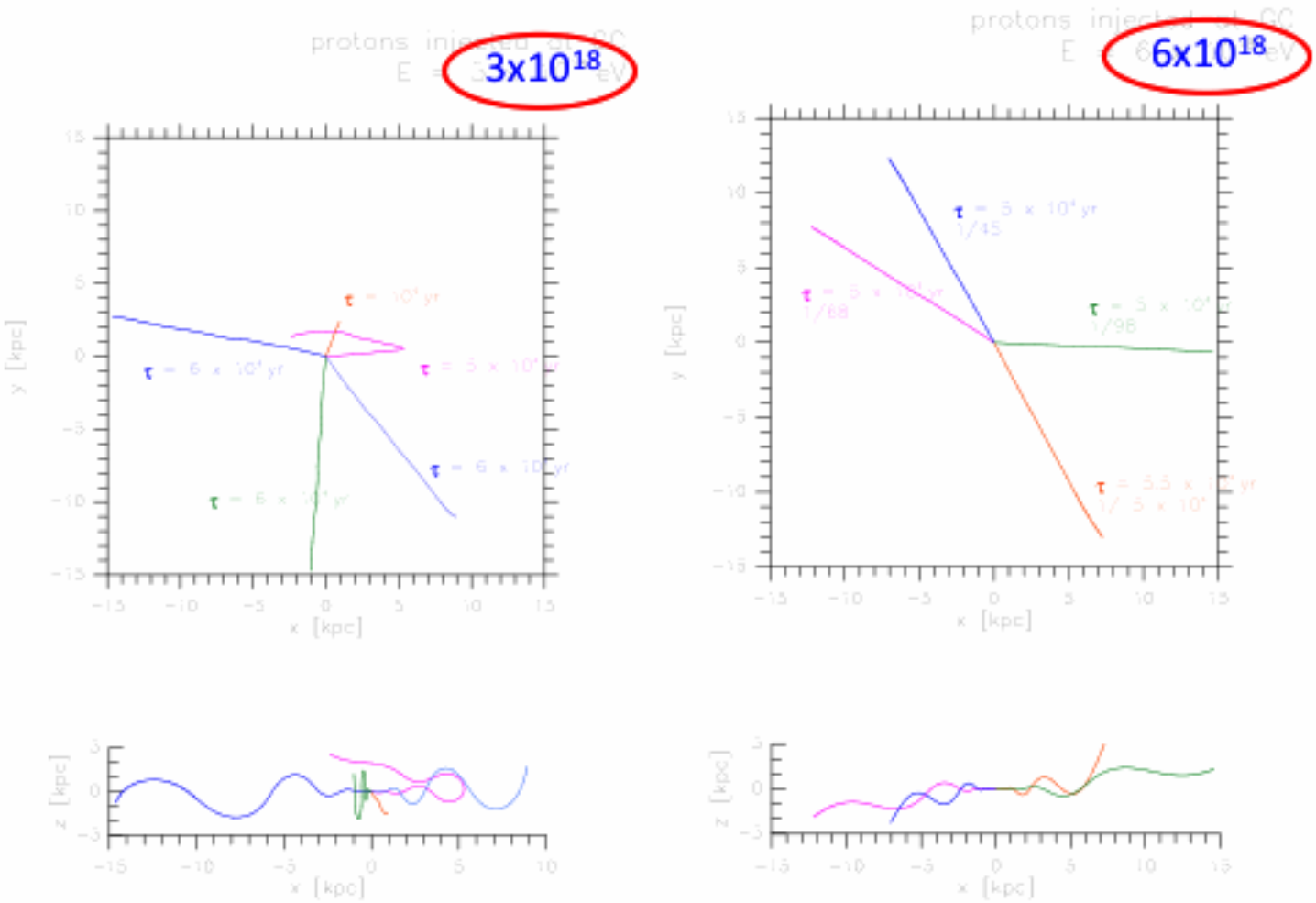

Medina Tanco & Watson (2001)

Deflection as a function of arrival direction

Simple GMF model: single regular BSS_S component – no dipole (which underestimates GC contribution)

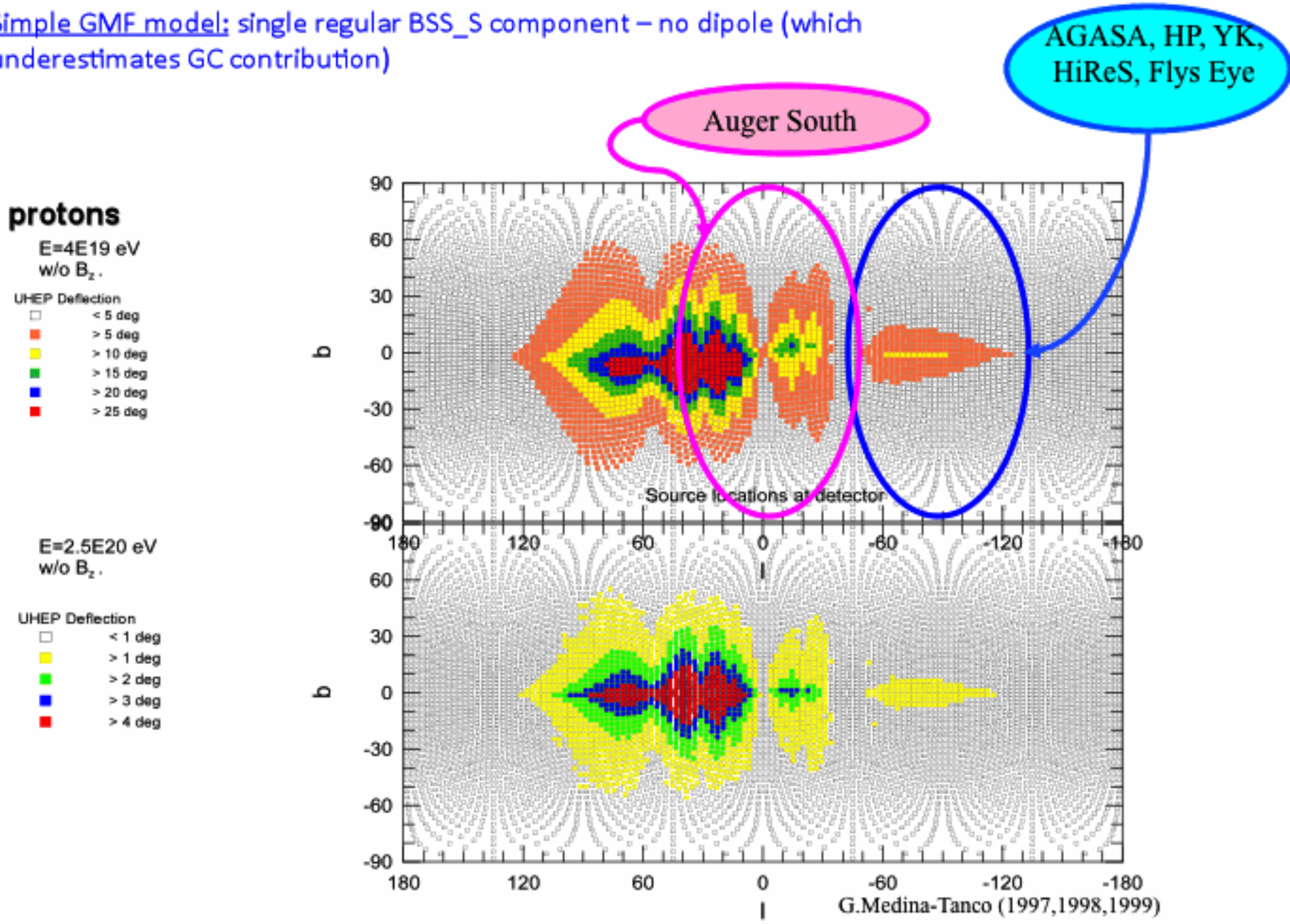

Deflection as a function of arrival direction

iron E=4E19 eV
w/o Bz

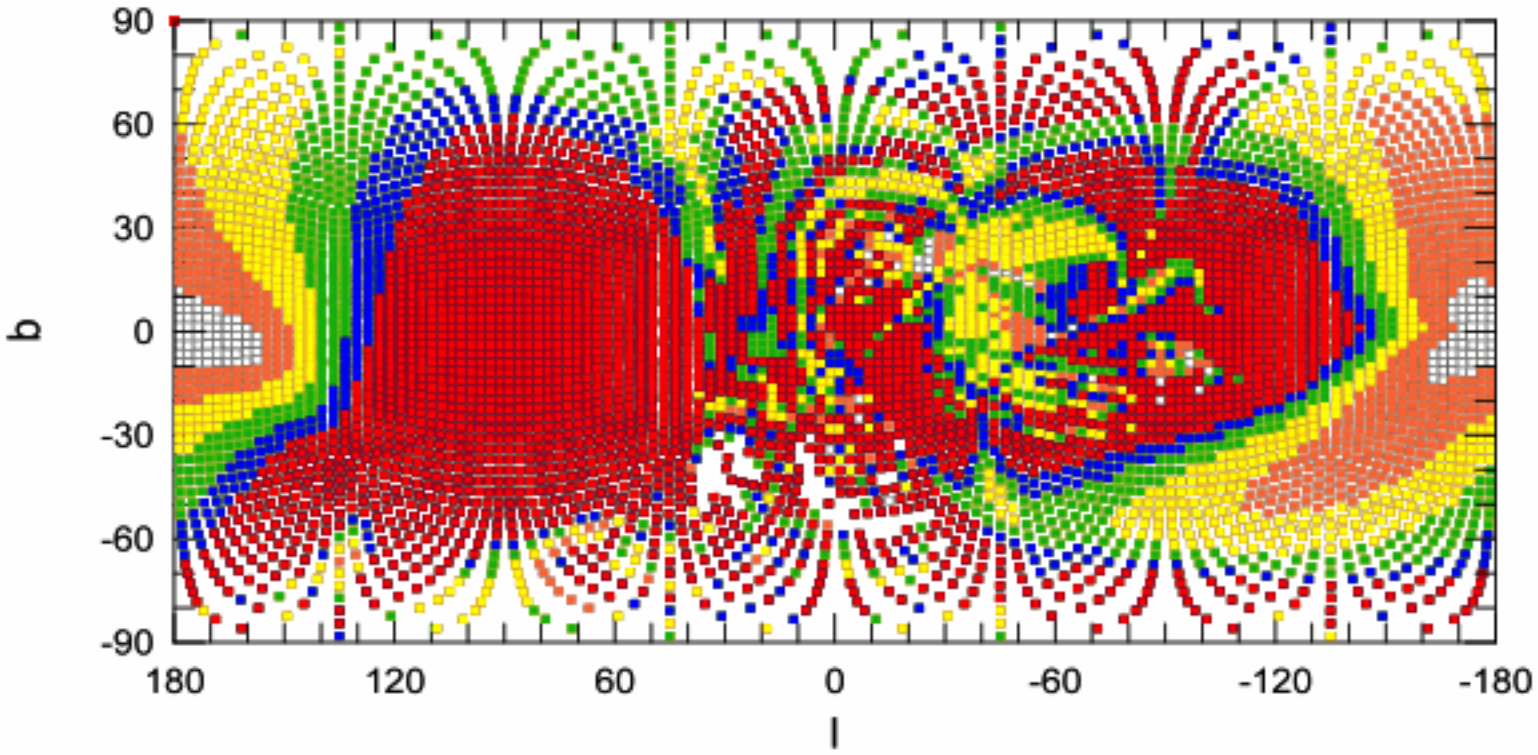

UHEP Deflection

- < 10 deg
- > 10 deg
- > 20 deg
- > 30 deg
- > 40 deg
- > 50 deg

G.Medina-Tanco (1997,1998,1999)

Proton deflection in a more realistic environment?

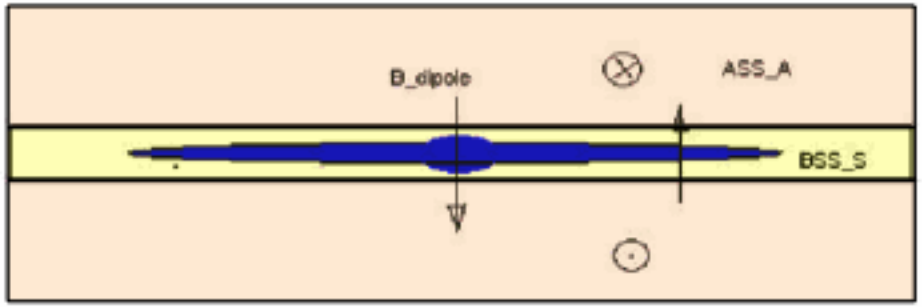

$E=10^{20}$ eV

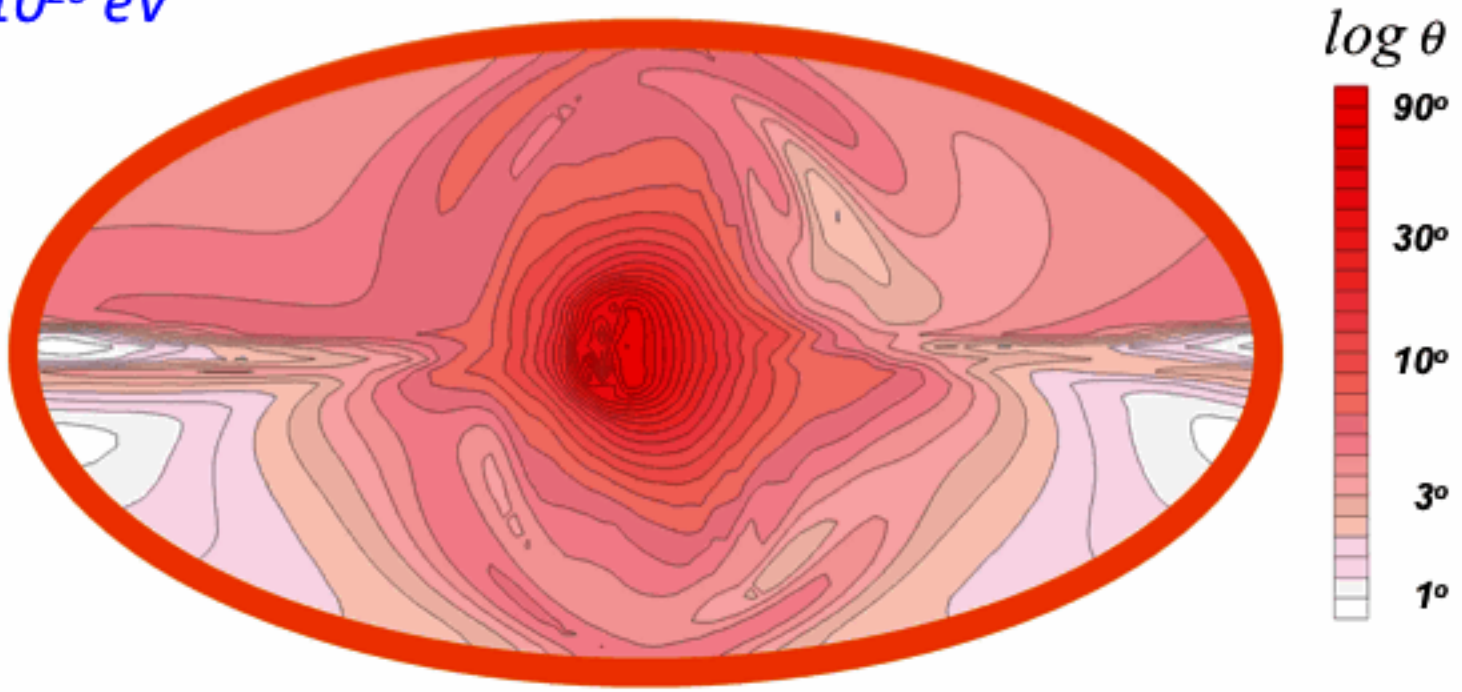

The Galactic center & extragalactic compact high energy regions

The Galactic center

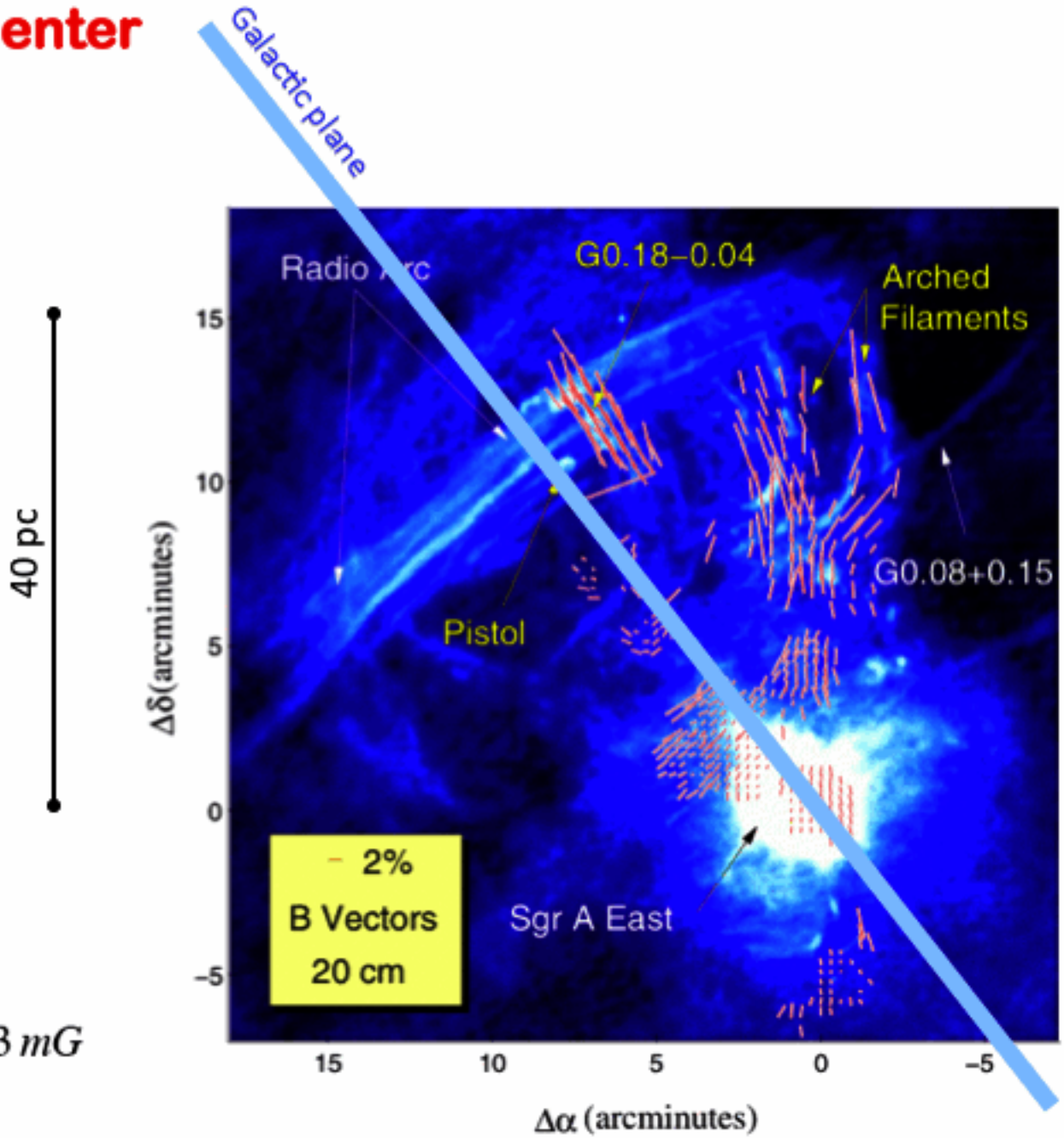

Chuss et al. (2003)

Polarimetry @ 350 μm

$$\langle B(r < 30\,pc) \rangle \approx 3\,mG$$

Gustavo Medina Tanco – gmtanco@gmail.com

The Galactic center

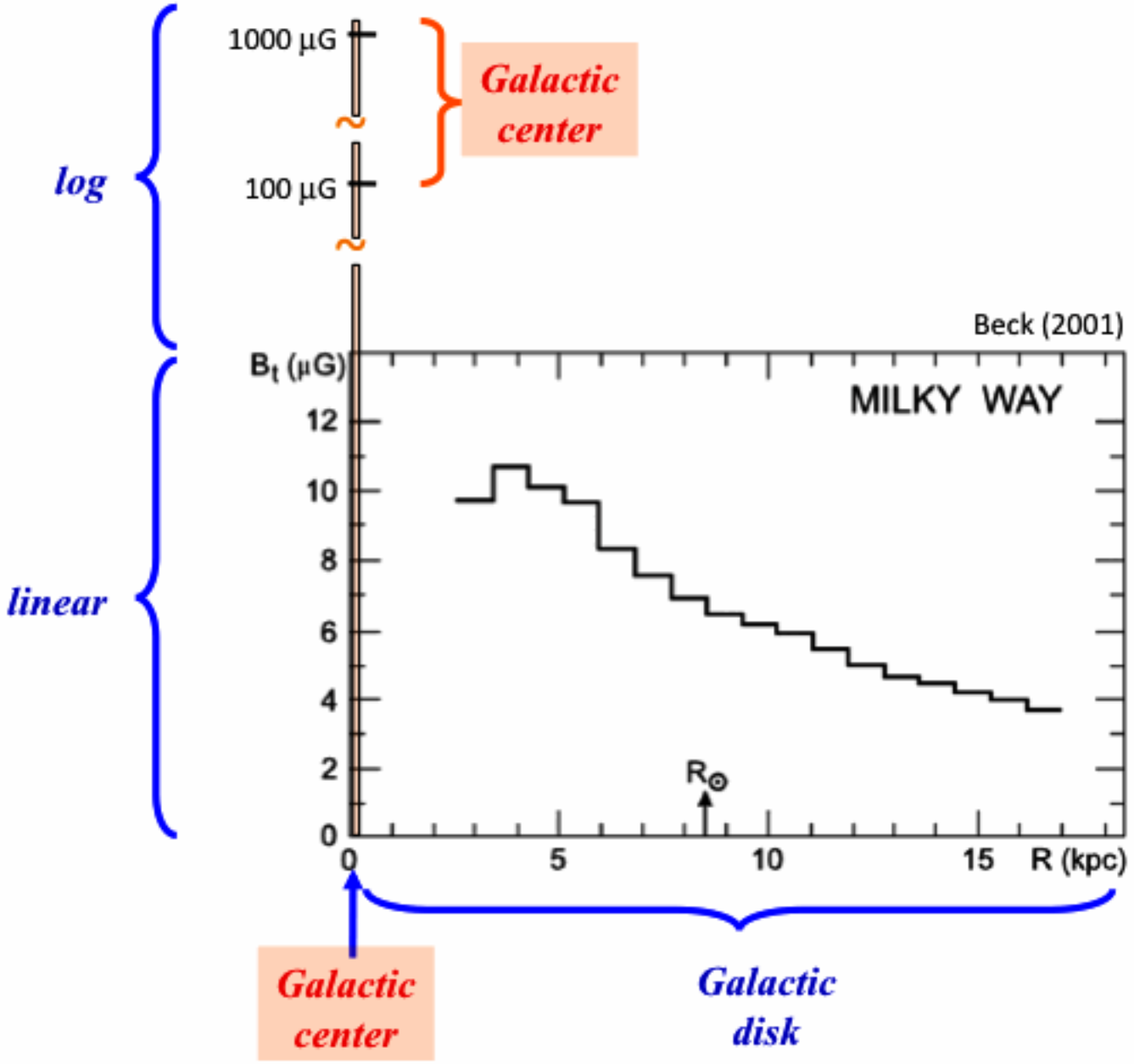

GC matter density distribution

Brogan et al. (2003) **740 MHz - CO**

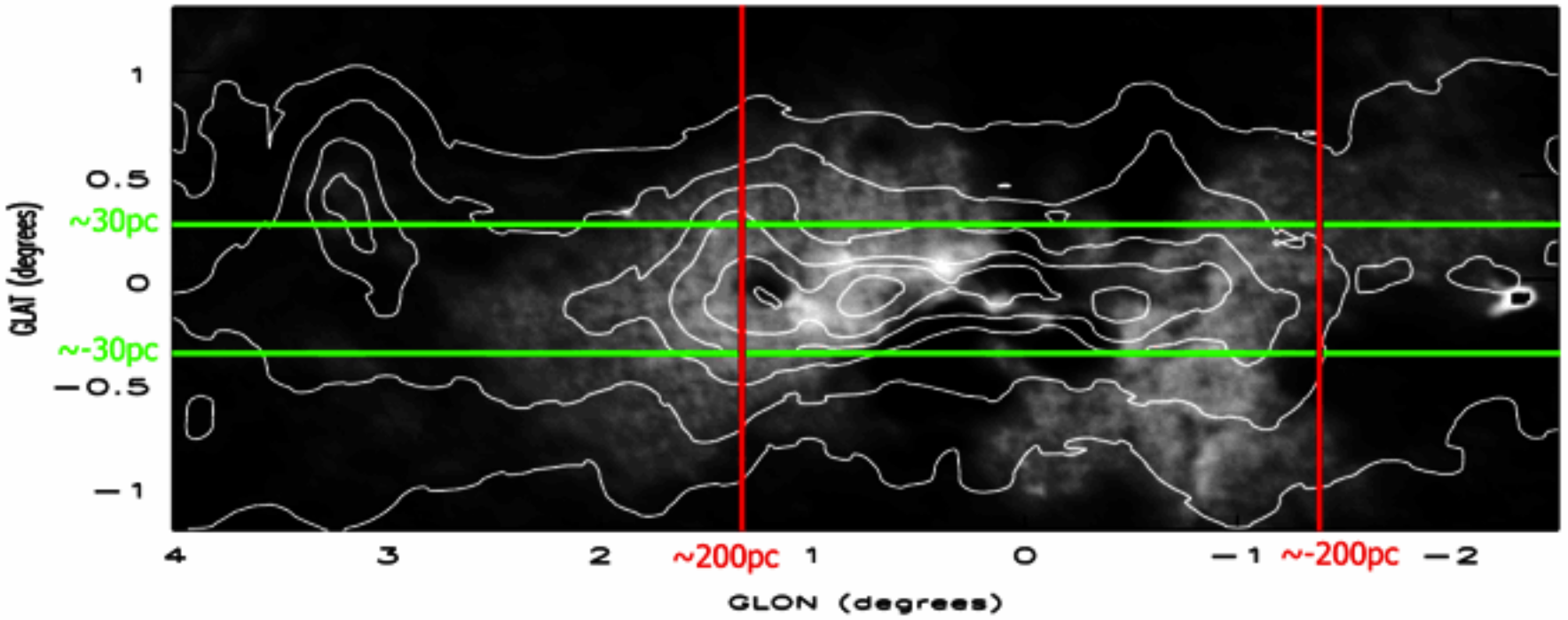

$$n(\rho, z) = n_0 e^{-z/Hz} = 10^{4.5} e^{-z[pc]/30pc} cm^{-3}$$

Gustavo Medina Tanco – gmtanco@gmail.com

Larmor radius of p & Fe nuclei at $\rho \sim$ *few x 10* pc and $\rho \sim$ *200* pc from the Galactic Center.

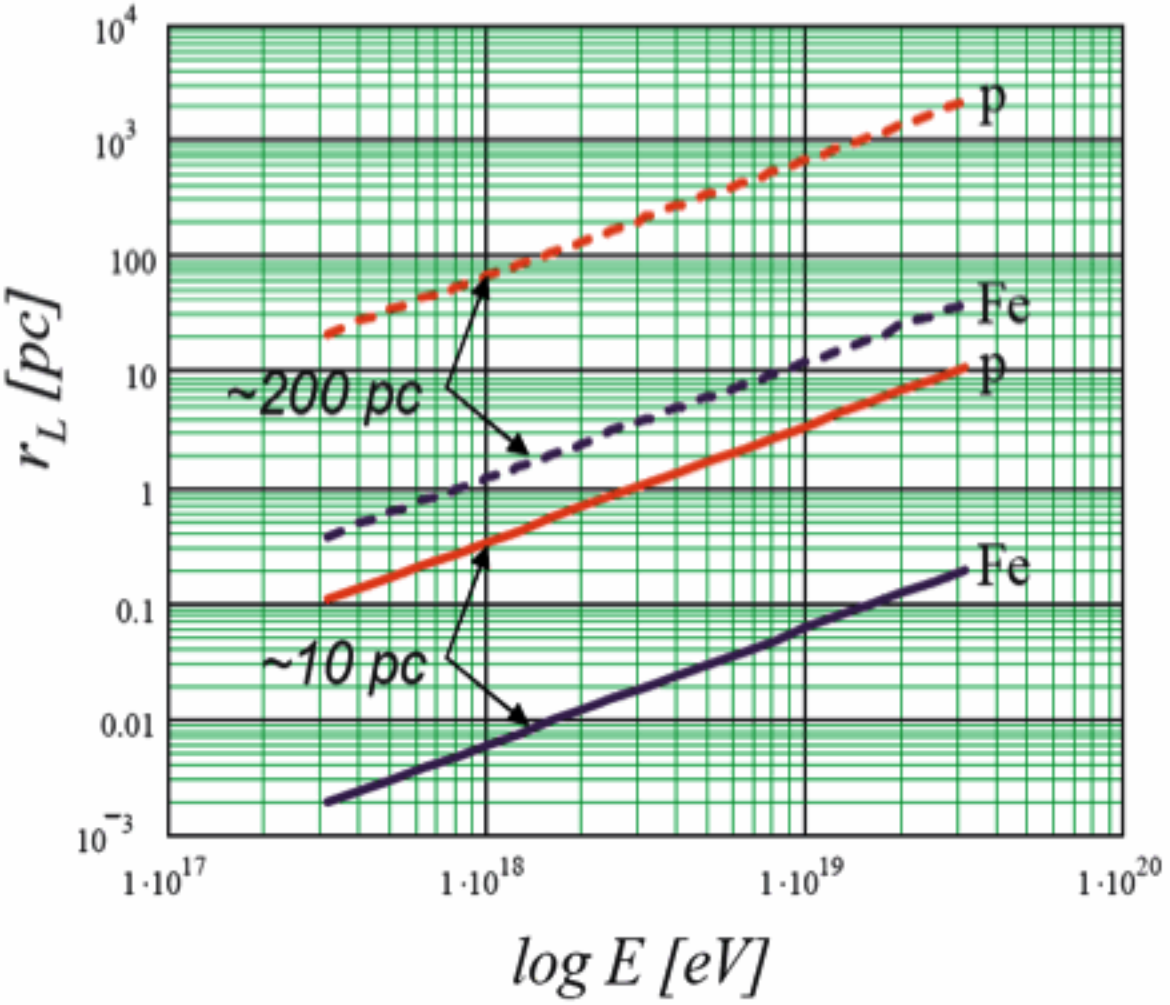

Gustavo Medina Tanco – gmtanco@gmail.com

Partial trapping of EeV CRs

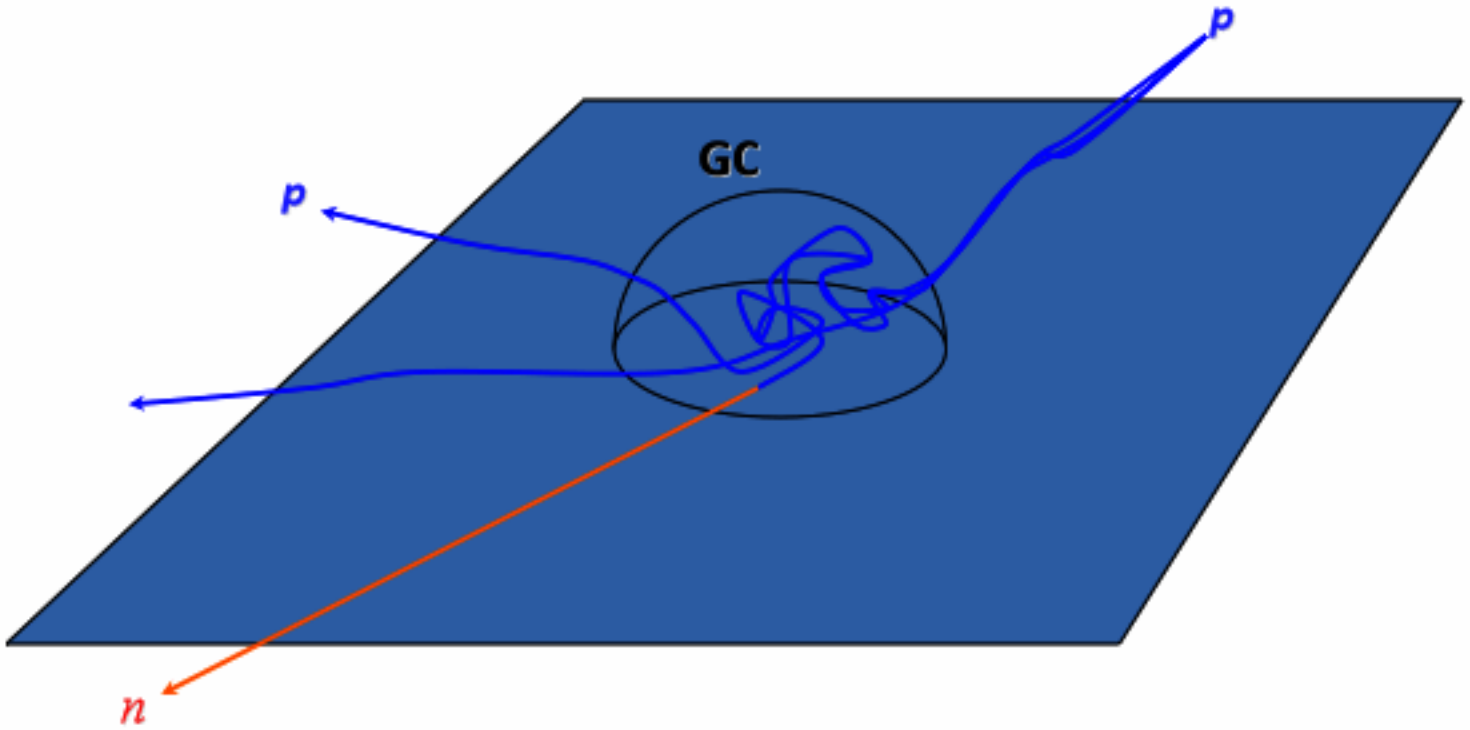

Gustavo Medina Tanco – gmtanco@gmail.com

Neutron conversion of "delayed" protons

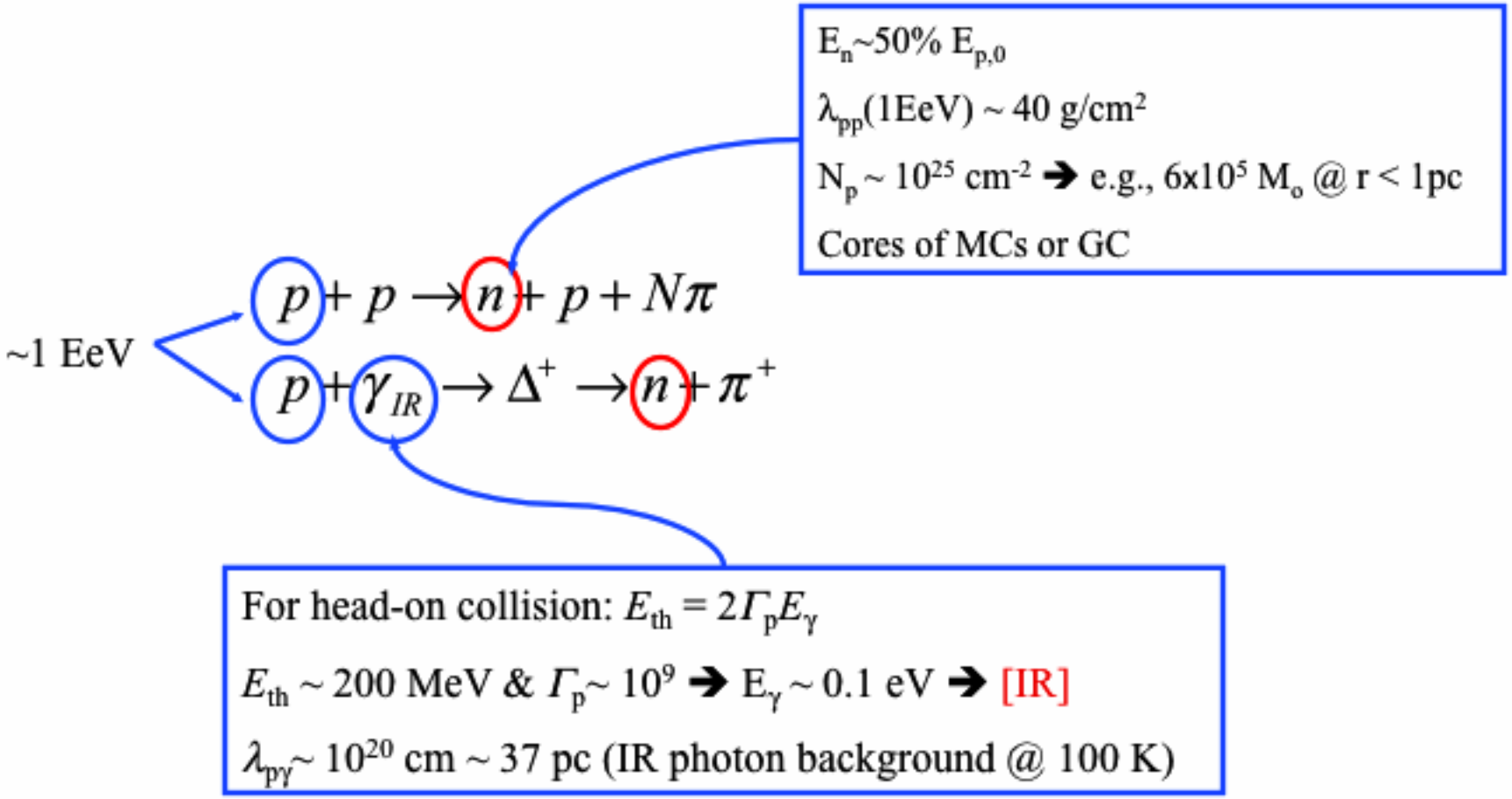

Gustavo Medina Tanco – gmtanco@gmail.com

NEUTRON PRODUCTION @ GC - SIMULATIONS – E ~ 1 EeV

REGULAR

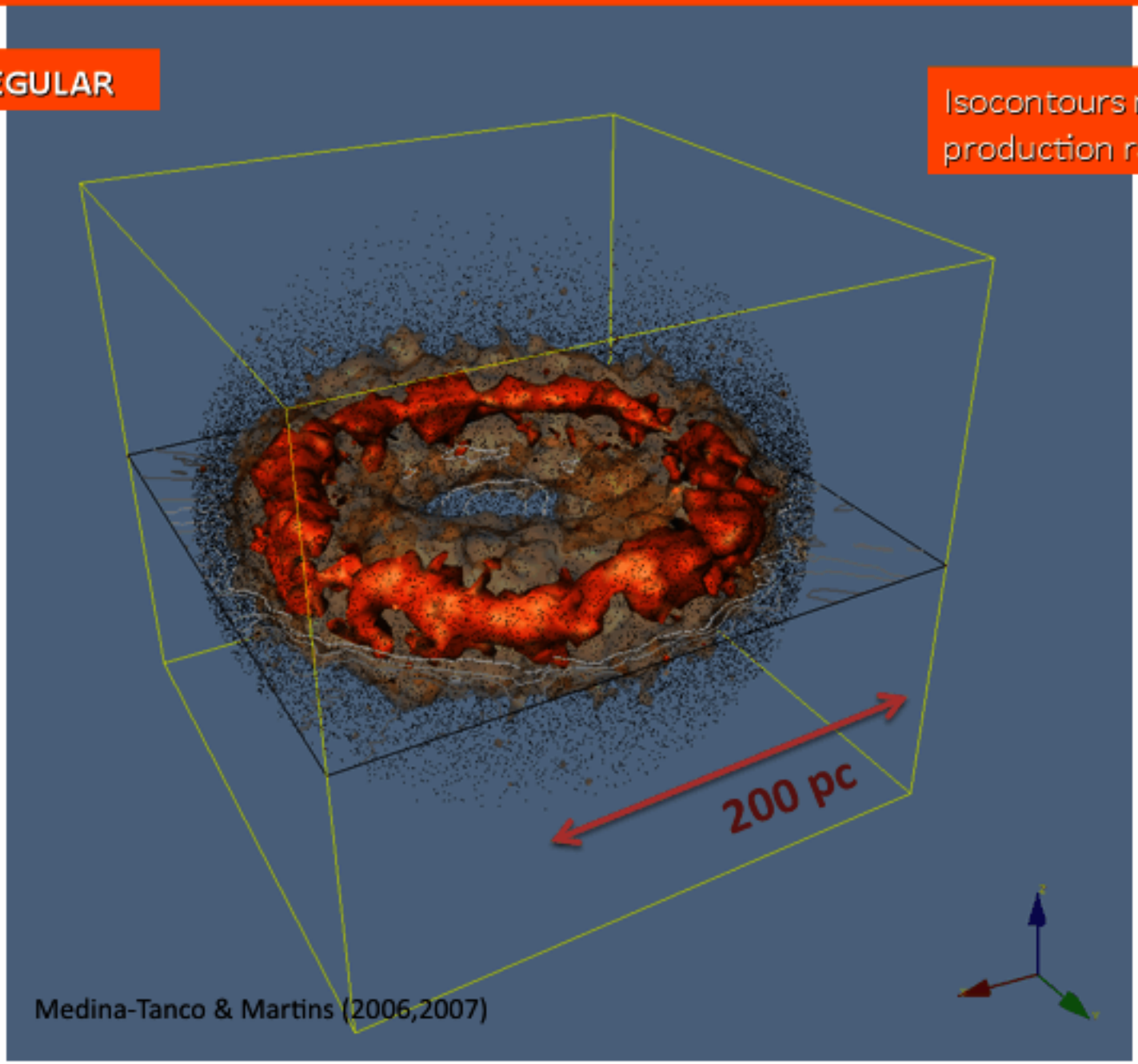

Neutron signal at Earth (@ 1 EeV)

[13n] GMF: ASS
Neutrons injected isotropically at the GC at 1 EeV

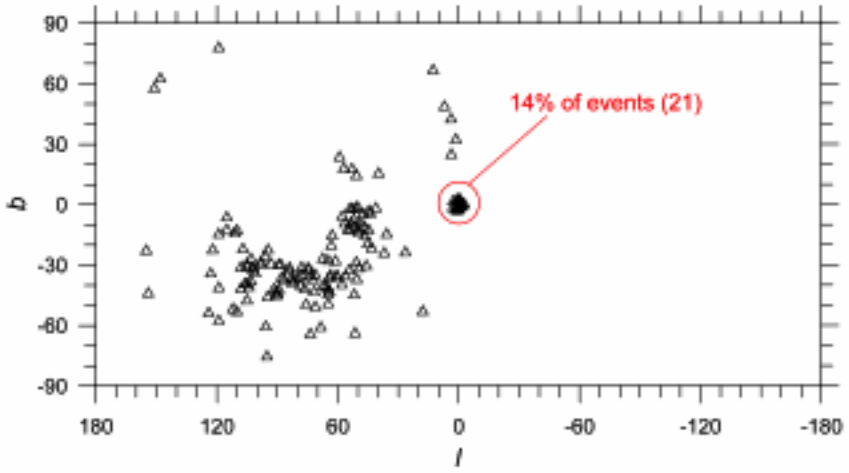

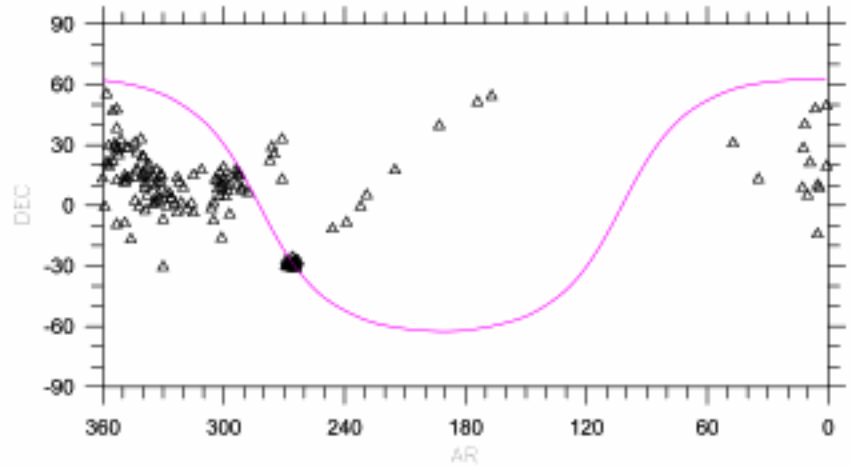

[14n] GMF: BSS
Neutrons injected isotropically at the GC at 1 EeV

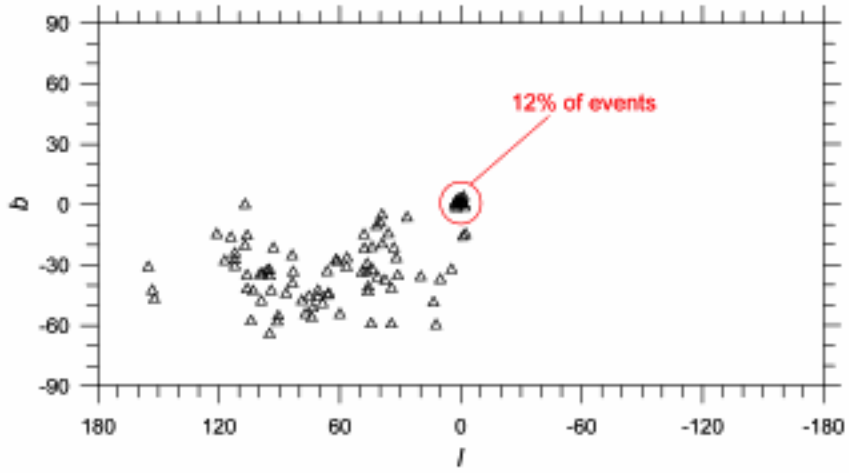

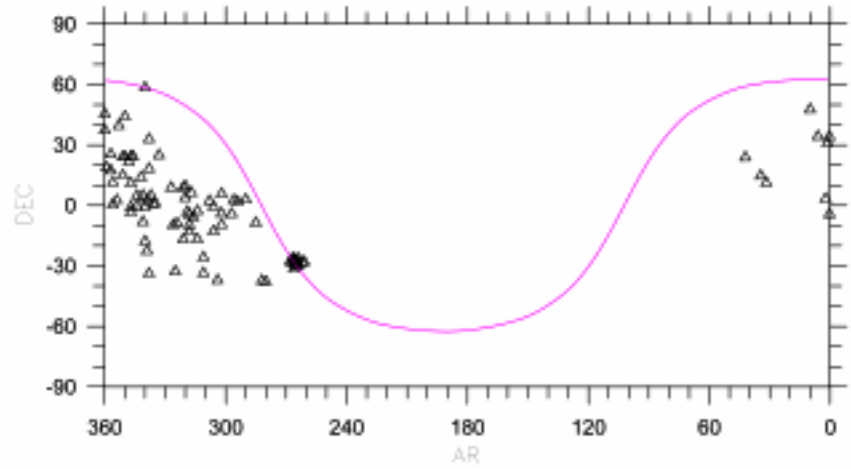

Gustavo Medina Tanco – gmtanco@gmail.com

Neutron signal at Earth (@ 1 EeV)

$\sigma \sim 1.5 - 3.5$

@ $E \sim 1$ EeV

@ $\tau > 5$ yr

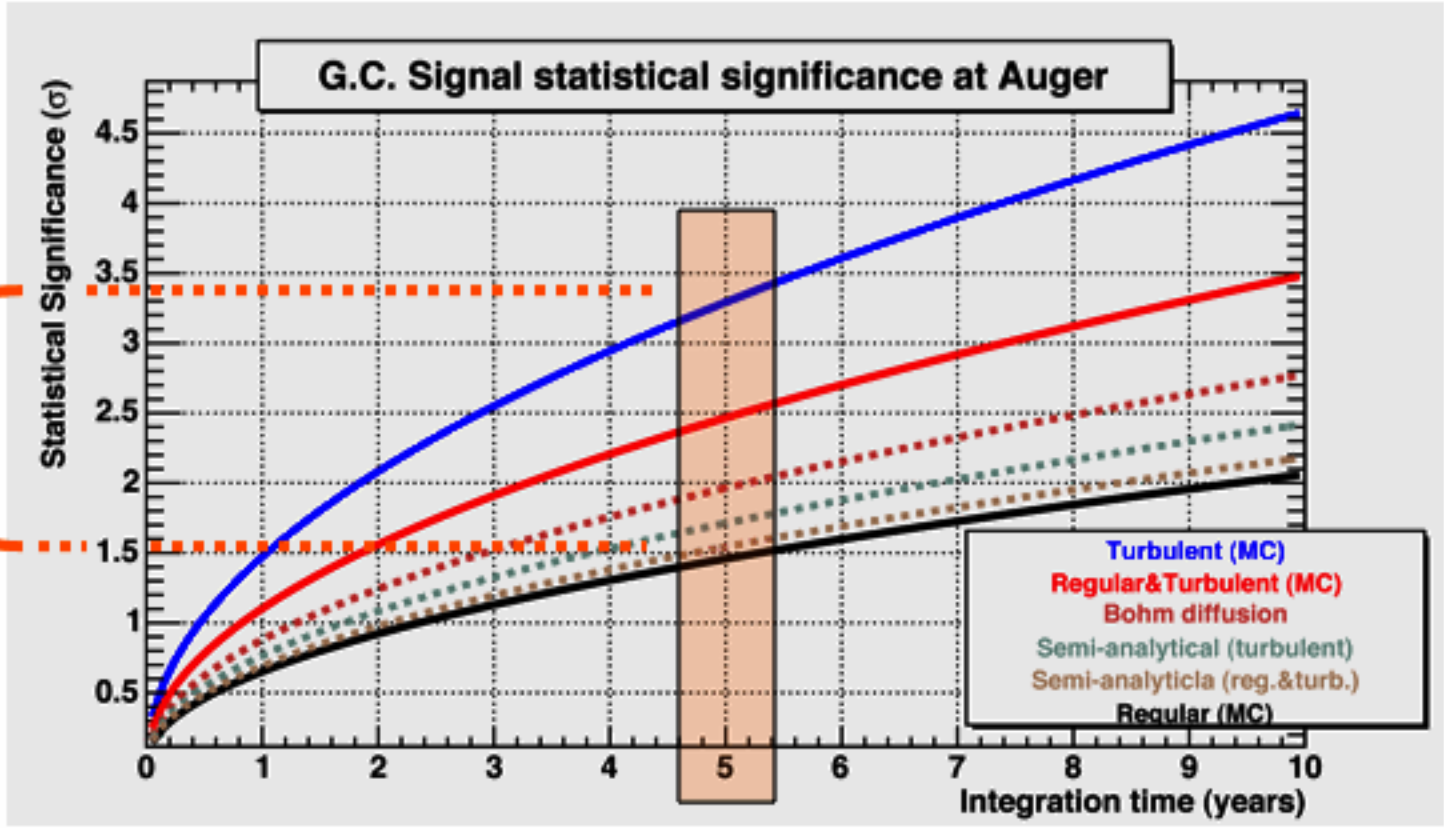

Medina-Tanco & Martins (2006,2007)

GC vs. equivalent extragalactic environments

Compact regions with high intensity magnetic fields, high gas density and/or high IR photon density could act as apparent UHECR sources in some energy range above ~ 10^{18} eV.

Lower energy Galactic CRs

CR energy spectrum

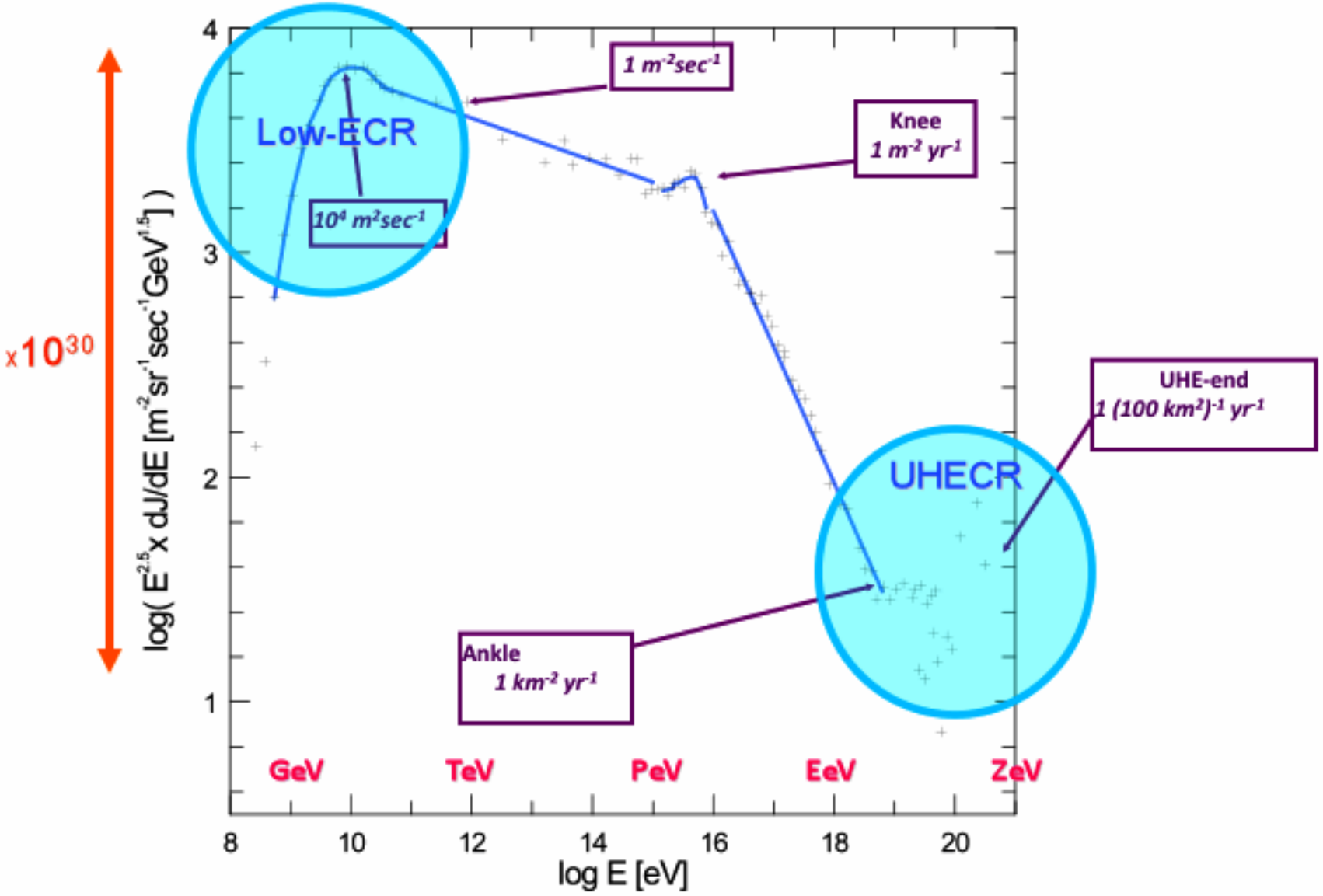

Gustavo Medina Tanco – gustavo.medinatanco@nucleares.unam.mx

CR abundances at the top of the atmosphere

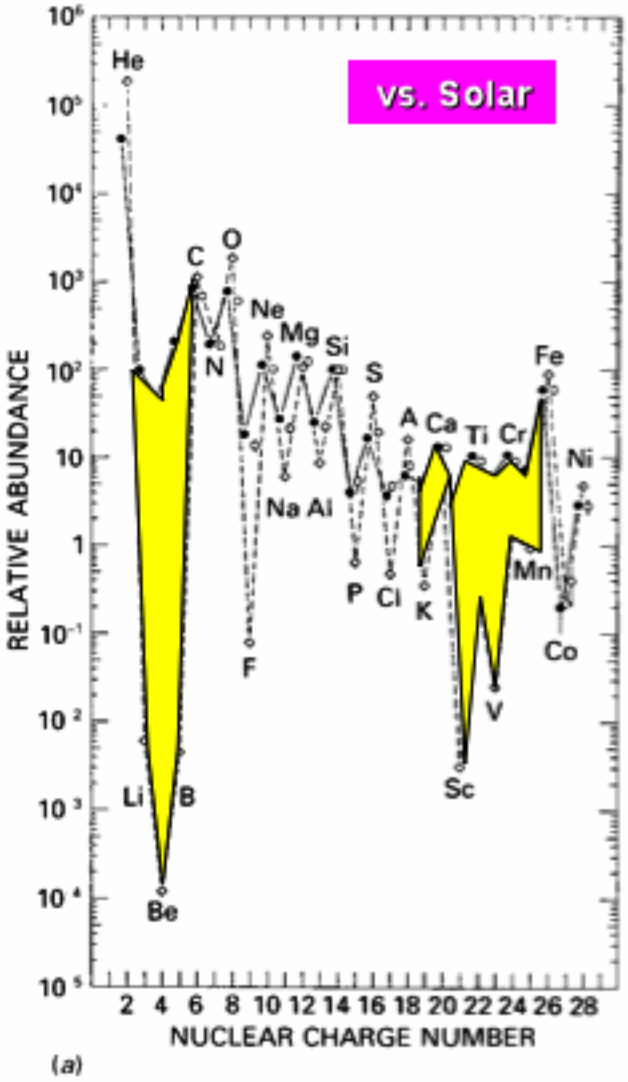

● 70-280 MeV/nuc

○ 1-2 GeV/nuc

◇ Solar System

Spallation in the ISM

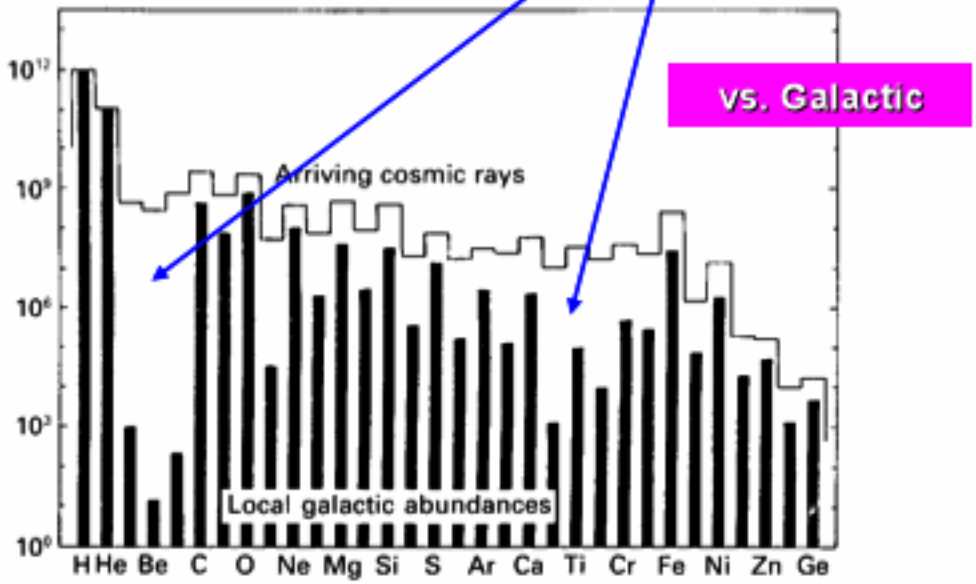

Magnetic fields, propagation and origin

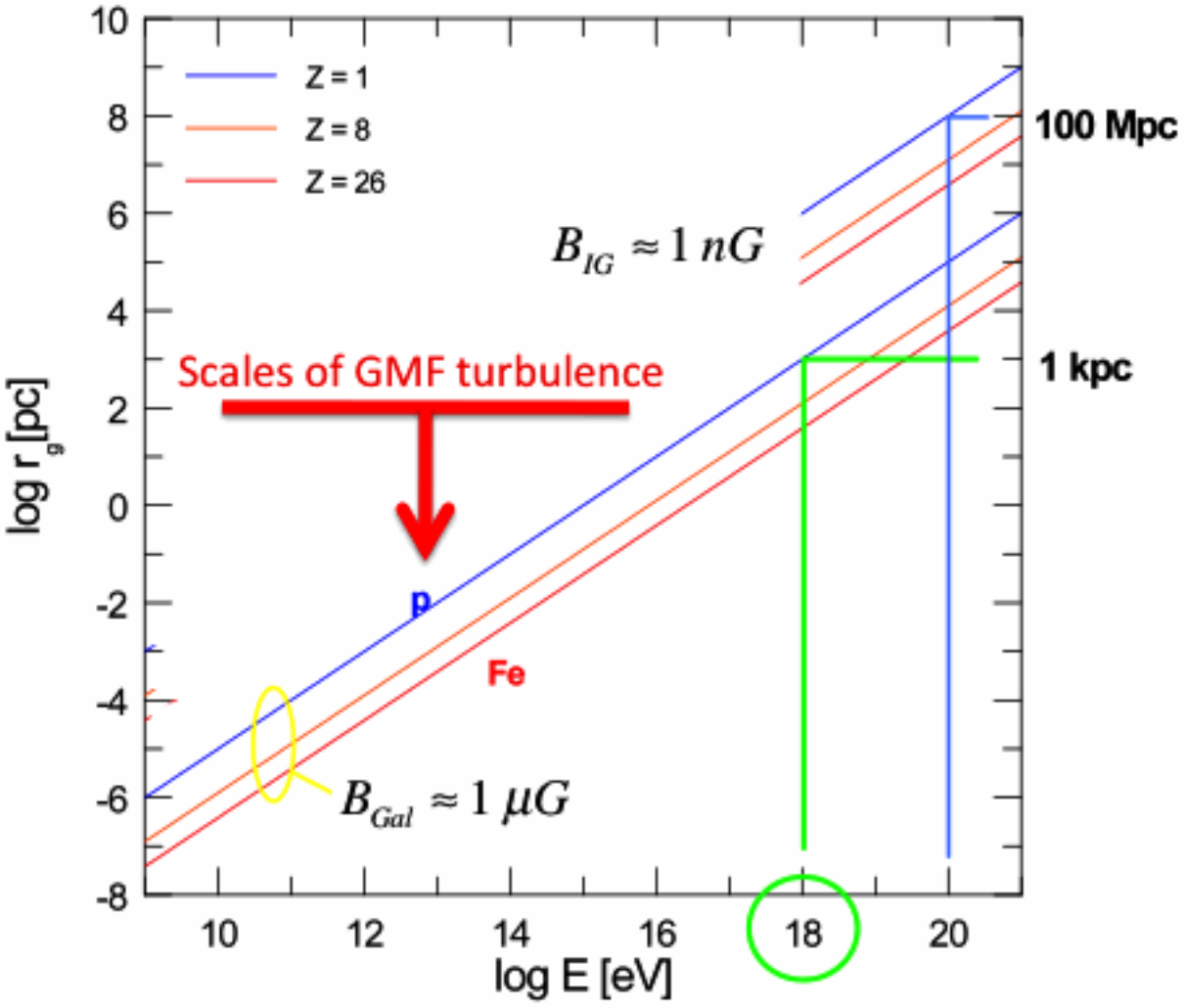

Scattering off magnetic irregularities

Magnetic disturbances are the main cause of momentum scattering of high energy particles.

Magnetic field is frozen in most cosmic media.

An ensemble of almost static MHD waves in some frame, tends to isotropize $f_{CR}(p)$ in that commoving frame

⇒ CR are coupled to the medium through the magnetic field. The coupling is described by the scattering frequency ν_s :

$$\nu_s = \frac{\langle \Delta\alpha^2 \rangle}{\Delta t}$$

The interaction between the particles and B is selective: a particle interacts with the field when its gyro-motion resonates with a Fourier component of wavelength equal to its Larmour radius.

$\lambda < r_L \longrightarrow \langle \Delta\alpha^2 \rangle = 0$

$\lambda > r_L \longrightarrow$ followed adiabatically (no jump in pitch angle)

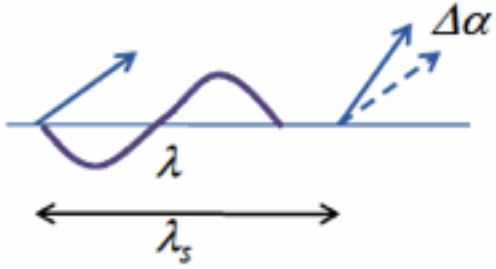

Scattering produces spatial diffusion

$$D_{\parallel} \equiv \frac{\langle \Delta x^2 \rangle}{2\Delta t} = \frac{1}{3} v^2 t_s \quad \text{with} \quad t_s \equiv \frac{1}{\langle \mu(t)^2 \rangle} \int_0^{\infty} \langle \mu(t)\mu(t-\tau) \rangle d\tau$$

$$D_{\perp} = D_{\parallel} \frac{1}{1 + (\omega_L t_s)^2}$$

$B_0 \equiv 0 \Rightarrow D_{\perp} \equiv D_{\parallel}$

$B_0 \approx B \Rightarrow D_{\perp} \ll D_{\parallel}$

Typial values of the diffusion coefficient

Intergalactic space

$D \approx 3\times10^{21}\,\beta P_{GV}\ \mathrm{cm}^2/s$

$D \approx 10^{34}\ \mathrm{cm}^2/\mathrm{s},\ \mathrm{at}\ 10^{19}\ \mathrm{eV}$

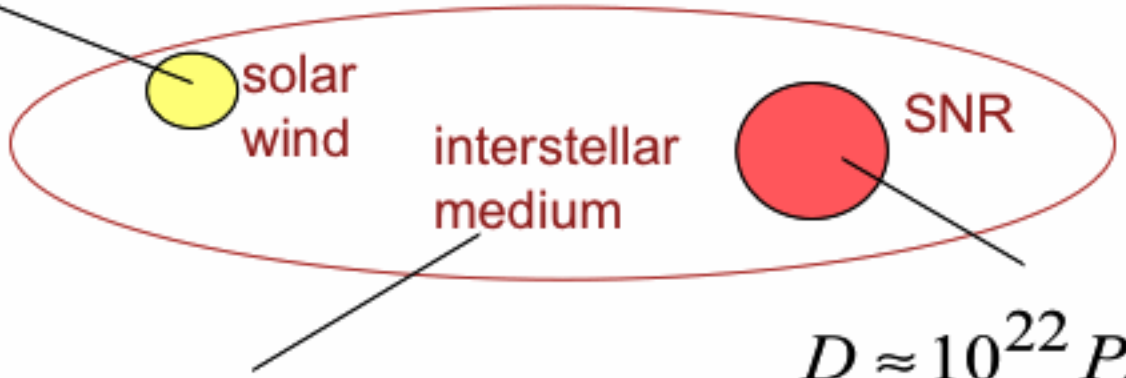

$D \approx 10^{22} P_{GV}\ \mathrm{cm}^2/s$

$D \approx 3\times10^{28} P_{GV}^{a}\ \mathrm{cm}^2/\mathrm{s},\quad a = 0.3-0.5$

$P = \frac{pc}{Z}$ - magnetic rigidity

Transport equation

$N_i(E,x,t)dE$ ➔ Density of particles of type i at x with energy in E, $E+dE$

diffusion

Energy losses and acceleration

convection

Source term

$$\frac{\partial N_i}{\partial t} = \nabla\cdot\left(D_i\nabla N_i\right) - \frac{\partial}{\partial E}\left[b_i(E)N_i(E)\right] - \nabla\cdot\vec{u}N_i(E) + Q_i(E,t)$$

$$- p_i N_i + \frac{vp}{m}\sum_{k\geq i}\int\frac{d\sigma_{i,k}(E,E')}{dE}N_k(E')dE'$$

Losses of nuclei i by collision and decay

Feed-down from higher energy: e.g., nuclear fragmentation

$$p_i = \frac{v\rho\sigma_i}{m} + \frac{1}{\gamma\tau_i}$$

Confinement region extends beyond the Disk

Halo: magnetic field but
almost no matter traversed

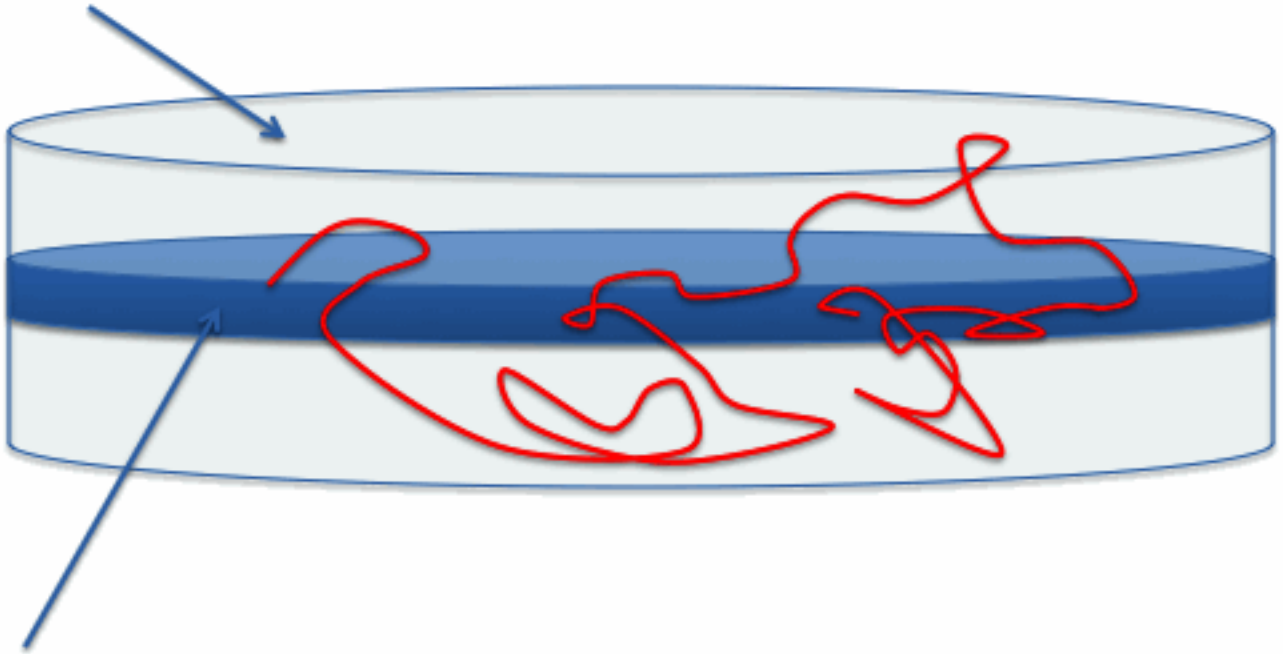

Disk: both, magnetic field
and matter

Testing the SNR acceleration / diffusion model

The Galactic Diffuse Emission

Diffuse emission is readily calculated … with only a few assumptions

Galactic cosmic-ray distribution of electrons and nucleons (+ He, heavies)

Galactic matter distribution of atomic, molecular, and ionized hydrogen

$$j(E_{\tilde{a}}, l, b) = \frac{1}{4\pi}\int (c_e \cdot q_{eb} + c_n \cdot q_{nn}) \times (n_{\mathrm{H\,I}} + n_{H2} + n_{\mathrm{H\,II}})\, d\rho +$$

$$\frac{1}{4\pi}\sum_i \int c_e \cdot q_{ic,i} \cdot u_{ic,i}\, d\rho \quad [\mathrm{ph\ cm^{-2}\ s^{-1}\ sr^{-1}\ GeV^{-1}}]$$

Gamma-ray production functions electron bremsstrahlung, nucleon-nucleon (π^o), and inverse Compton Synchrotron emission is not significant

Low-energy photon energy density cosmic microwave background, infra-red, visible, and ultraviolet

Testing the SNR acceleration / diffusion model

EGRET diffuse γ data modeling

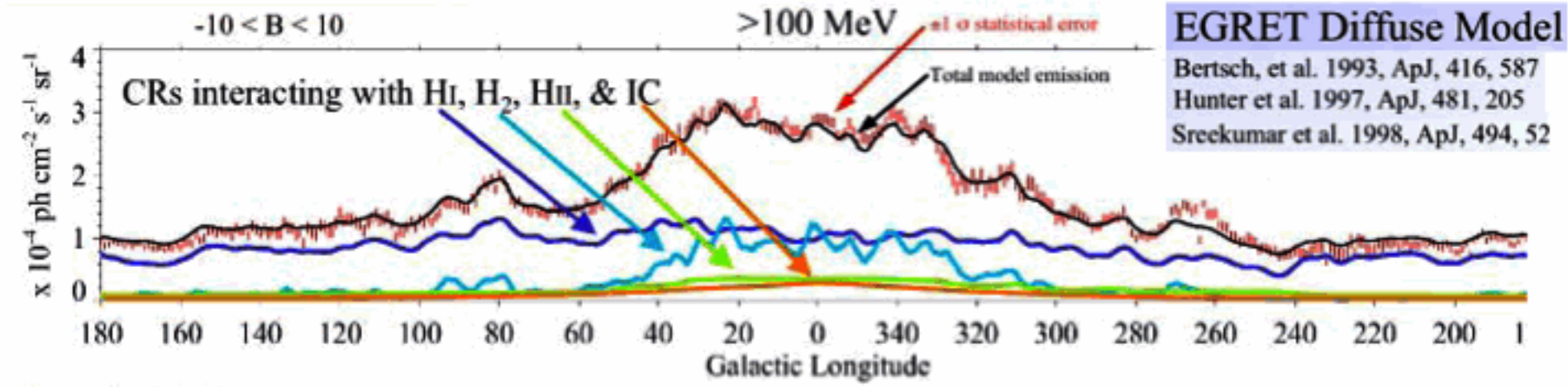

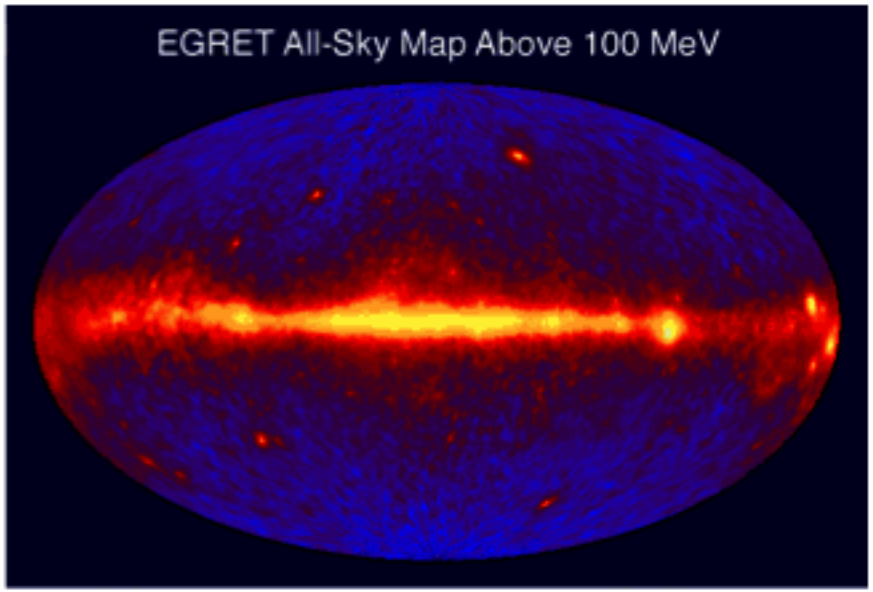

2D correlation in arrival directions & “intrinsic” point spread function

2D Correlation function of arrival directions in galactic coordinates (AGASA)

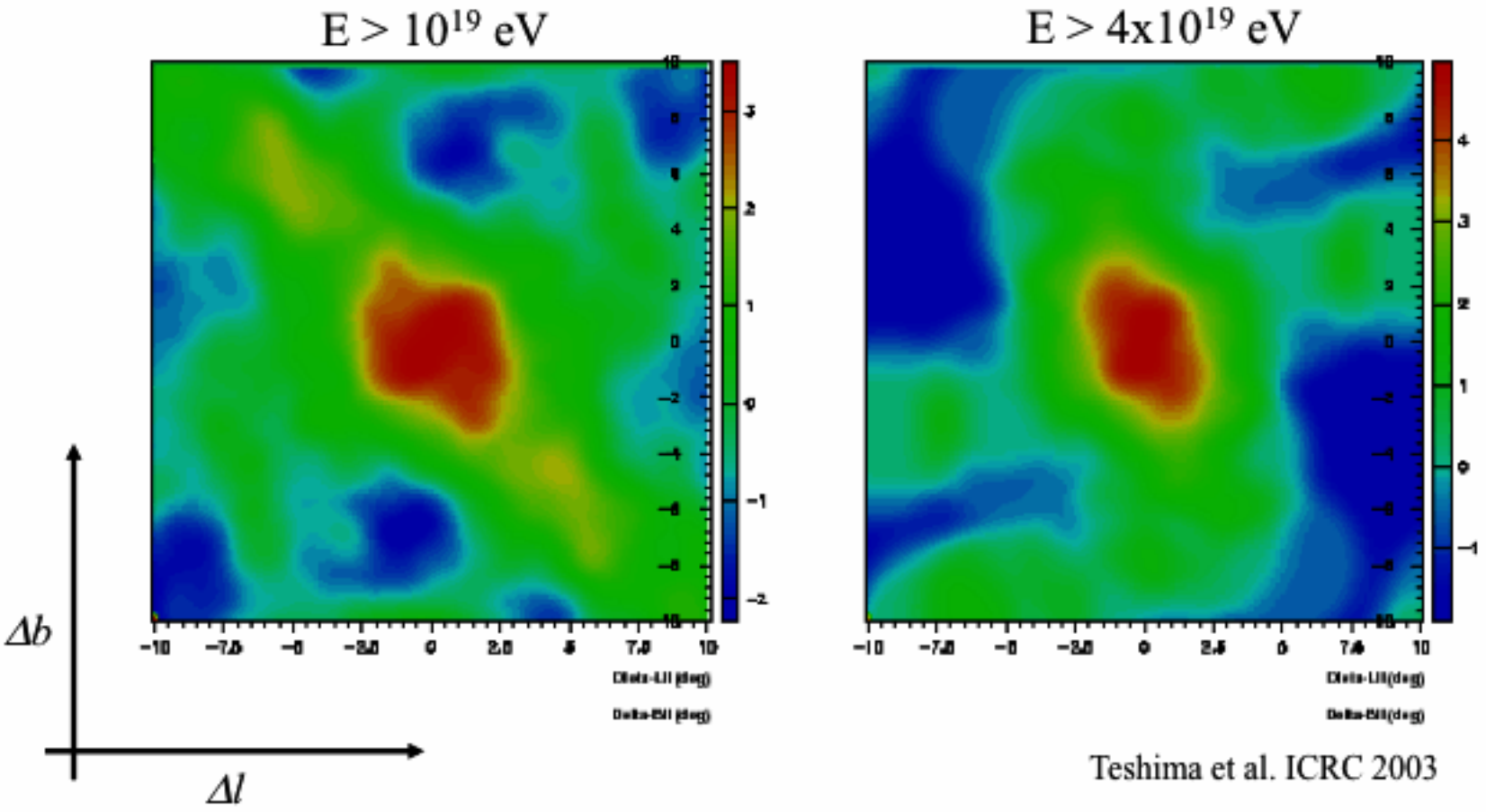

Teshima et al. ICRC 2003

2D Correlation function of arrival directions

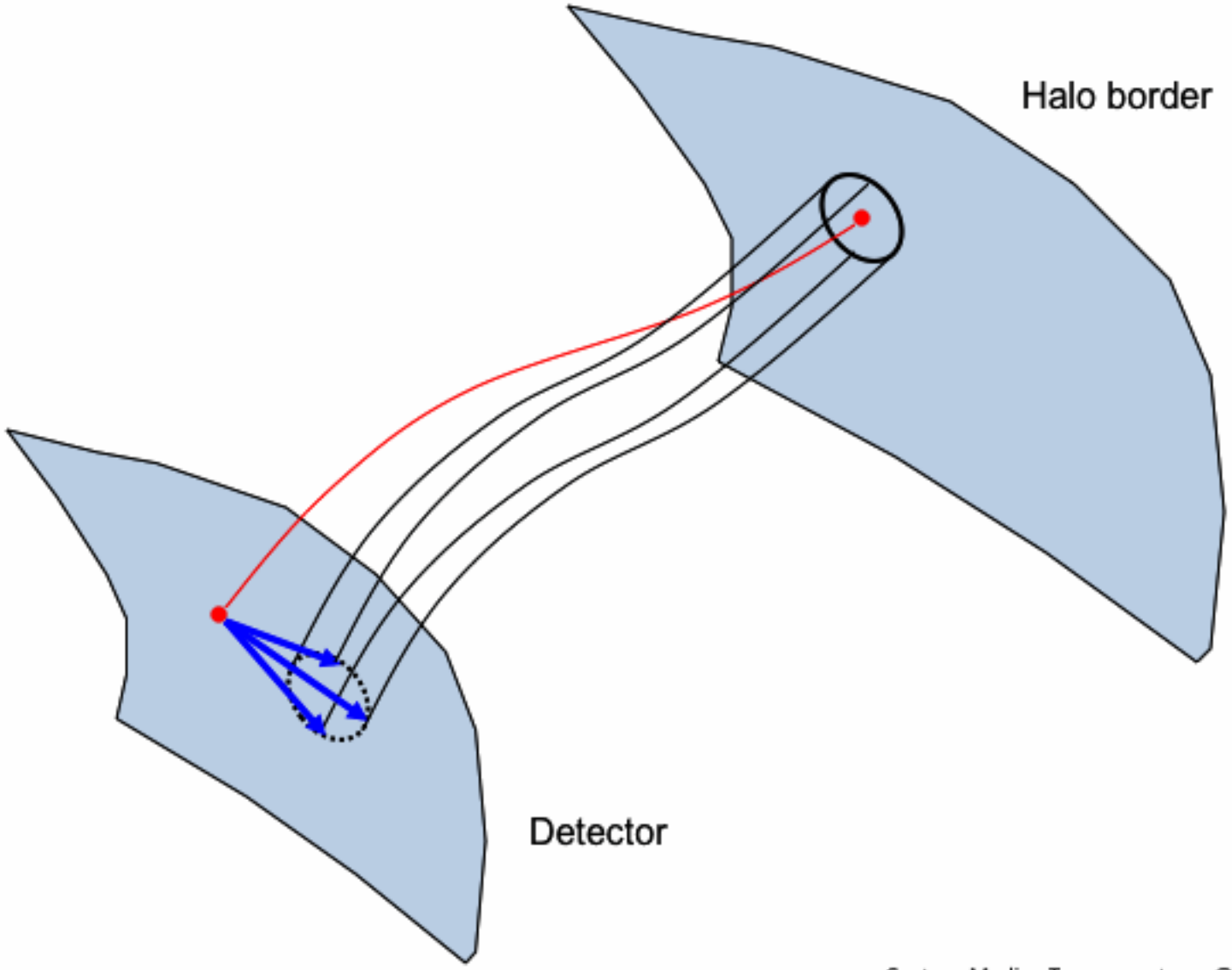

Gustavo Medina Tanco – gmtanco@nucleares.unam.mx

2D Correlation function of arrival directions

CHARGED UHECR + large scale regular GMF

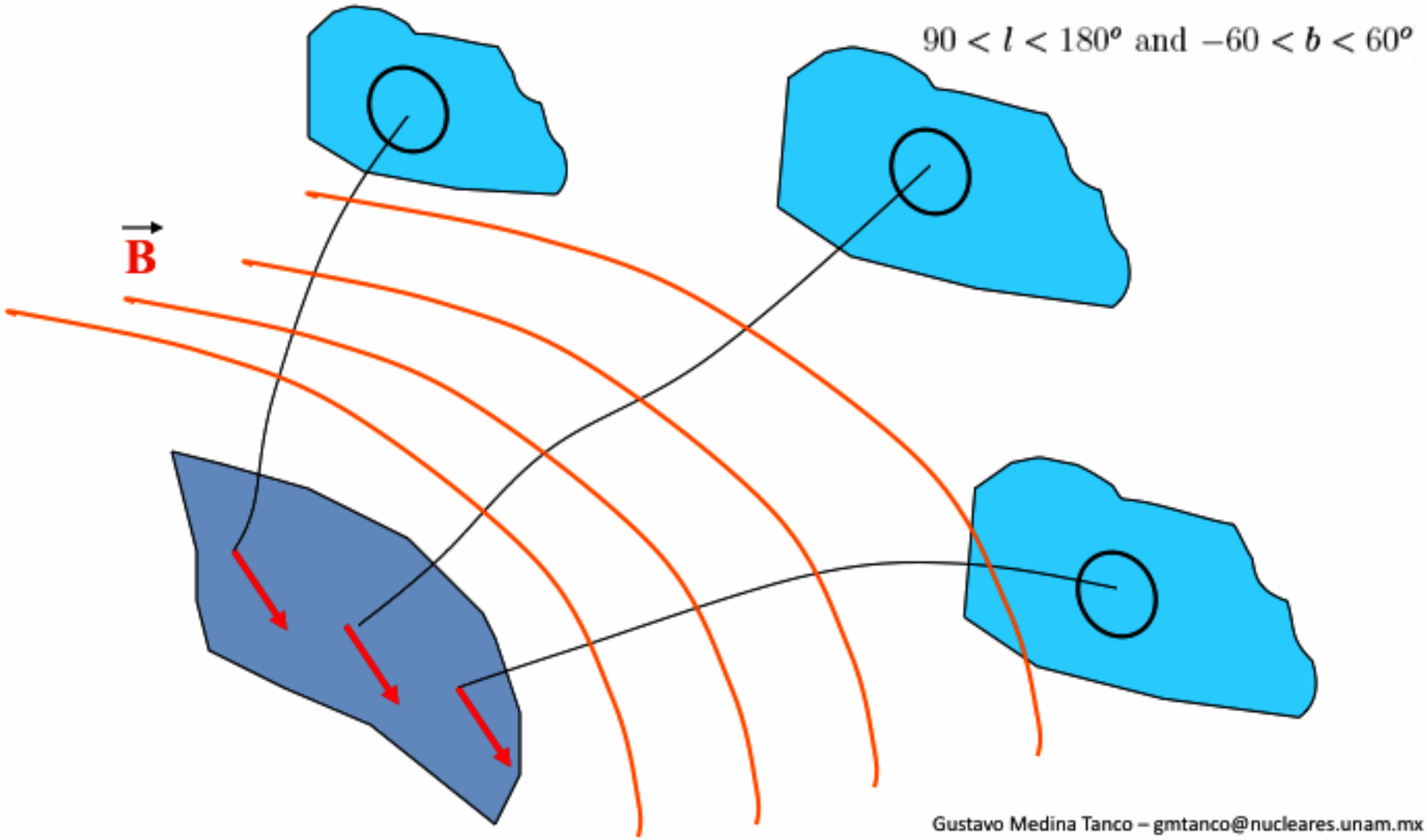

Gustavo Medina Tanco – gmtanco@nucleares.unam.mx

2D Correlation function of arrival directions

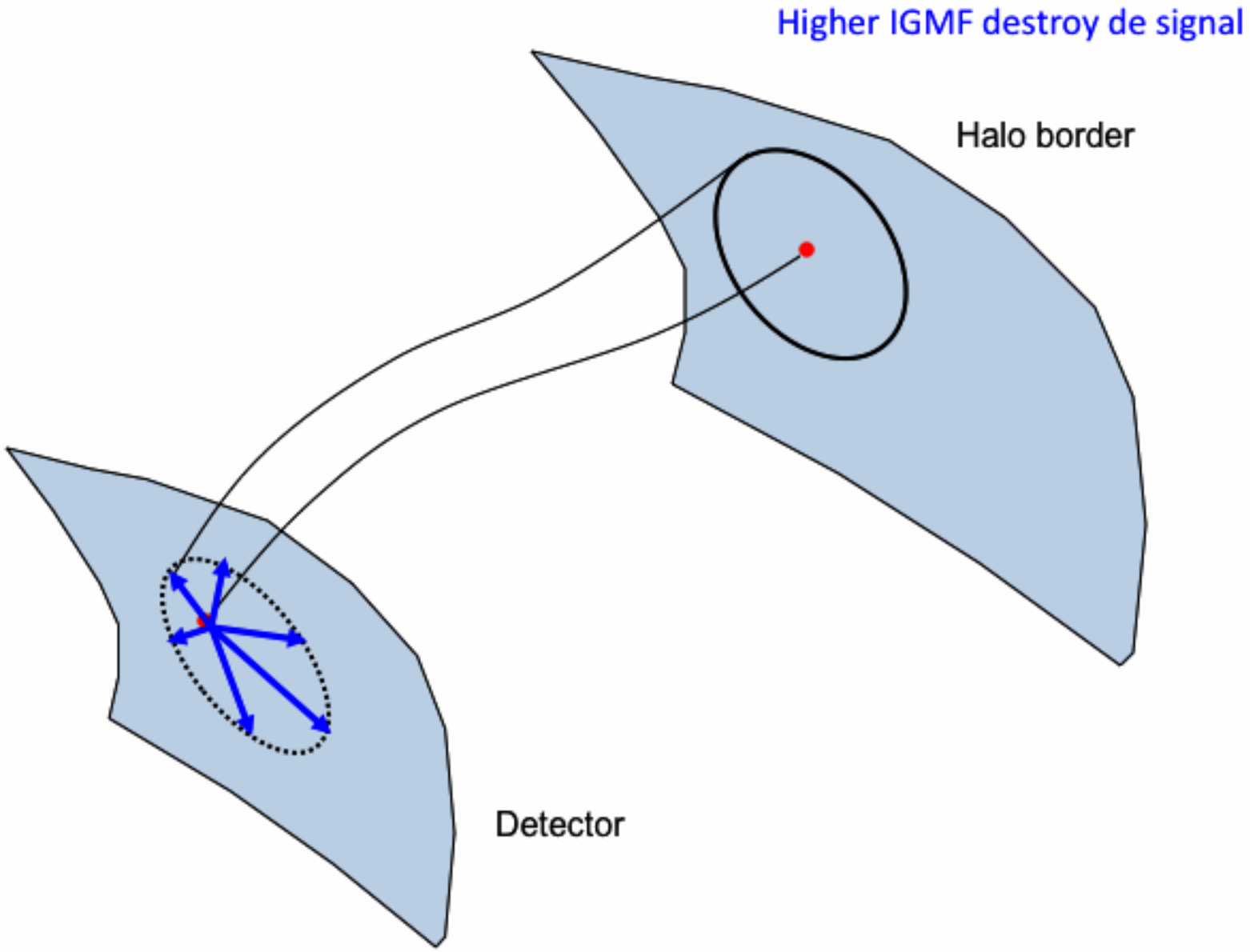

NEARBY sources + low IGMF

$$\delta\theta \sim 0.07^{o} \times Z \times \left(\frac{E}{10\,EeV}\right) \times \left(\frac{D}{L_c}\right)^{1/2} \times \left(\frac{L_c}{1Mpc}\right) \times \left(\frac{B}{10^{-9}G}\right)$$

$$\delta\theta < 2^{o}\ , E \approx 10^{19}\,\mathrm{eV}, L_c \approx 1\ \mathrm{Mpc} \Rightarrow \boxed{B < \frac{3\times 10^{-8}\,\mathrm{G}}{D_{\mathrm{Mpc}}^{1/2}}}$$

Along the line of sight to the point sources responsible for the linear signal

A consistent picture is difficult to obtain unless one assumes that the linear feature in the 2D correlation function is the result of:

1. charged UHECR particles,
2. a large scale regular component of the magnetic field extending through the Galactic plane and halo,
3. the existence of at least a few relatively nearby point sources of UHECR and
4. a relatively low intergalactic magnetic field between those nearby sources and the external border of the Galactic halo.

For 2D signal individual sources do not need to be resolved, but with higher statistics (JEM-EUSO?) they might be resolved… However, even then, IGMF + GMF can complicate severely the picture.

Point EG sources and IGMF & GMF

Source towards the **outskirts** of the MW

GMF most plausible model:
BSS@disk + ASS@Halo + dipole

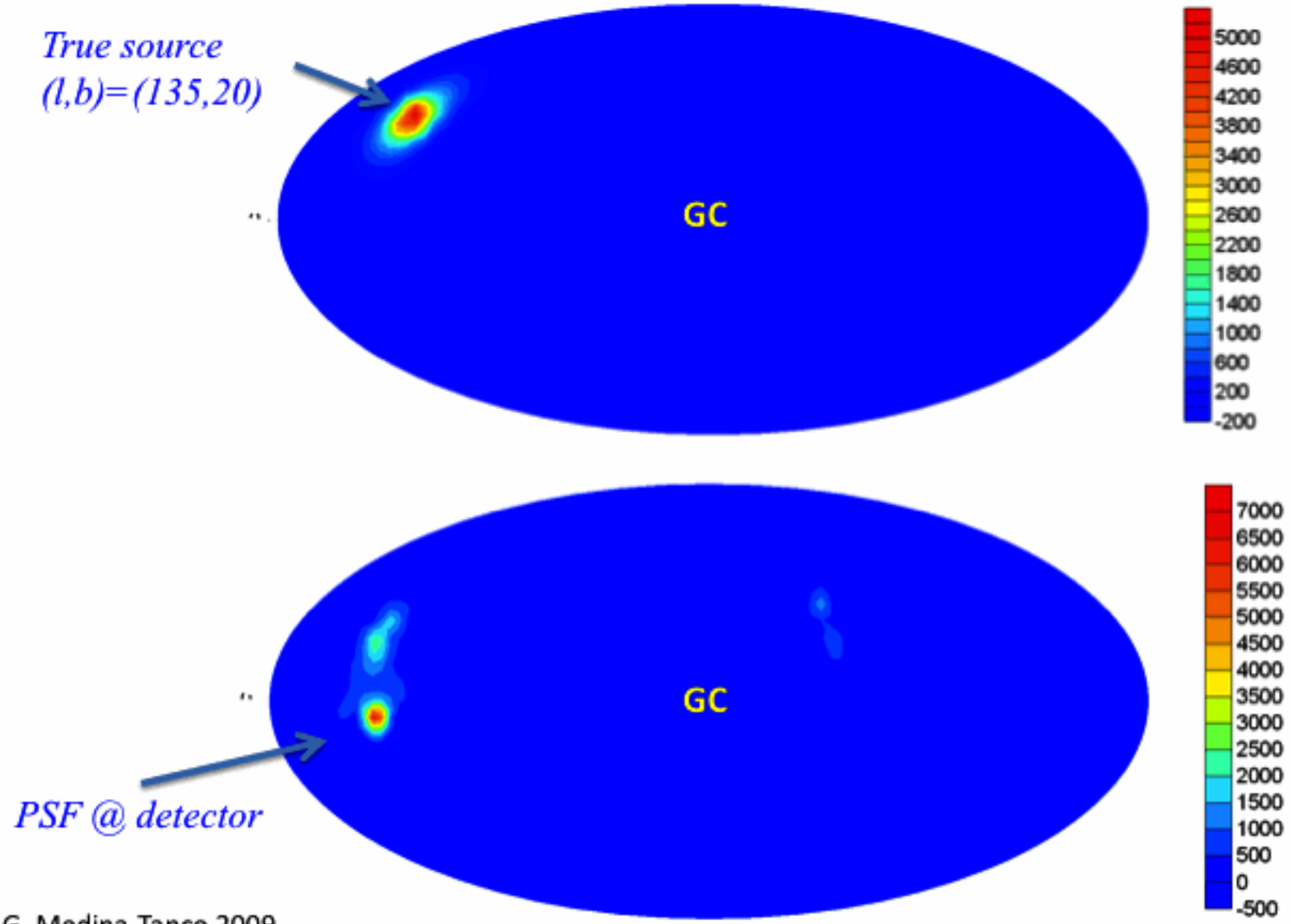

G. Medina-Tanco 2009

Point EG sources and IGMF & GMF

Source towards the **outskirts** of the MW

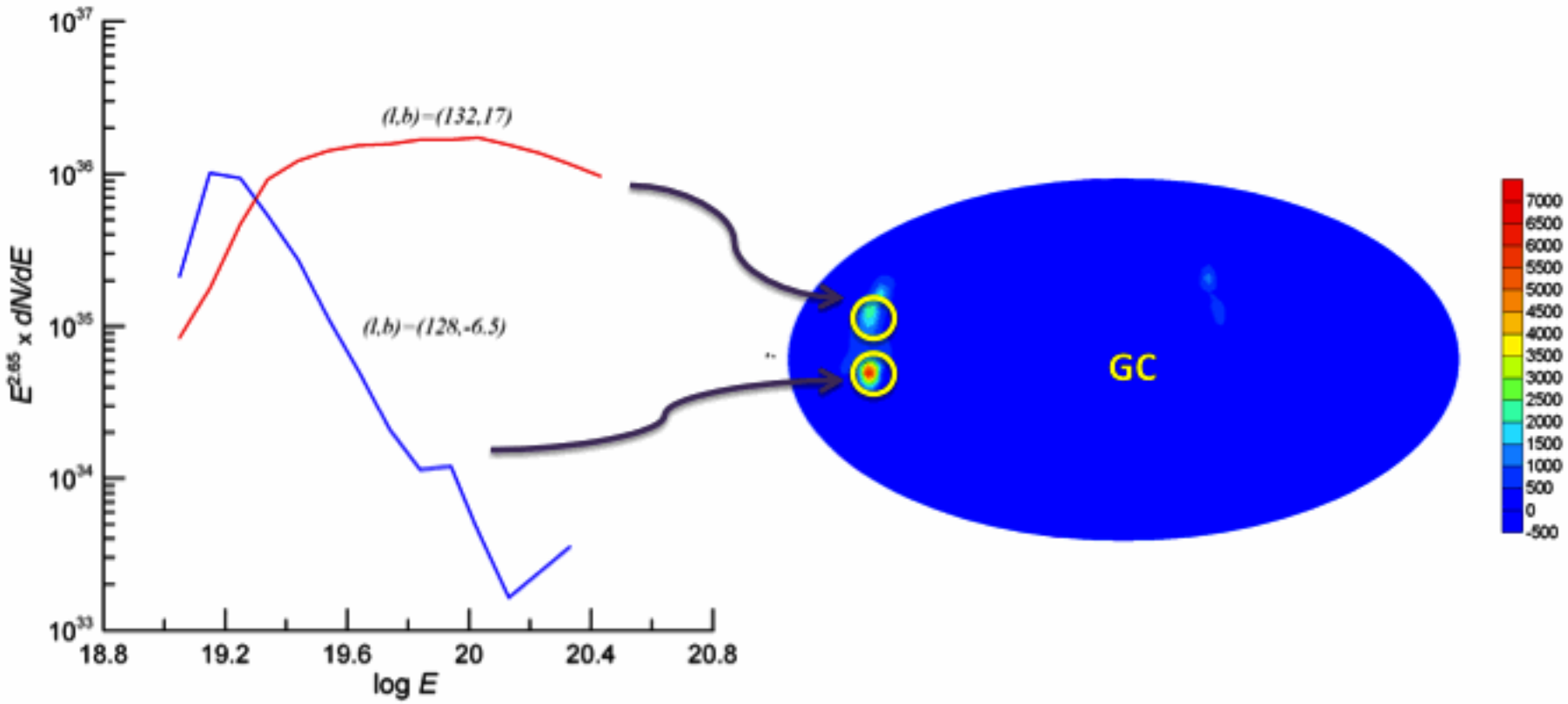

G. Medina-Tanco 2009

PSF & IGMF: spectra as a function of assumed radius

D ~ 5 Mpc
(~ Cen A)

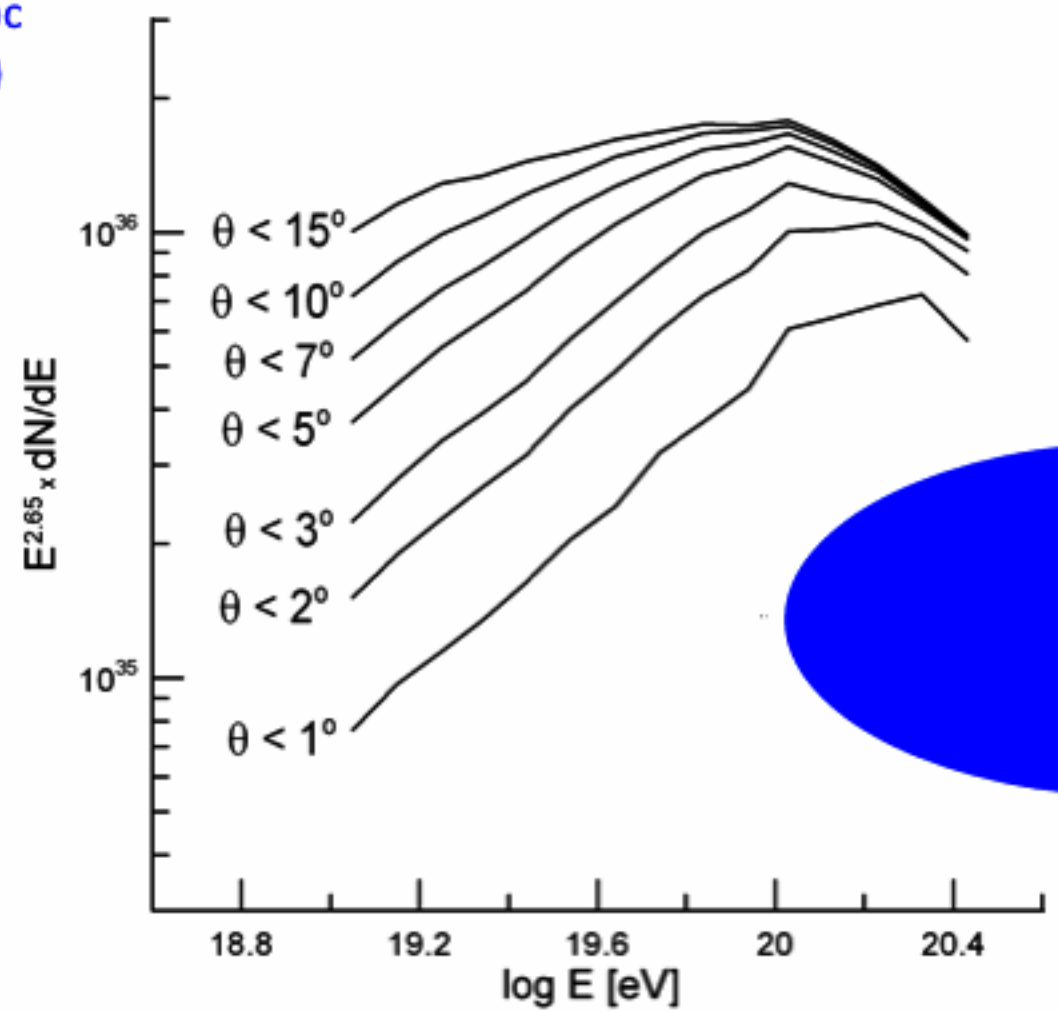

Circles of varying radius centered at true source position on the sky

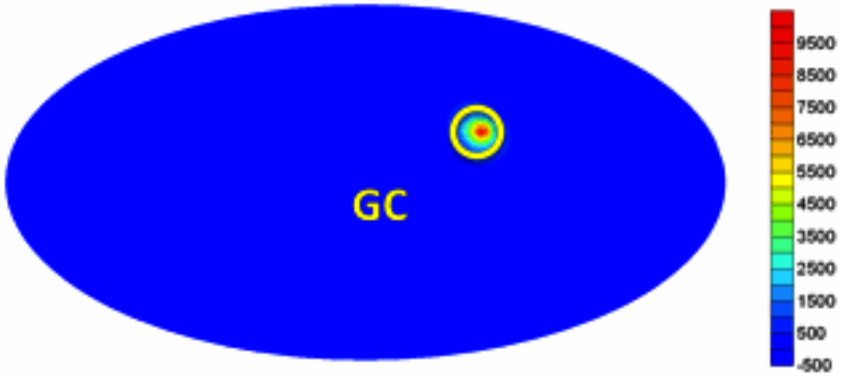

The hardness of the spectrum strongly depends on the radius of the PSF

G. Medina-Tanco 2009

“Intrinsic” point spread functions

- PSFs can extend for several degrees on the sky, giving the spurious impression of linear structures in the source distribution.
- The combined signal for all the sources inside a patch of sky would constitute a 2D polarization signal

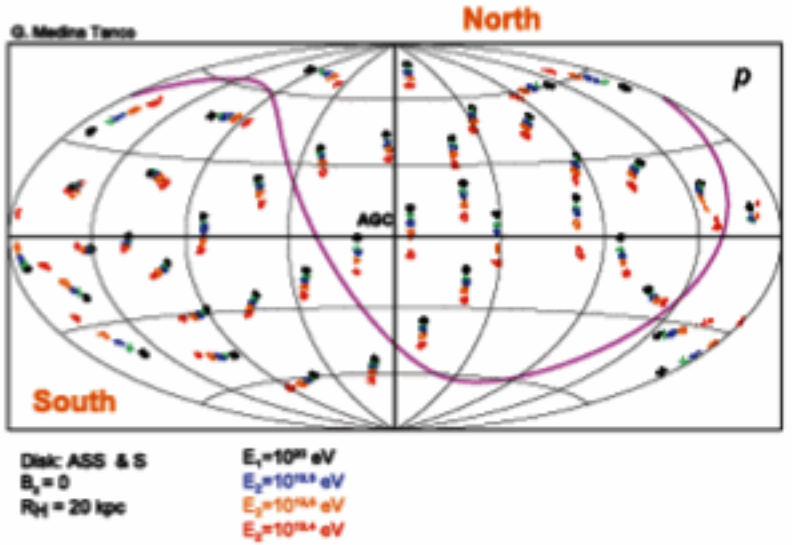

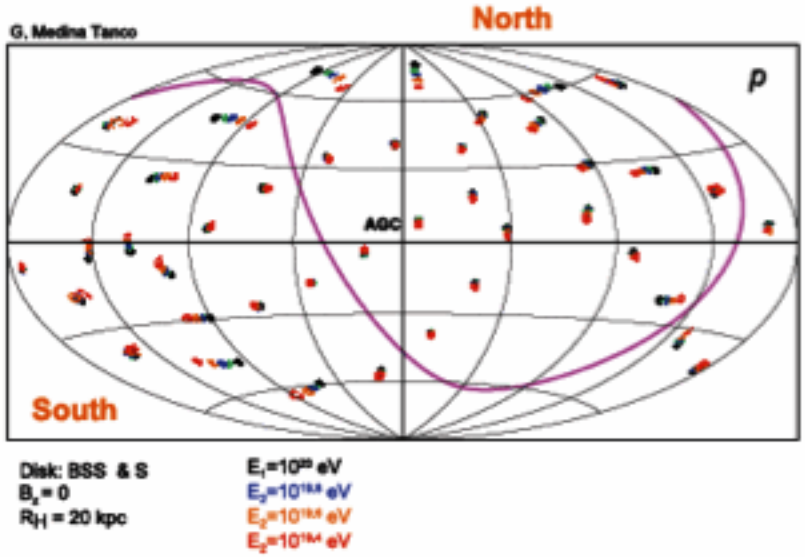

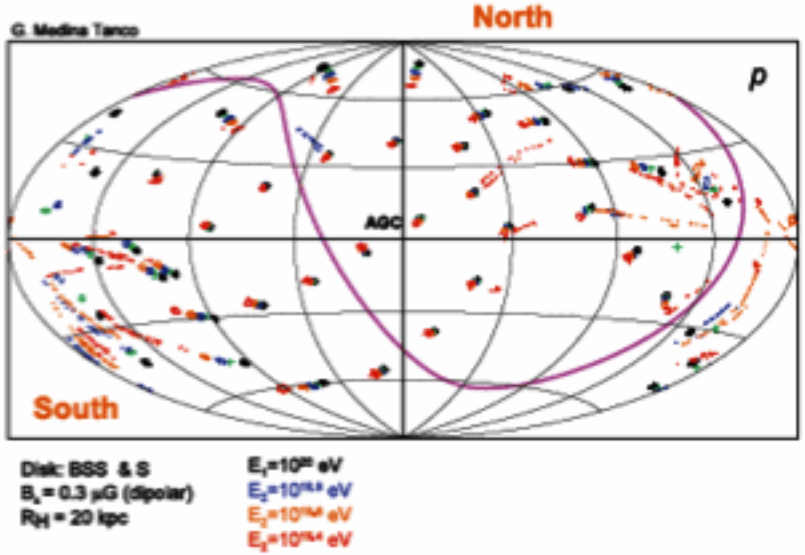

Medina Tanco, Teshima & Takeda (2003)

Auger North

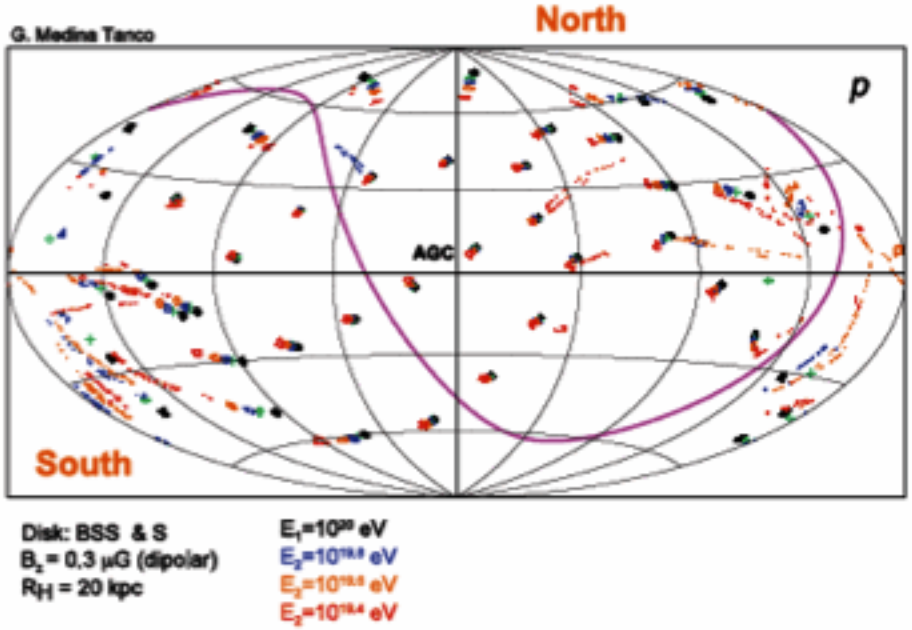

Auger South

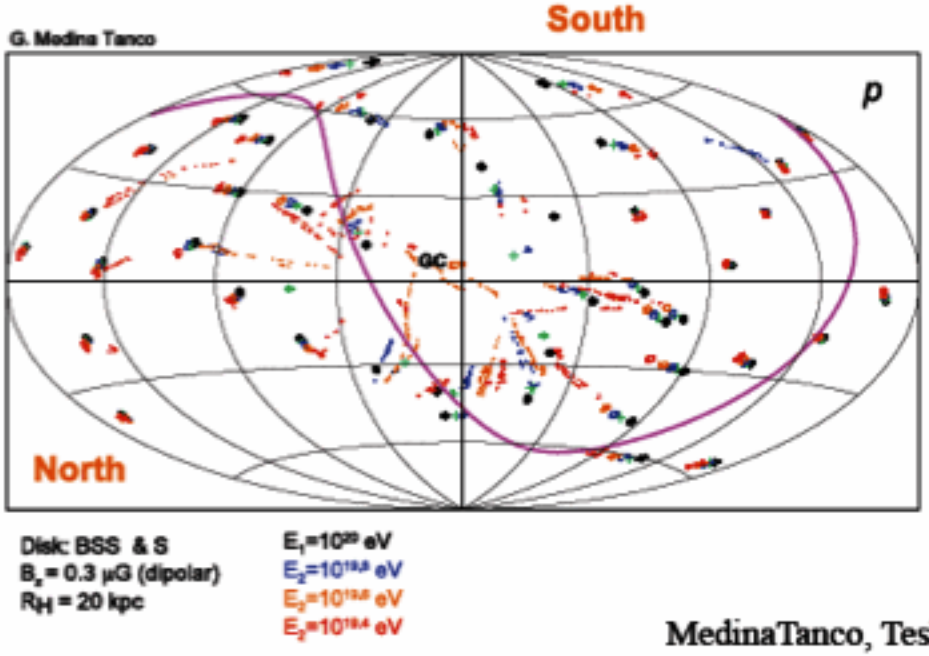

MedinaTanco, Teshima & Takeda, 2003

Grand scale isotropy & anisotropy

The immediate neighborhood

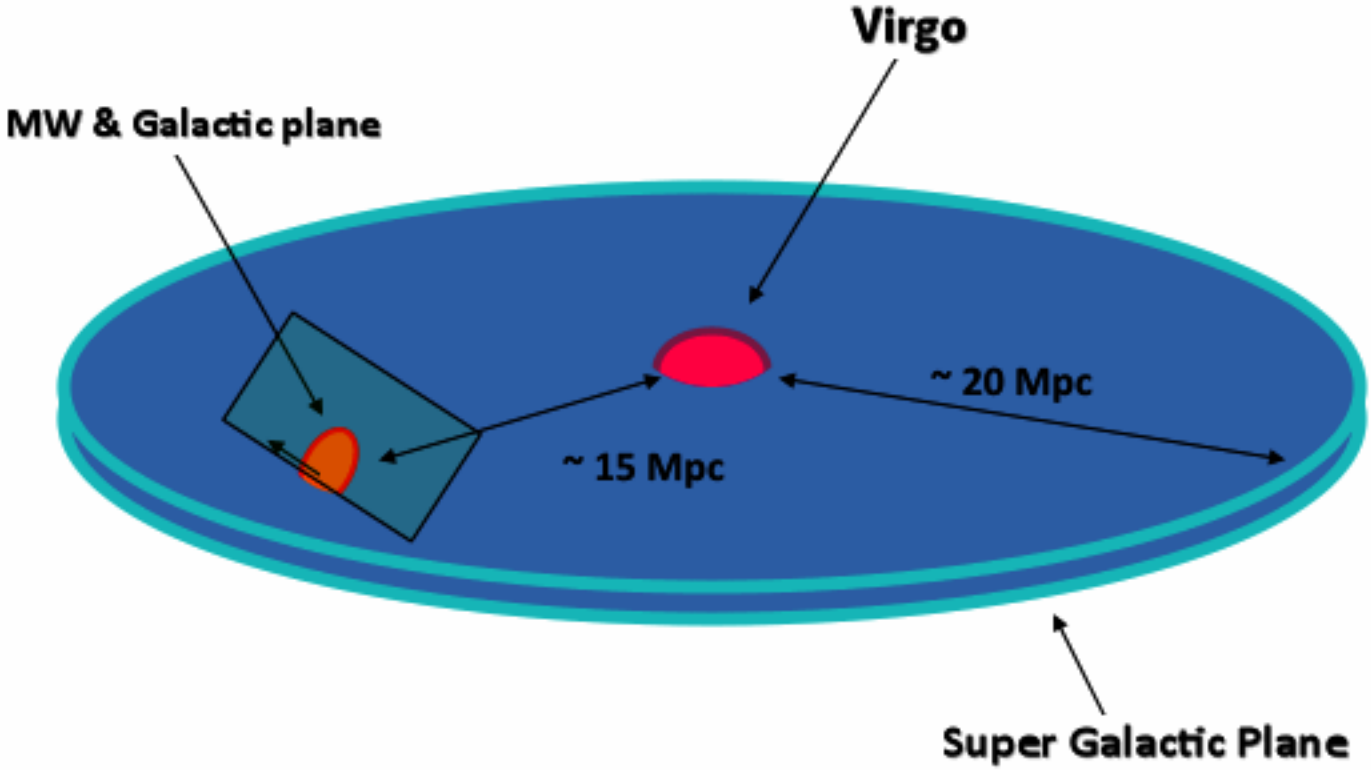

G. Medina Tanco – gmtanco@gmail.com

The curse of isotropy

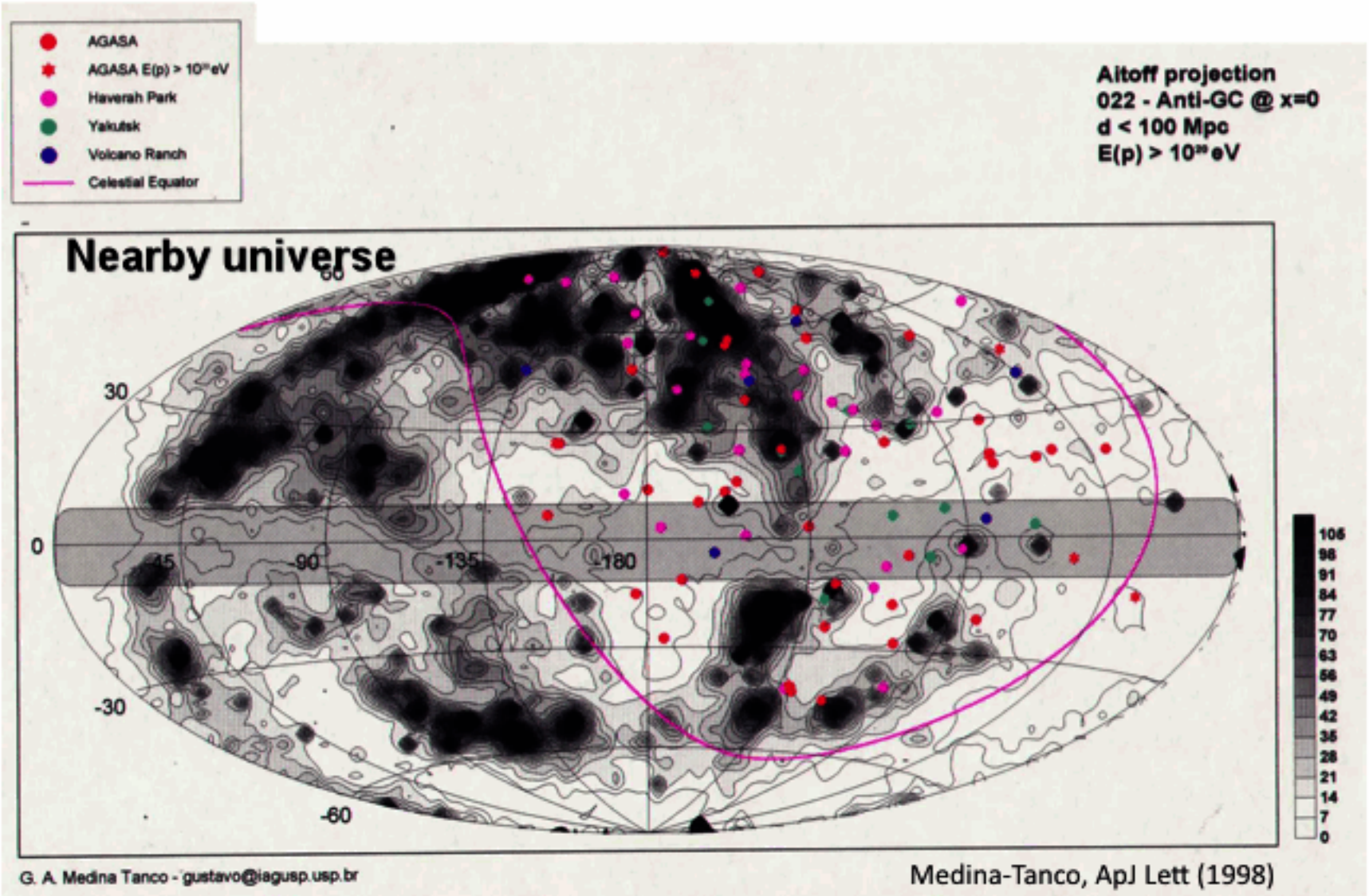

The curse of isotropy: Auger

E @ EeV
71147 events

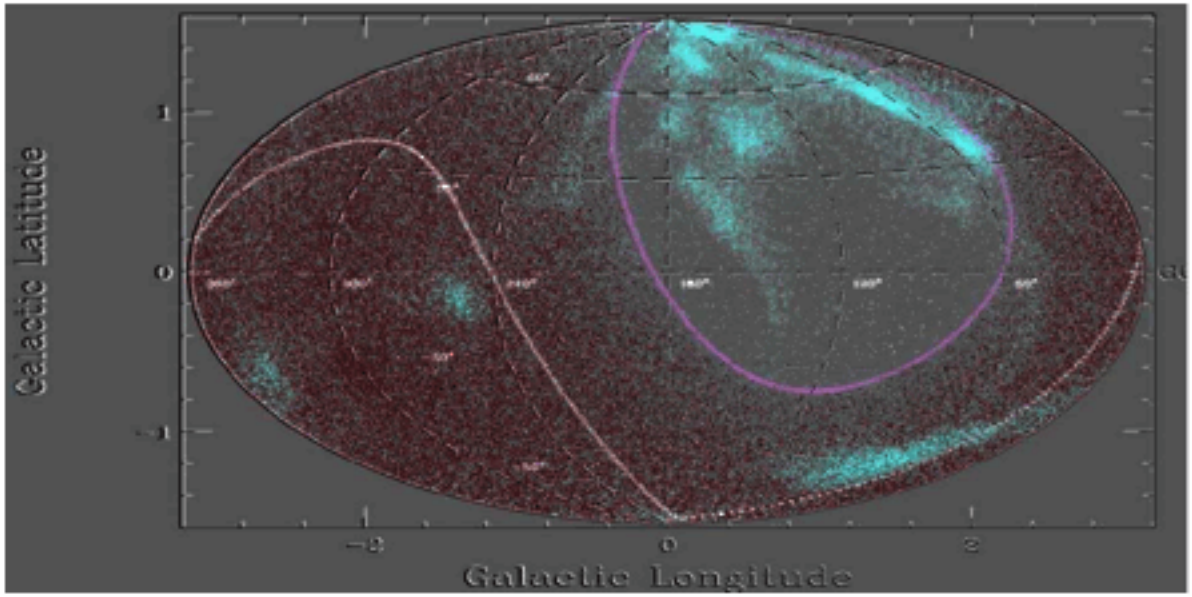

E>10 EeV
638 events

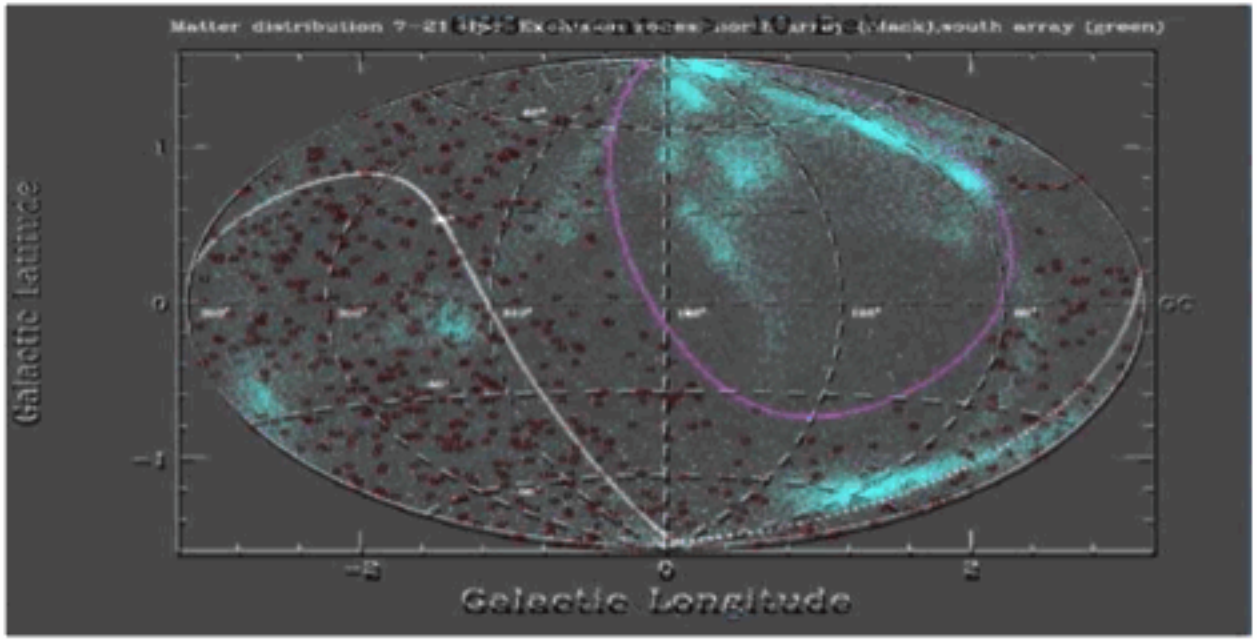

UHECR & AGN correlation

Auger Collaboration, Science, Nov. 9, 2007

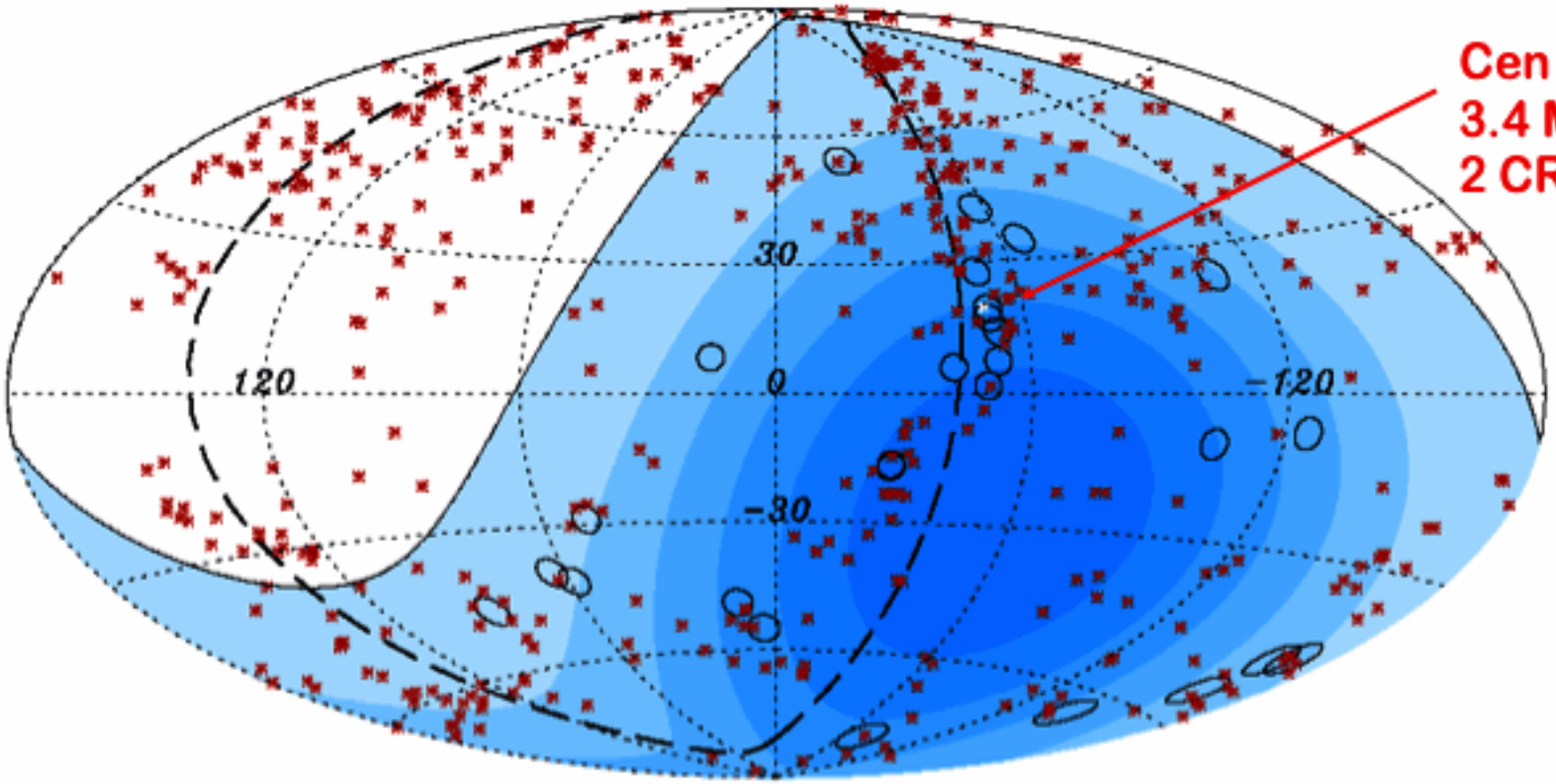

Whole data set scan: $\psi < 3.2°$, $z < 0.017$ (71 Mpc) and $E > 57$ EeV

Chance probability that the sample is isotropic ~ 10^{-5}

ANISOTROPY (58 events @ E>55 EeV)
Evolution as a function of arriving events (~time)

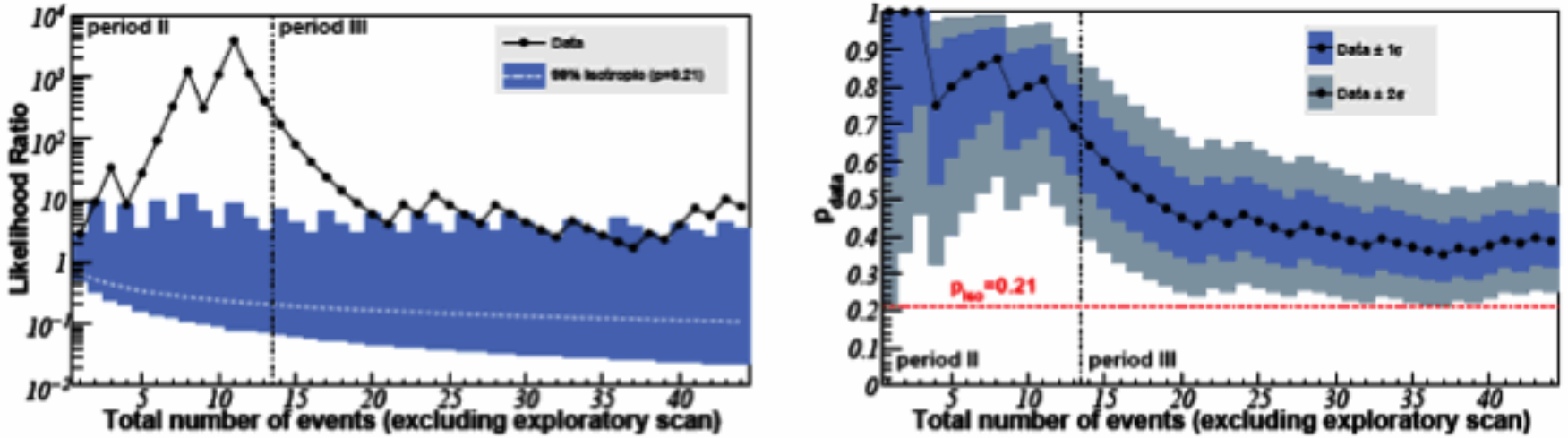

Fig. 1. Monitoring the correlation signal. *Left:* The sequential analysis of cosmic rays with energy greater than 55 EeV arriving after 27 May, 2006. The likelihood ratio $\log_{10} R$ (see Eqn (2)) for the data is plotted in black circles. Events that arrive within $\psi_{\rm max} = 3.1^\circ$ of an AGN with maximum redshift $z_{\rm max} = 0.018$ result in an up-tick of this line. Values above the area shaded in blue have less than 1% chance probability to arise from an isotropic distribution ($p_{\rm iso} = 0.21$). *Right:* The most likely value of the binomial parameter $p_{\rm data} = k/N$ is plotted with black circles as a function of time. The 1σ and 2σ uncertainties in the observed value are shaded. The horizontal dashed line shows the isotropic value $p_{\rm iso} = 0.21$. The current estimate of the signal is 0.38 ± 0.07. In both plots events to the left of the dashed vertical line correspond to period II of Table I and those to the right, collected after [1], correspond to period III.

$$P = \sum_{j=k}^{N} \binom{N}{j} p_{\rm iso}^{\,j} (1 - p_{\rm iso})^{N-j}$$

$$R = \frac{\int_{p_{\rm iso}}^{1} p^k (1-p)^{N-k}\, dp}{{p_{\rm iso}}^k (1-p_{\rm iso})^{N-k+1}}$$

Likelihood ratio: This quantity is the ratio between the binomial probability of correlation – marginalized over its range of possible values and assuming a flat prior – and the binomial probability in the isotropic case (piso = 0.21).

Bottom Line: Still evidence for anisotropy at level of 6 x 10^{-3}

The anisotropy signal today

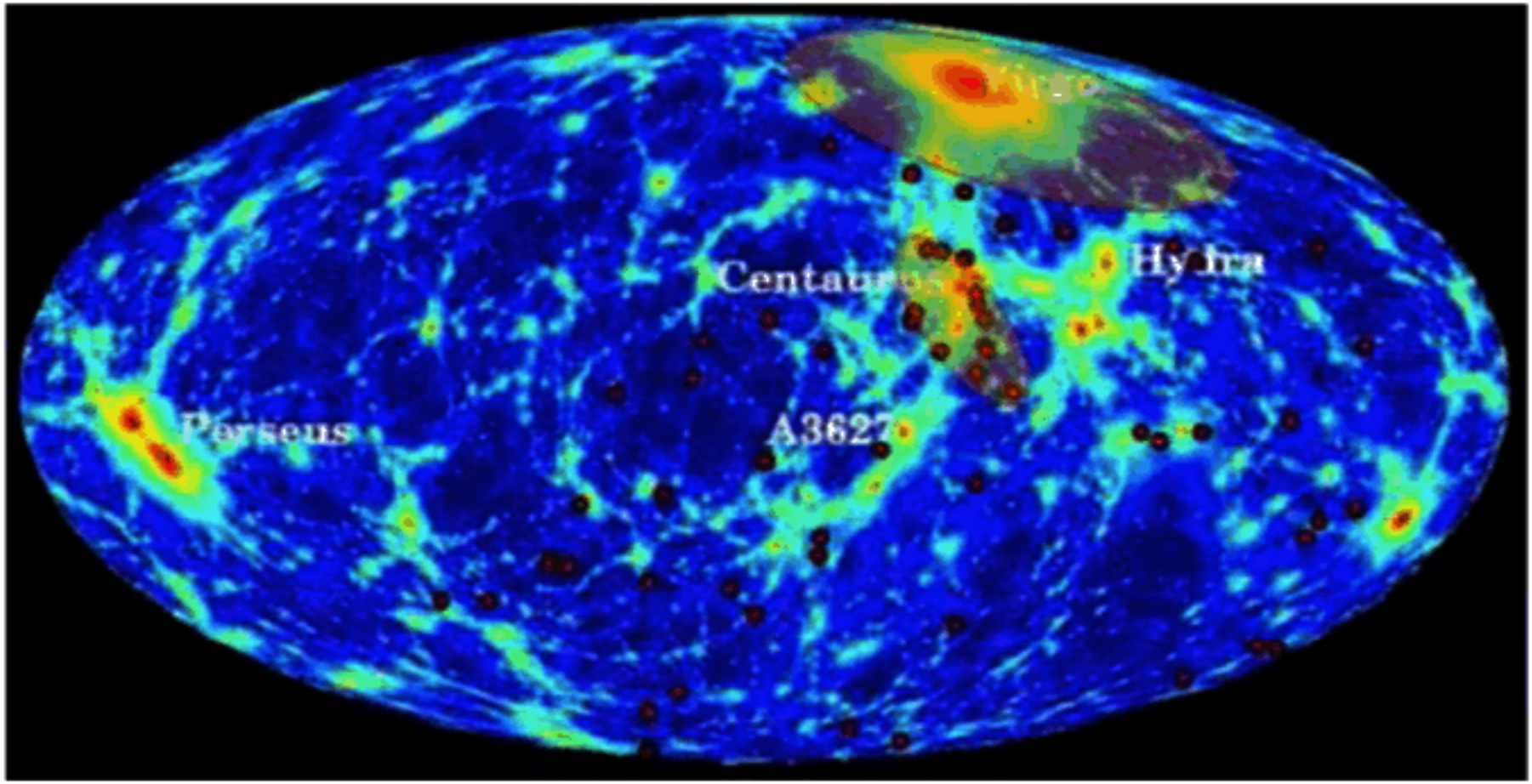

Nearby extragalactic magnetic fields

$$\delta\theta \sim 0.42^{o} \times Z \times \left(\frac{E}{60\,EeV}\right) \times \left(\frac{D}{L_c}\right)^{1/2} \times \left(\frac{L_c}{1Mpc}\right) \times \left(\frac{B}{10^{-9}G}\right)$$

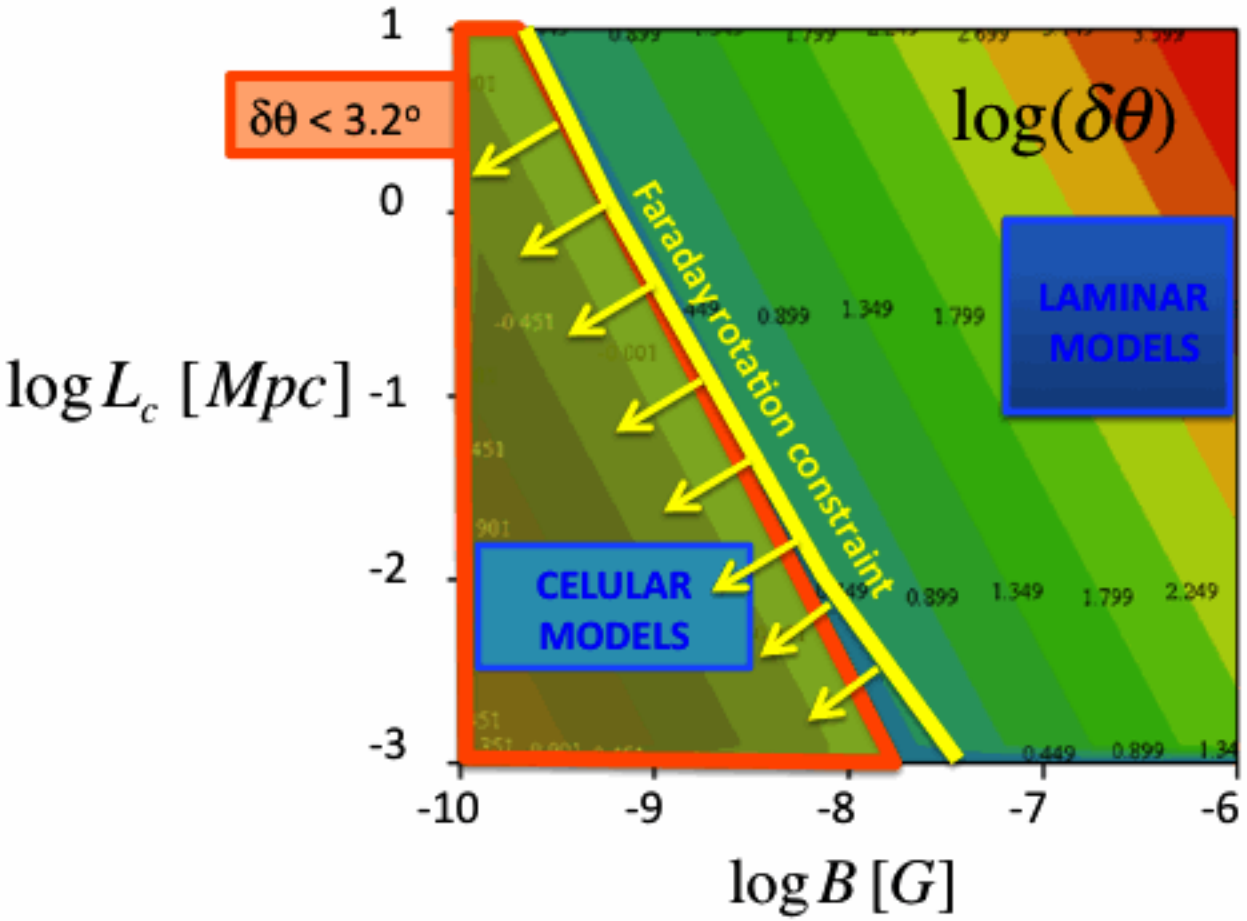

D=70 Mpc
E=60 EeV

Galactic magnetic fields

Deflection after propagation through the galaxy and 20 kpc Halo (BSS-S)

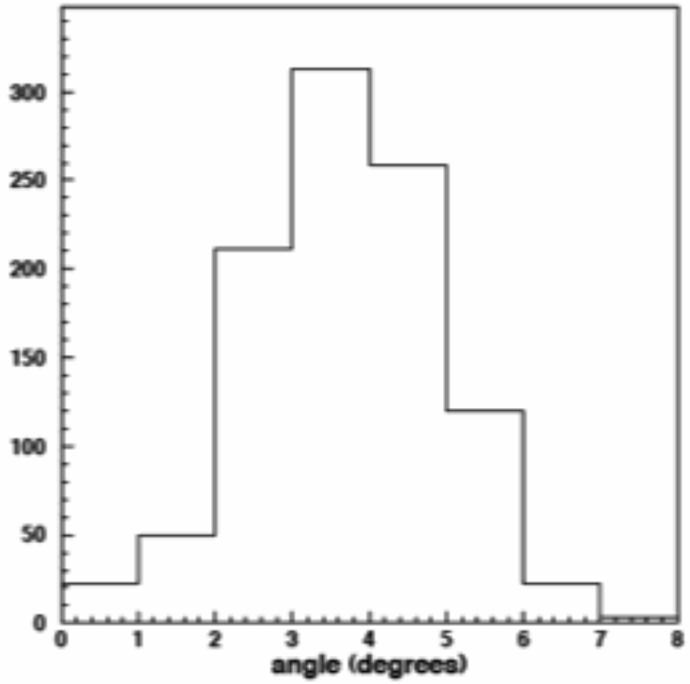

1000 isotropic events

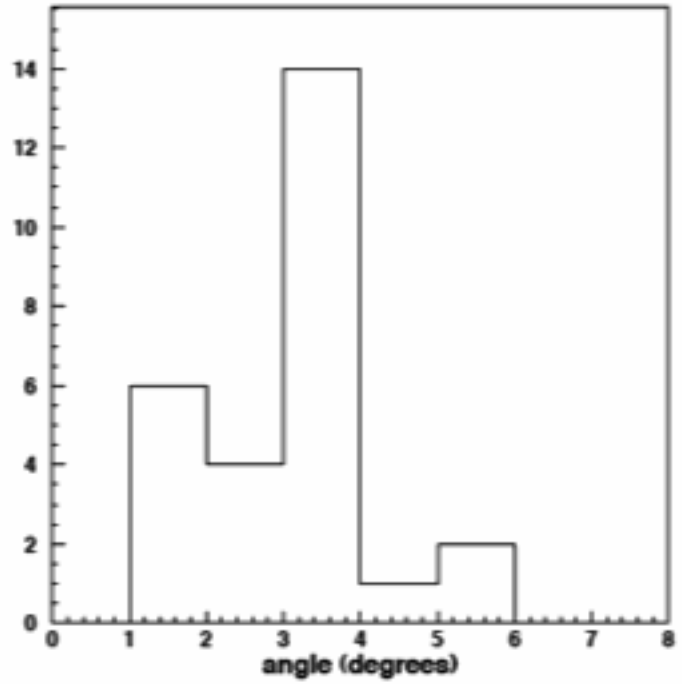

27 real events E > 57 EeV

Nearby extragalactic magnetic fields

$$\delta\theta \sim 0.42^{o} \times Z \times \left(\frac{E}{60\,EeV}\right) \times \left(\frac{D}{L_c}\right)^{1/2} \times \left(\frac{L_c}{1Mpc}\right) \times \left(\frac{B}{10^{-9}G}\right)$$

IGMF too small?

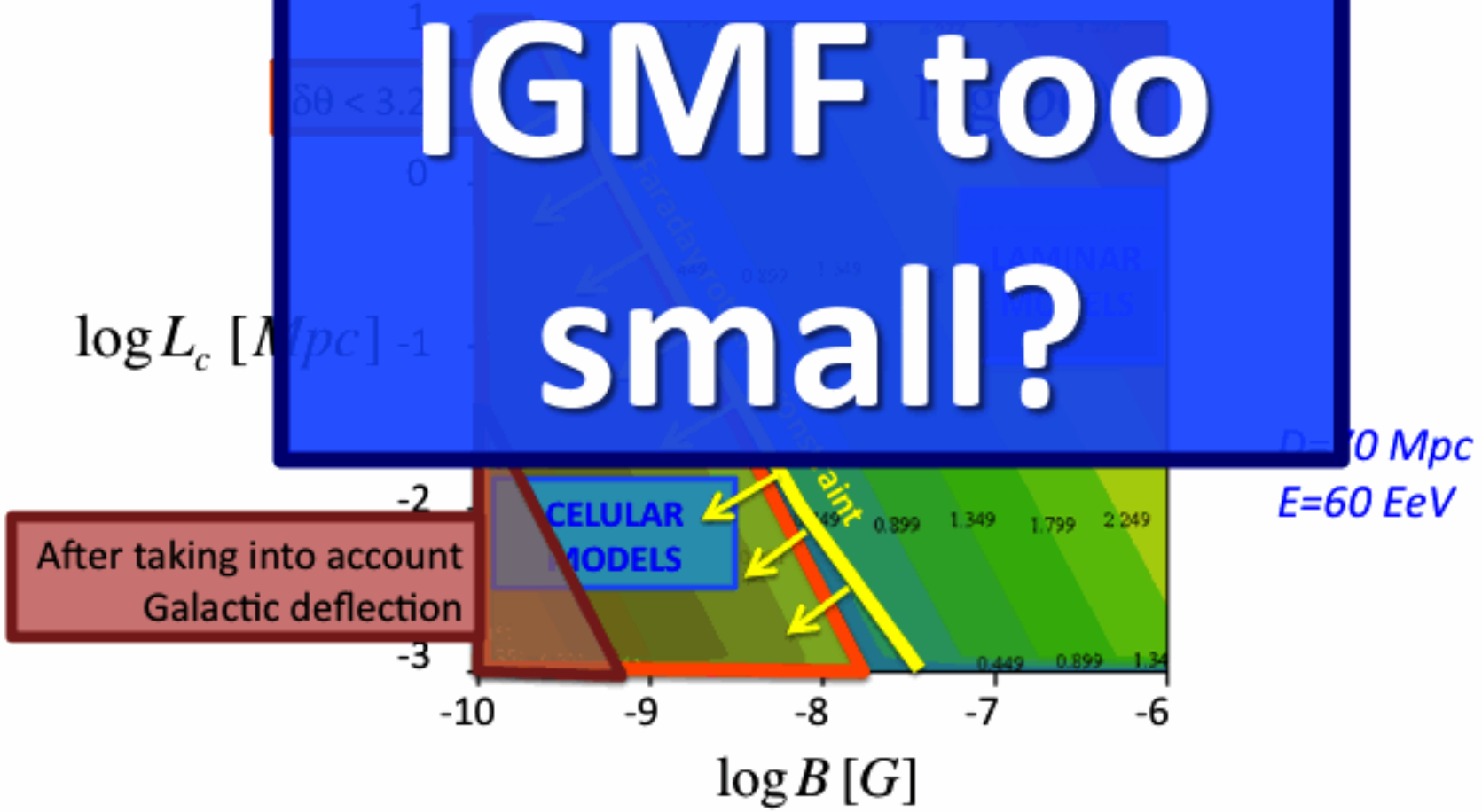

One source + diffuse background

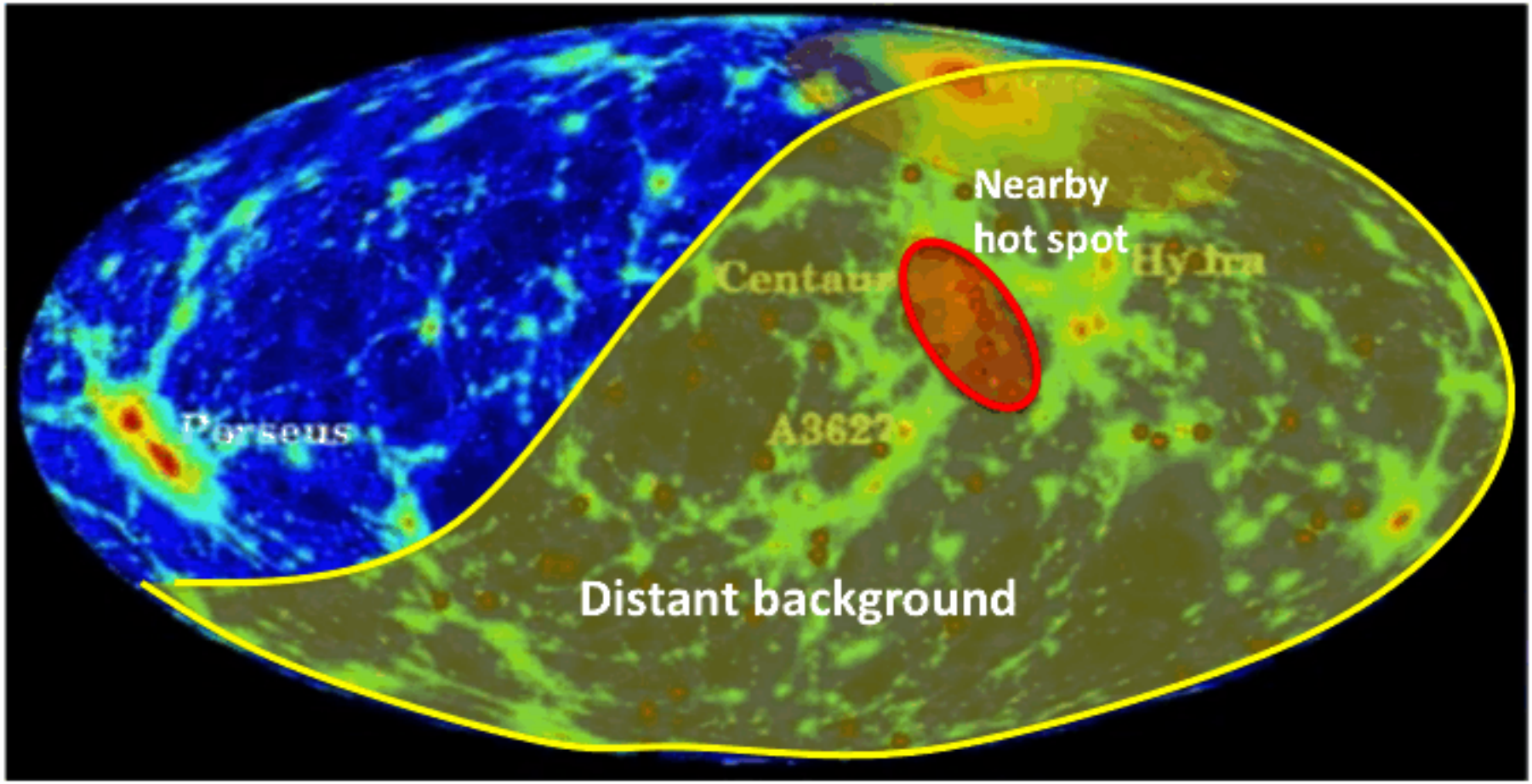

Nearby extragalactic magnetic fields

$$\delta\theta \sim 0.42^{o} \times Z \times \left(\frac{E}{60\,EeV}\right) \times \left(\frac{D}{L_c}\right)^{1/2} \times \left(\frac{L_c}{1Mpc}\right) \times \left(\frac{B}{10^{-9}G}\right)$$

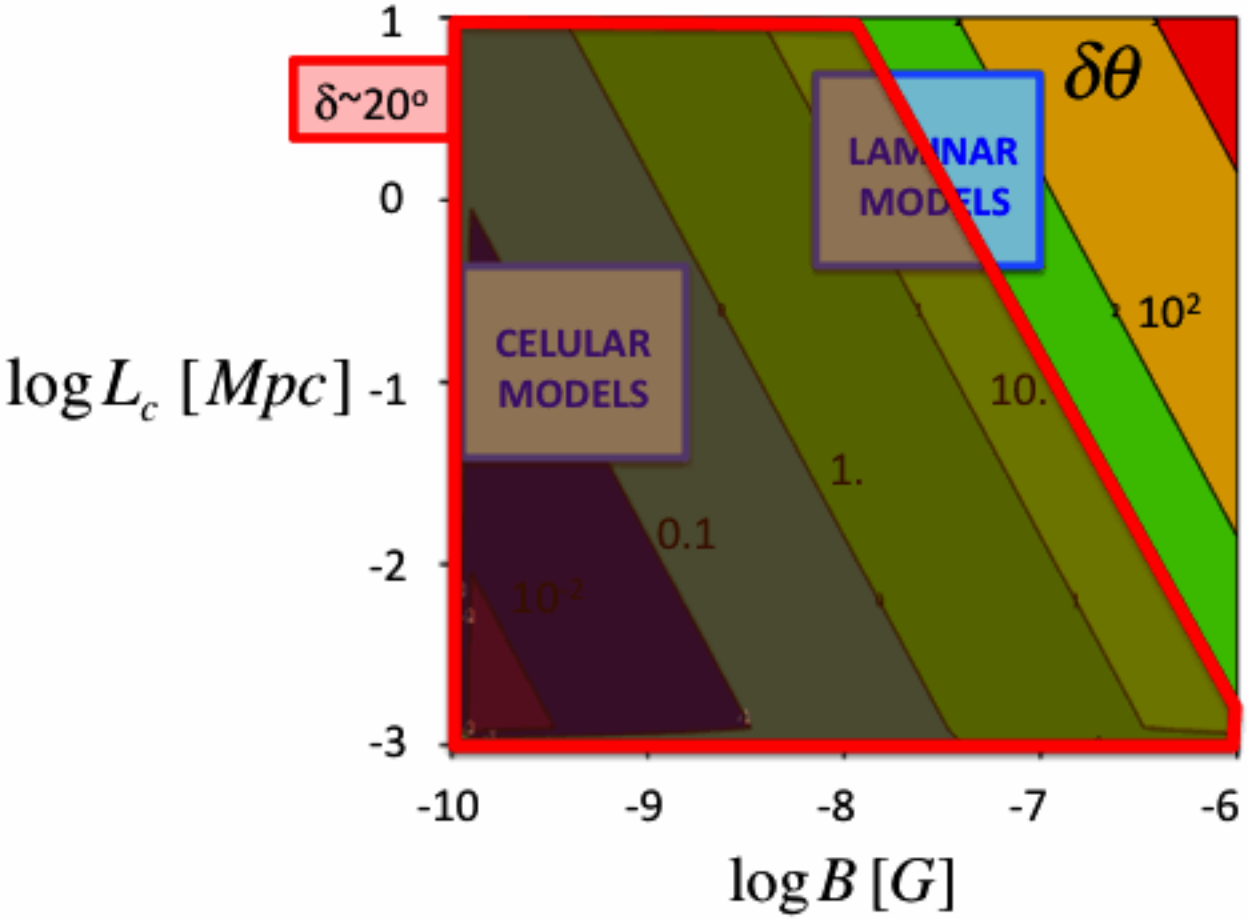

Cen A
D=4 Mpc
E=60 EeV

The Galactic Halo does mater

Deflection: magnetic field intensity

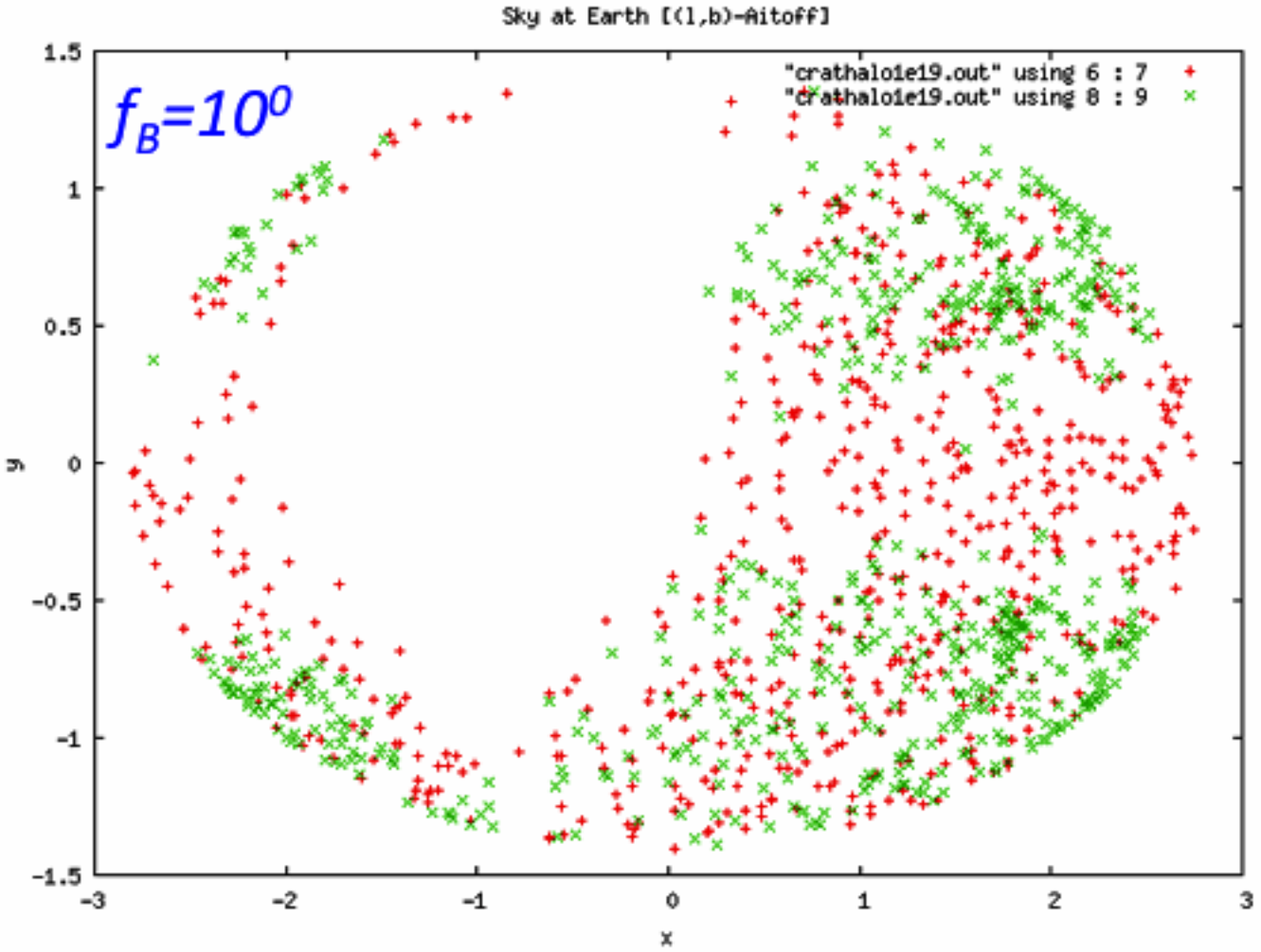

No dipole component
BSS_S
R_H~30 kpc

Events with Auger exposure
& angular distribution
$E > 10^{19}$ eV

G. Medina Tanco (2008)

Deflection: magnetic dipolar component

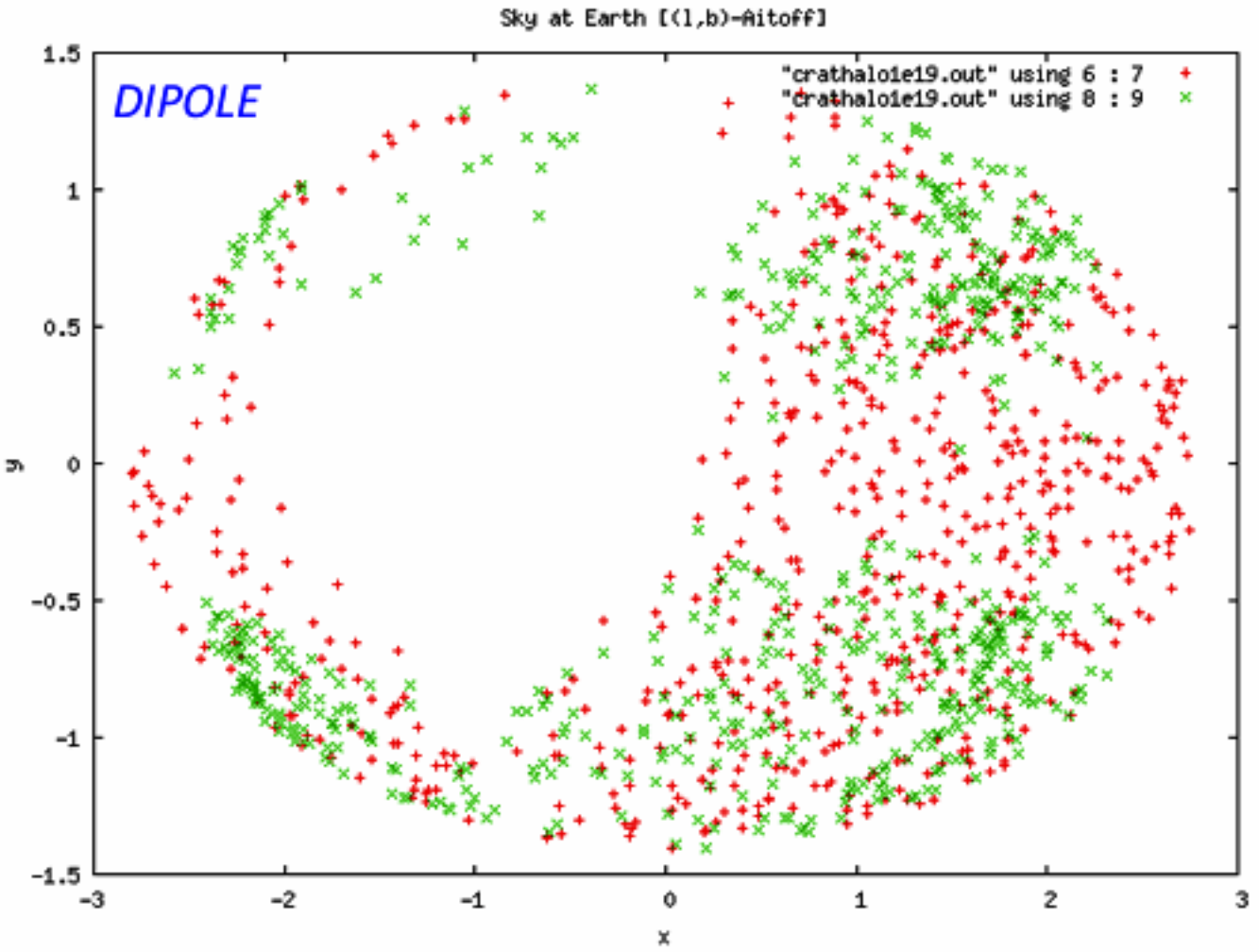

No dipole component
BSS_S
R_H~30 kpc

Events with Auger exposure
& angular distribution
$E > 10^{19}$ eV

G. Medina Tanco (2008)

Deflection by a magnetized Halo

With turbulence

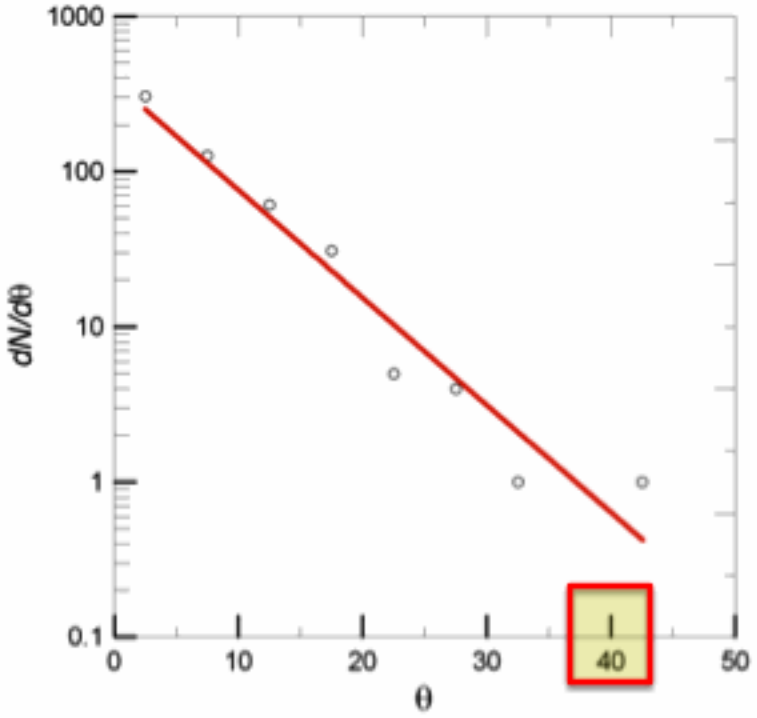

Without turbulence

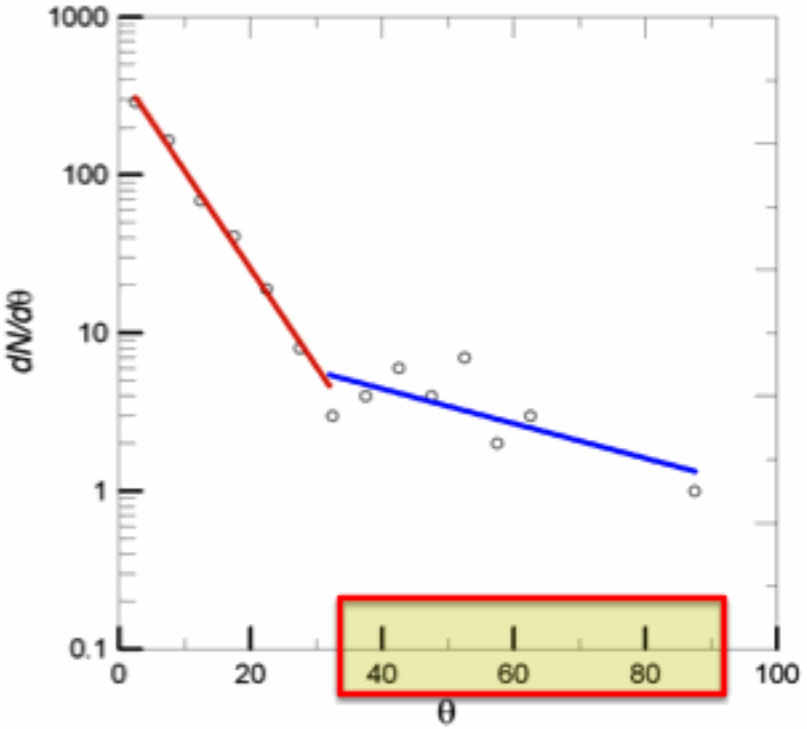

No dipole component
BSS_S
R_H~30 kpc

Events with Auger exposure
& angular distribution
$E > 10^{19}$ eV

Magnetic lensing by the Halo

UHECR vs. AGN correlation

NO Parker-like Galactic wind

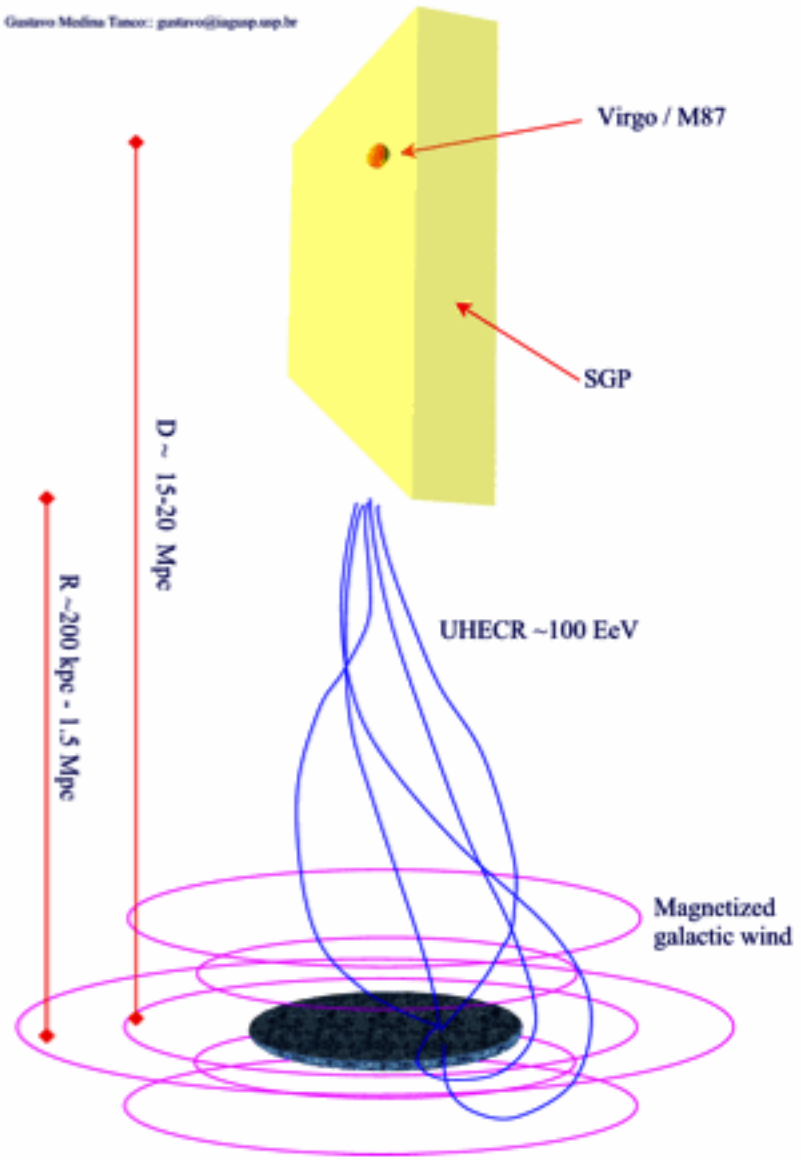

Biermann, Ahn, Medina Tanco & Stanev, 2000, 2001

Halos might bear quite amazing structures

Elongation rate vs. anisotropy result

Remember:
$\delta\theta \sim Z$

Too heavy ?

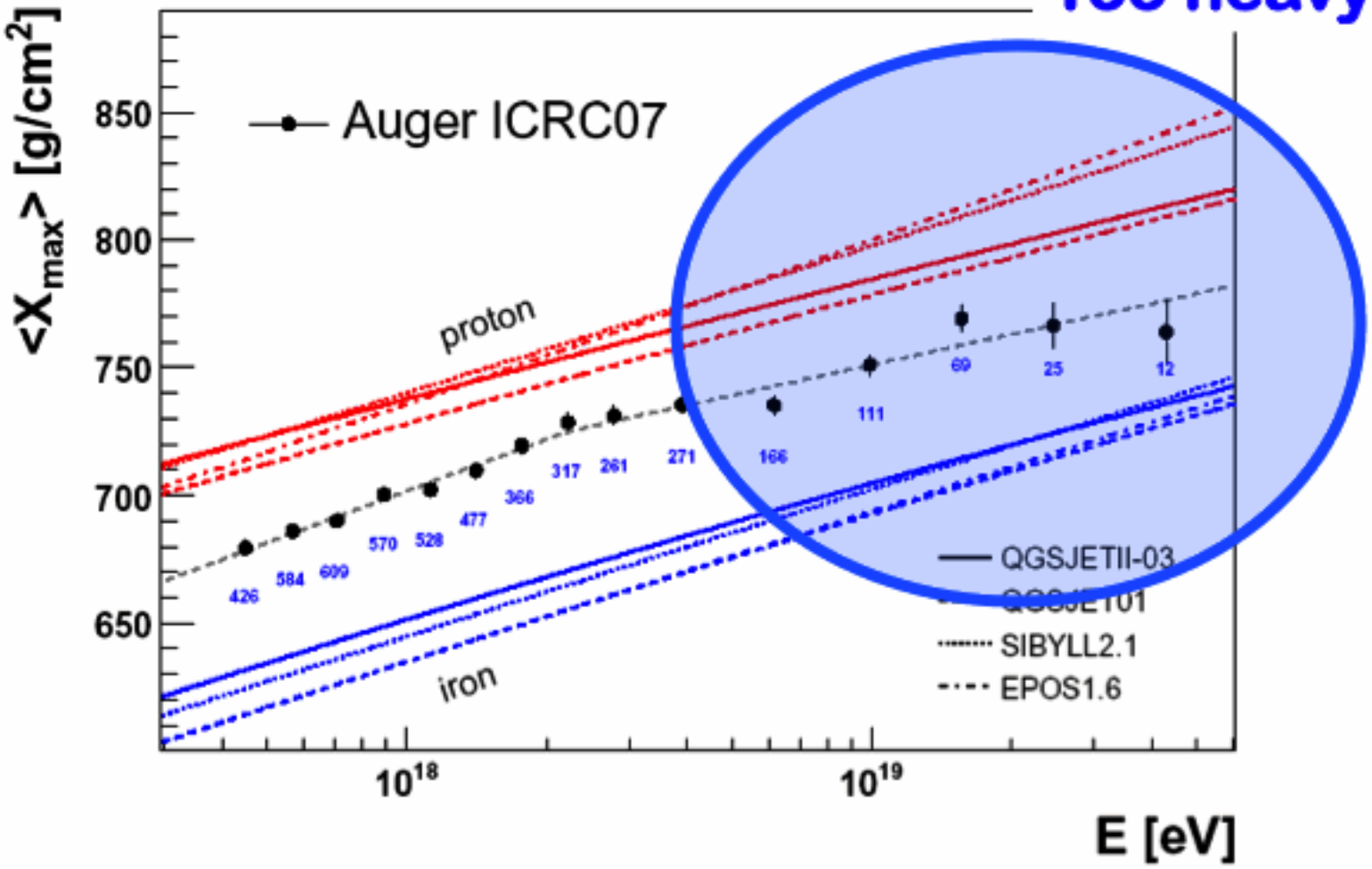

Is the particle physics Correct?

Conclusions 1

1. Circumstantial evidence may come from:

   SPECTRAL FEATURES
   COMPOSITION
   ANISOTROPY

2. Smoking gun:

   Anisotropy: (point source)
   IDENTIFICATION OF AN ASTRONOMICAL COUNTERPART

As in the case of GRBs & BeppoSAX

But, it will more difficult than in the GRB case to achieve the identification of an astrophysical source, since the GMF & IGMF will distort the picture

LARGE STATISTICS @ HIGHEST ENERGIES

Conclusions

Astrophysical interpretation of the data in terms of source discrimination and distance scales **MUST** take into account the uncertainties posed by the intervening magnetic fields.

Once we have solved this basic problem, UHECR will be a tool to probe magnetic fields in low density regions of the cosmos where emission is negligible and have remained so far beyond our observational reach.

Repository

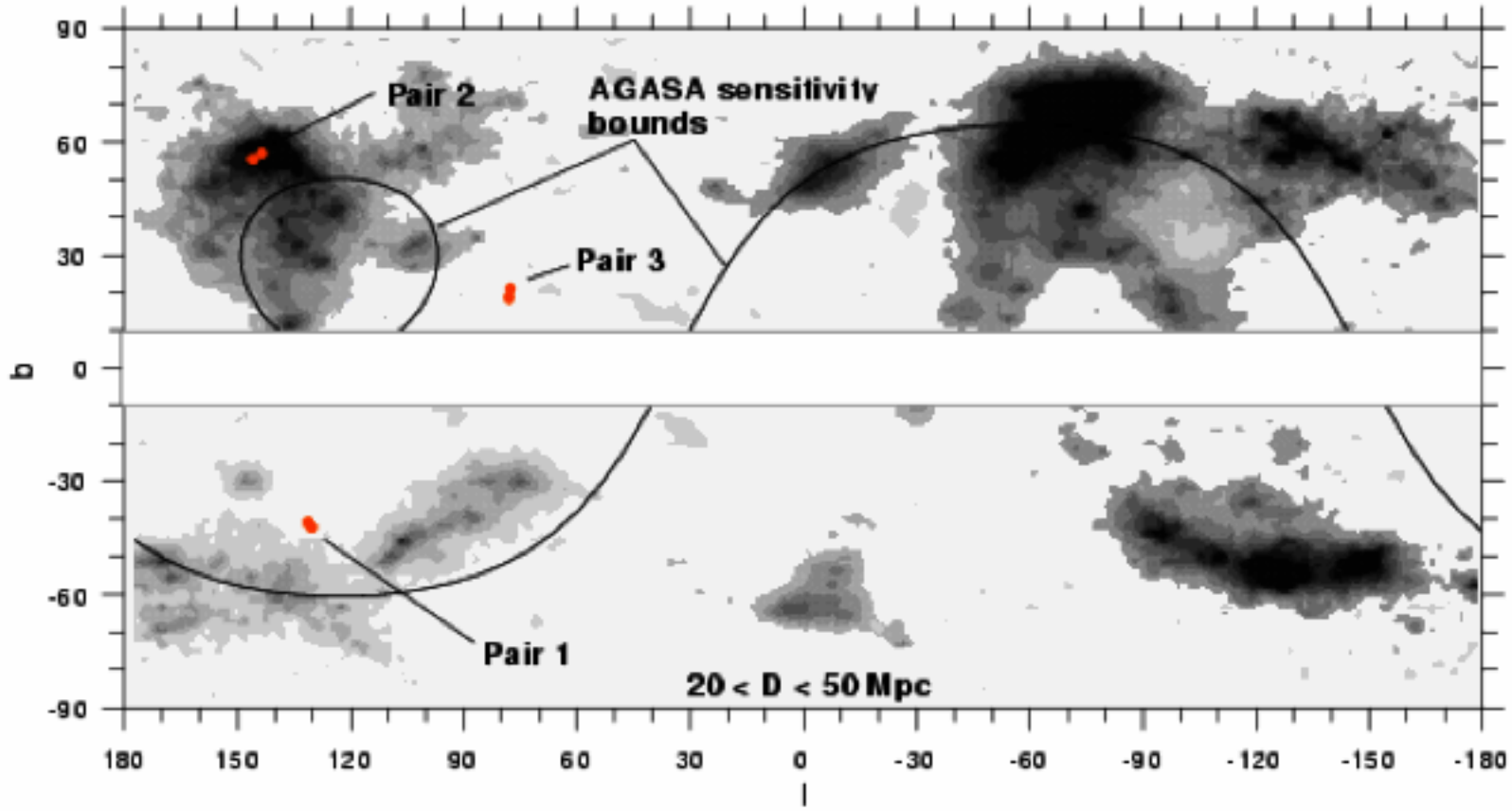

Medina Tanco, ApJ Lett, 1998

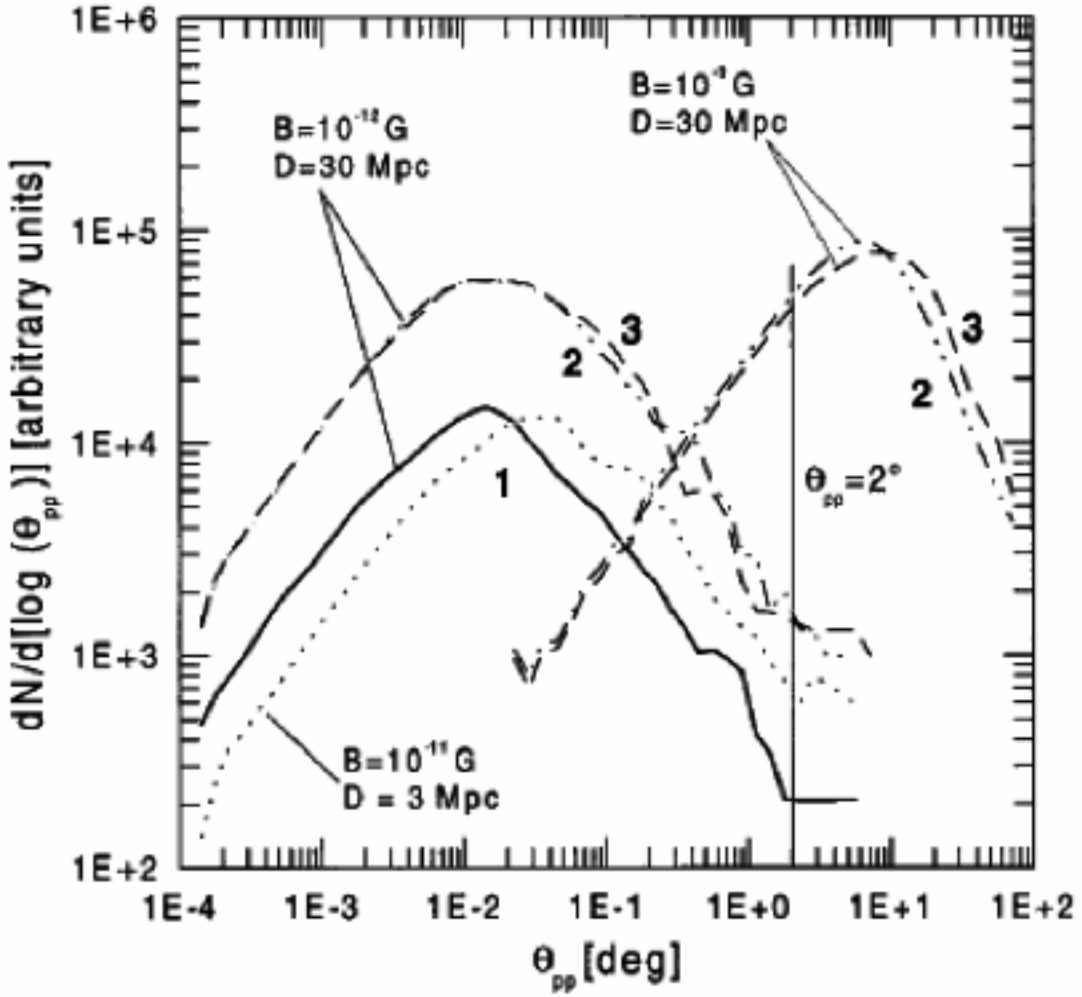

Pair Number	Date	Δt_{obs} (yr)	Energy (EeV)	Type	l_{gal}	b_{gal}
1	1993 Dec 3	1.90	210	A	131.2	−41.1
	1995 Oct 29	...	51	...	130.2	−42.3
2	1992 Aug 1	2.49	55	B	143.5	56.9
	1995 Jan 26	...	78	...	145.8	55.3
3	1991 Apr 20	3.21	43	B	77.9	18.6
	1994 Jul 6	...	110	...	77.6	21.1

* Adapted from Hayashida et al. 1996.

First 3 AGASA doublets

Medina-Tanco, ApJ Lett, **495**,71,1998

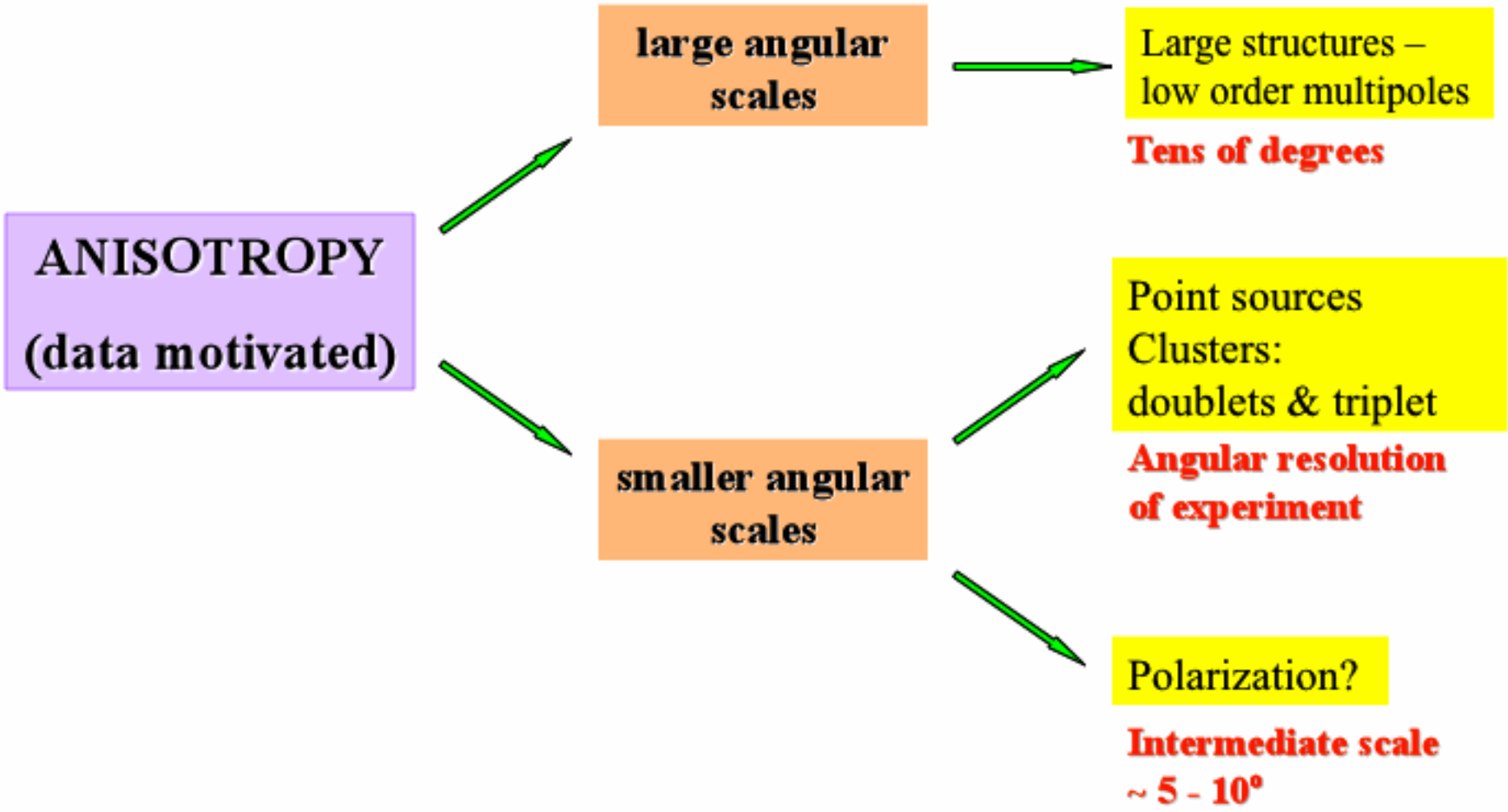
ANISOTROPY
(data motivated)
large angular scales
smaller angular scales
Large structures – low order multipoles
Tens of degrees
Point sources
Clusters: doublets & triplet
Angular resolution of experiment
Polarization?
Intermediate scale ~ 5 - 10°

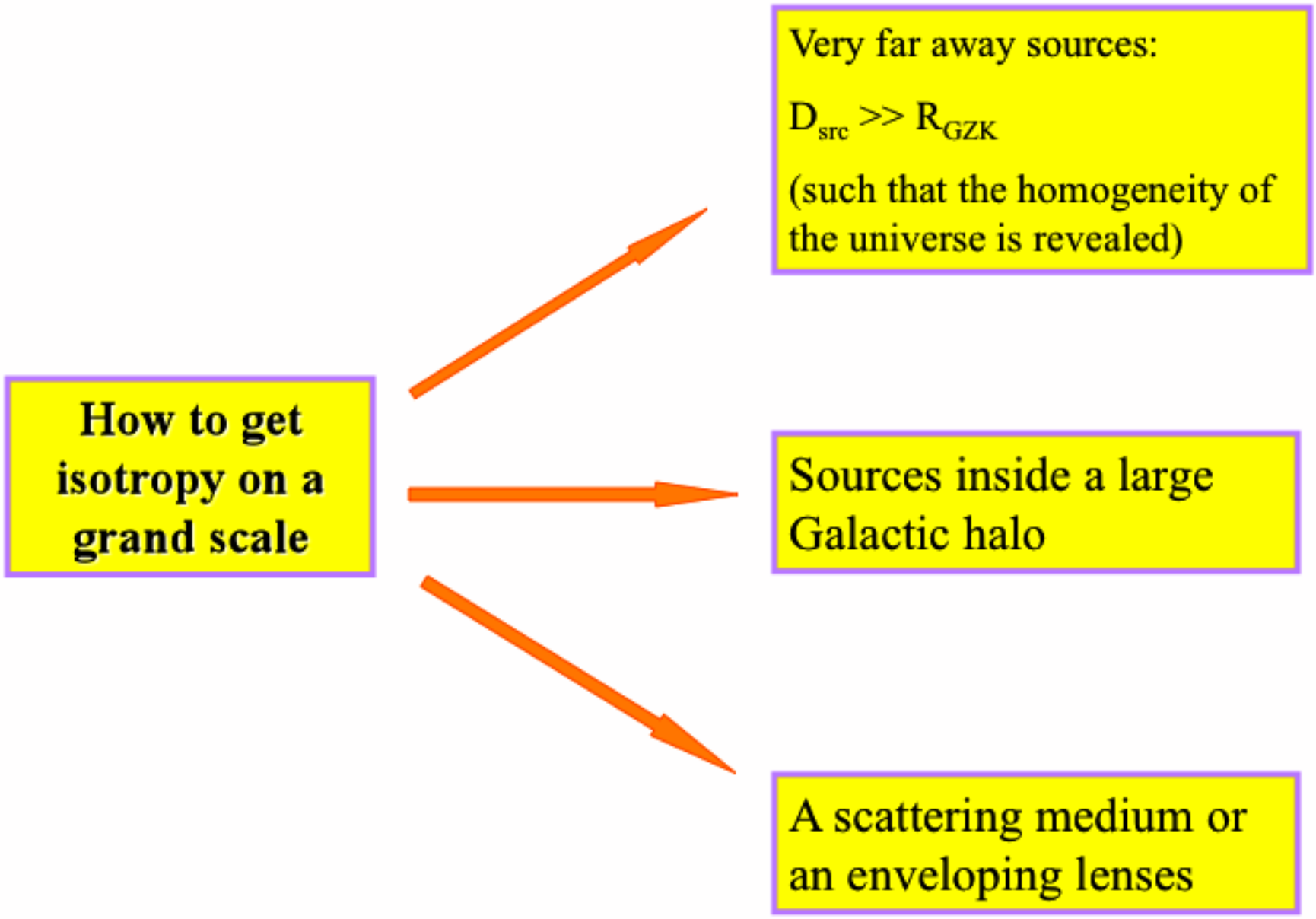
How to get isotropy on a grand scale
Very far away sources:
$D_{src} >> R_{GZK}$
(such that the homogeneity of the universe is revealed)
Sources inside a large Galactic halo
A scattering medium or an enveloping lenses

The Galactic center

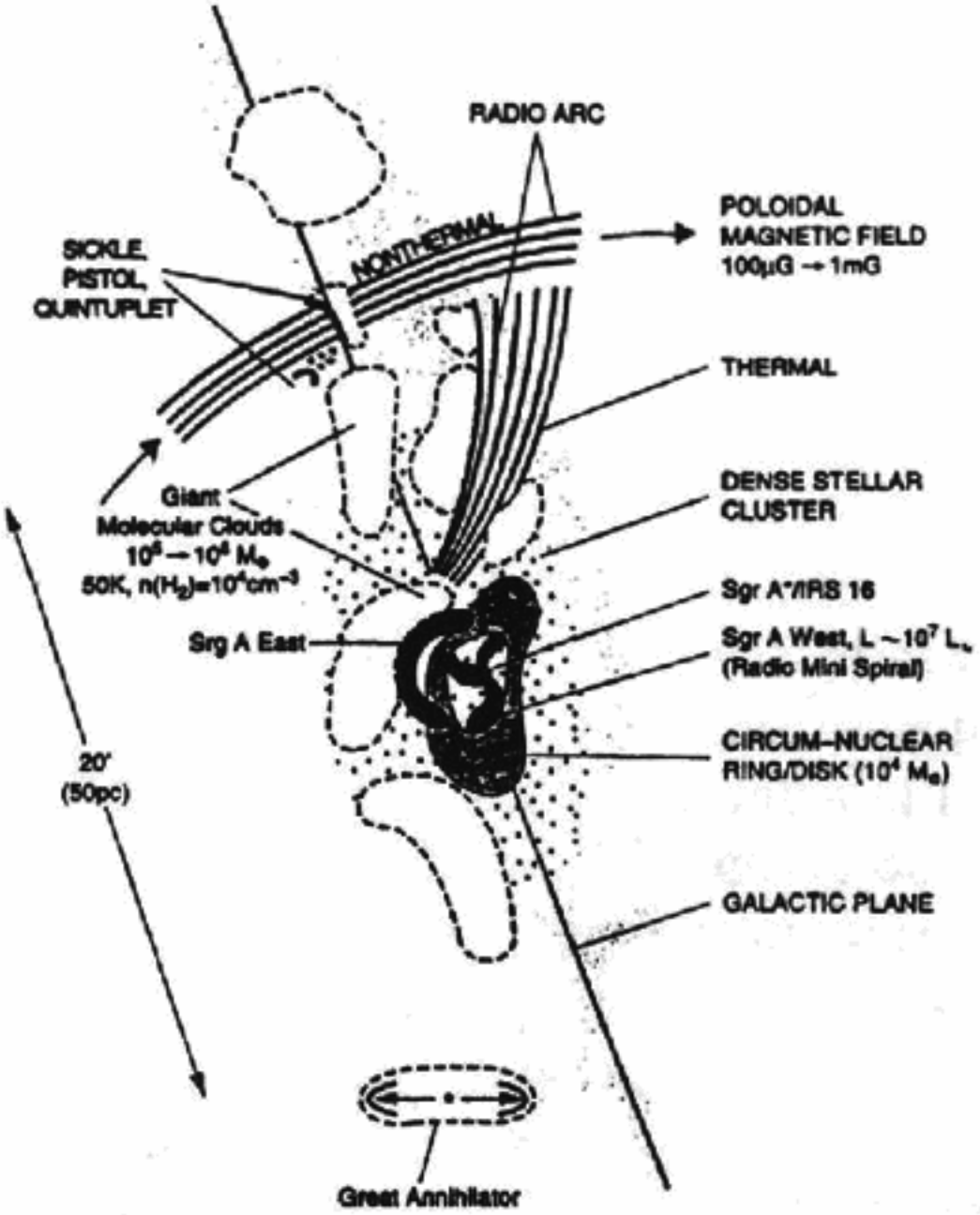

Magnetic field evolution in spiral galaxies

The magnetic field evolution in a spiral galaxy is shown. The velocity and density distribution are obtained from a particle simulation with gas clouds and stars. The time evolution of gas velocity and density are taken as the input for the induction equation to follow the magnetic field evolution under the action of a turbulent dynamo (The azimuthal averaged velocity is subtracted in the movie). The diffusivity (scaled with the density) reflects the spiral structure and leads to interarm magntic fields. The non-axisymmetric velocity of the gas clouds responsible for the spiral structure gives magnetic fields within the optical arms. Both effects together show more or less magnetic fields within the arms. The dynamo with azimuthal averaged rotation and diffusivity is shown for comparison.

See next slide...

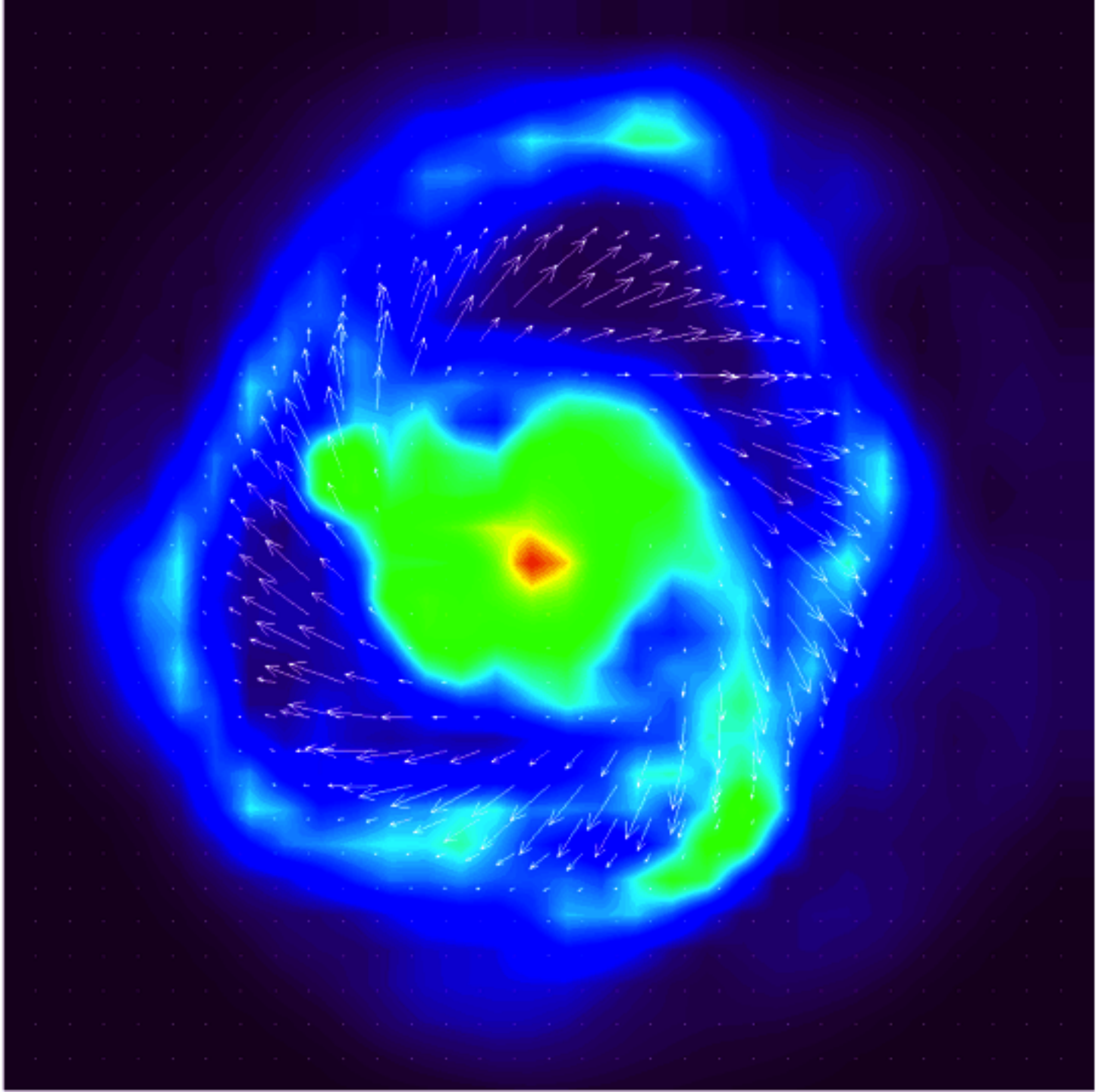

Detlef Elstner
AIP, Germany

Field generation and amplification

The amplification and maintenance or periodic regeneration of magnetic fields by the action of conducting moving fluids is called a dynamo or generator

$$\frac{\partial \vec{B}}{\partial \vec{t}} = -\vec{\nabla} \times \vec{E}$$ Induction equation

$$\vec{E} = \eta \vec{J} - \vec{v} \times \vec{B} - \frac{\vec{\nabla} p}{n_e e} + \ldots$$ Ohm's law

$$\vec{J} = \frac{1}{\mu_0} \vec{\nabla} \times \vec{B} + \ldots$$ Ampere's law

$$\frac{\partial \vec{B}}{\partial \vec{t}} = \underbrace{\vec{\nabla} \times \left(\vec{v} \times \vec{B} \right)}_{\text{convection}} + \underbrace{\frac{\eta}{\mu_0} \nabla^2 \vec{B}}_{\text{diffusion}} + \underbrace{\vec{\nabla} \times \left[\frac{\vec{\nabla} p}{n_e e} \right]}_{\text{battery (non-uniform rotation or non-spherically symmetric chemical composition in a star)}} + \ldots$$

$\int \vec{B}.d\vec{S}$ is conserved for any commoving cross-section $\vec{S}$ *frozen-in* field